9-1-1993

Photolithography model parameter extraction from in-situ measured development rates

Patrick G. Drennan

PHOTOLITHOGRAPHY MODEL PARAMETER EXTRACTION FROM IN-SITU MEASURED DEVELOPMENT RATES

by

Patrick G. Drennan

A Thesis Submitted

in

Partial Fulfillment

of the

Requirements for the Degree of

MASTER OF SCIENCE

in Electrical Engineering

Approved by: **Prof, B. Smith, Thesis Advisor**

Prof. L. Fuller

Prof. I. R. Turkman

Prof. R Unnikrishnan

DEPARTMENT OF ELECTRICAL ENGINEERING

COLLEGE OF ENGINEERING

ROCHESTER INSTITUTE OF TECHNOLOGY

ROCHESTER, NEW YORK

SEPTEMBER, 1993

TABLE OF CONTENTS

LIST OF TABLES

LIST OF FIGURES

Figures 43 - 45 : In-situ development rate versus depth (dose = 66, 90, and 114mJ/cm^2).

Figures 46 - 48 : In-situ thickness versus time (dose = 66, 90, and 114mJ/cm^2).

Figure 49 : Error in fit versus PEB diffusion length constant.

Figures 50 - 52 : Comparison of simulated and measured development rate versus depth in resist (dose = 66, 90, and 114mJ/cm^2).

LIST OF SYMBOLS

I = light intensity.

R = development rate.

a_1 = absorbtion coefficient for the PAC.

a_2 = absorbtion coefficient for the ICA.

a_3 = absorbtion coefficient for the novolac binder.

m_1 = molar concentration of the PAC.

m_2 = molar concentration of the ICA.

m_3 = molar concentration of the novolac binder.

C = the fractional decay rate of the PAC per unit intensity of light.

I_o = light intensity at the resist surface.

m_o = initial PAC concentration.

A = the dynamic component of the extinction coefficient.

B = the static component of the extinction coefficient.

α = the dynamic attenuation coefficient.

R_1 = development rate for fully exposed resist.

R_2 = development rate for unexposed resist.

R_3 = a sensitivity parameter.

R_4 = characteristic length for the surface development rate inhibition.

R_5 = ratio of the surface development rate to the bulk development rate.

R_6 = ratio of the surface development rate to the bulk development rate for no exposure.

R_{bulk} = bulk development rate for the Kim model.

R_{max} = the maximum development rate for the Mack development model.

R_{min} = the minimum development rate for the Mack development model.

n' = the developer selectivity.

α' = a simplification parameter.

M_{th} = the point of inflection on the development rate versus PAC concentration curve.

$R_{bulk,MACK}$ = bulk development rate for the Mack development model.

R_{sb} = the ratio of the surface development rate to bulk development rate for fully exposed resist.

L = the characteristic length of the surface development rate inhibition.

m' = the molar PAC concentration after pre-bake.

M' = the normalized PAC concentration after pre-bake.

K_t = a rate constant for a given temperature in the pre-bake model.

t_b = pre-bake time.

A_r = Arrhenius coefficient for the pre-bake model.

E_a = activation energy for the pre-bake model.

z' = the interim depth for the PEB model.

D = the diffusion coefficient for the PEB model for a given temperature.

t_{PEB} = the PEB bake time.

M^* = the modified PAC concentration after PEB.

Δthick = the width of the resist sublayer.

D_o = the Arrhenius coefficient for the PEB model.

E_{PEB} = activation energy for the PEB model.

T_r = transmitted light intensity.

W = the total resist thickness.

ϵ_o = the dielectric constant.

$R_{inhibit}$ = the modification factor for the surface development rate inhibition.

S = the interference signal.

d_o = the instantaneous resist thickness.

1.0 ABSTRACT

In order to truly represent photolithography through simulation, the exposure, bake and development models and model parameters must be accurate. Models for the pre-bake, exposure, post-exposure/pre-development bake, and the development have been developed and are available with most commercial simulators [1-5]. The extraction of the exposure parameters has been established [1-3]. However, the extraction of the bake and development model parameters have been subject to question [6-13] given the immersion type development that has been required for the measurement of the development rate and henceforth the extraction of these parameters.

A new approach for the measurement of the in-situ development rate is presented. This method uses a circularly polarized tungsten light source to generate interference curves at eight different wavelengths. Patterned wafers were sampled individually as they spun on the development module of a wafer-track. Previous work has demonstrated the robustness of this technique to ambient light, developer spray, bubbles in the developer and the red cloud effect [14]. The Marquardt-Levenberg nonlinear regression algorithm was then used to determine the development rate from the eight interference curves.

Using the models for the pre-bake, exposure, post-exposure bake, and development [1,2,4,5], a one-dimensional photolithography simulator was written in C. With this simulator, it was demonstrated that the exposure and development parameters were highly correlated with each other in terms of the development rates.

Next, the model parameters were extracted for Shipley 812 resist with Shipley MF312 developer. Development rates for exposures of 66, 90 and 114mJ/cm^2 were measured. The model parameters $A=0.581\mu m^{-1}$, $B=0.082\mu m^{-1}$, $C=0.013cm^2/mJ$, $R_1=25.559\mu m/min$, $R_2=10.451\mu m/min$, $R_3=1.879$, $R_4=0.112$, $R_5=1.586$, $R_6=0.000\mu m$, and sigma=$0.0016\mu m$ were extracted. A comparison of simulated data using the extracted model parameters with the measured data demonstrated the need for model adequacy checks.

2.0 INTRODUCTION

2.1 Introduction

As the drive for smaller line-width geometries at the expense of increasing cost and process development time continues in semiconductor manufacturing, the value and convenience of accurate, process specific modeling parameters is becoming increasingly vital. Time and money invested up-front in the determination of the model parameters can be realized and compensated in subsequent process optimizations or process trouble-shooting.

Figure 1 contains a cause and effect diagram (a.k.a. Ishikawa diagram) [15] for photolithography. Factors that effect the desired resist line quality are categorized in this diagram in a hierarchical structure. In order to consistently achieve high quality resist lines and spaces, the factors listed must be understood, if not controlled. Here, the factors have been segregated into four areas: resist coat, exposure and development and the ambient conditions. Generally speaking all of the factors can be controlled to a large degree, but more specifically the ambient conditions are typically more difficult to control. These factors may be labeled as covariates; factors that cannot be controlled but can be measured, monitored and perhaps compensated. Most of the

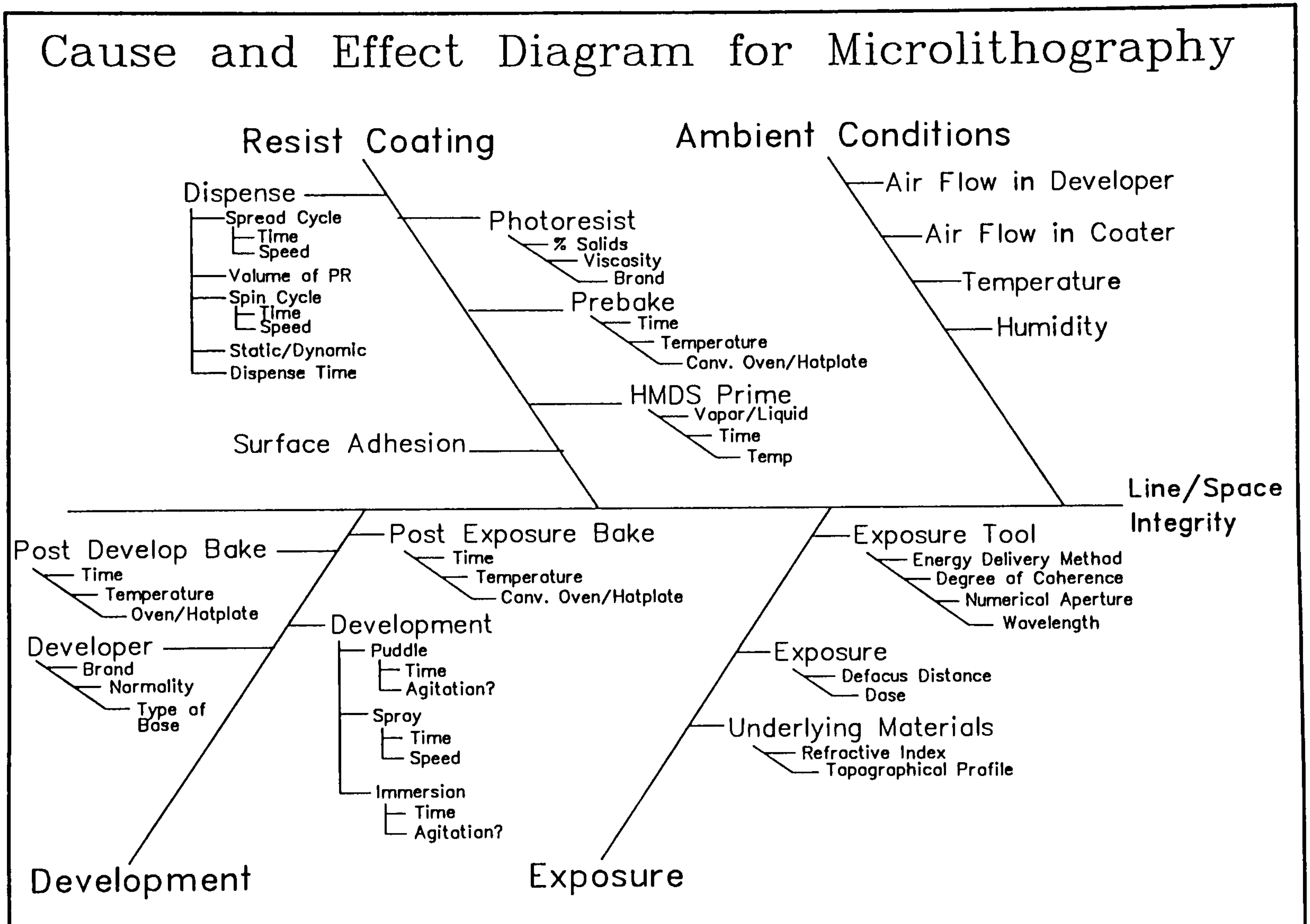

Figure 1 : Cause and effect diagram for microlithography.

factors, such as chemistry and exposure wavelength can be controlled but are usually not varied in the fabrication facility in order to minimize the process development cycle time. Other factors such as the exposure time, bake times and temperatures are frequently optimized. Hence, accurate models and model parameters that relate these factors to measures of the resist quality are desired.

Traditionally, the nature of photolithography simulation has been descriptive rather than predictive [16]. Often times, the difficult and involved parameter extraction techniques prohibit process specific parameter extraction and the simulation is based upon a set of non-representative values [6-13]. Often times the validity and accuracy of these parameters are questionable but they are the best estimates available for simulation.

In the case of the photolithographic transfer of a desired pattern onto the wafer surface, resist and development parameters have been obtained using the Perkin Elmer Development Rate Monitor (DRM) [6-13]. The DRM requires an immersion development. This detracts from the validity of these parameters since production wafer processing is usually performed individually on a wafer track with a dispense or spray type development.

This thesis proposes an alternative technique for process specific parameter extraction for photolithography modeling. First, some background on photolithography chemistry is presented, current models are reviewed, and prior parameter extraction techniques are examined. Next, the development of a one dimensional photolithography simulator is derived. This simulator facilitated an evaluation of the correlation among model parameters. This evaluation reduced the parameter set to a fundamental and independent set of modeling parameters for extraction.

With this knowledge, the parameter extraction was applied to Shipley 812 photoresist. A technique for the in-situ measurement of development rate on a patterned wafer as it is processed on a wafer track is presented. This technique allowed for the process specific parameter extraction using non-linear regression.

Finally, a comparison of the simulated development rate using the extracted model parameters and the development rate measured from the wafers demonstrated the success of this approach. Further comments on the improvement of this technique are added for future development.

3.0 THEORY

3.1 Photolithography Processing

3.1.1 Introduction

During the course of semiconductor manufacturing, the defining patterns of the integrated circuit must be transferred unto the wafer surface [17]. In order to accomplish this, a photosensitive / etch-resistant material called photoresist is spin-casted onto the wafer. The defining pattern is then transferred from a template or mask to the wafer surface via an exposure to light. Although there are many types of resists, each of which may have unique development contrast phenomenon, this thesis has been limited to the case of conventional positive resist.

3.1.2 Conventional positive photoresist processing

The most common photoresist material used in microlithography today is a diazonaphthoquinone (DNQ) / novolac combination. This resist is comprised of three principle materials [17,18]. The first of these is the (DNQ) photo-active compound (PAC) which is responsible for the chemical alteration in the resist upon exposure to light. The second is the novolac (cresol formaldehyde) binding polymer used to provide the desirable physical attributes of the resist. The third is the casting solvent. Two of the more common casting solvents are ethyl cellosolve acetate and diglyme. This solvent allows the resist to be spin-cast onto the wafer surface and controls film thickness through viscosity.

Typical photolithography processing begins with the resist deposition. After depositing some quantity of resist on the wafer surface, the wafer is spun at a spin speed ranging from 2000 to 6000 RPM to obtain a coating that is uniform in thickness. Casting solvent is driven out of the resist with a pre-exposure bake (a.k.a. pre-bake or soft bake) on a hotplate or in a convection oven.

During the exposure step the photosensitive, the DNQ molecule forms a ketocarbene as below.

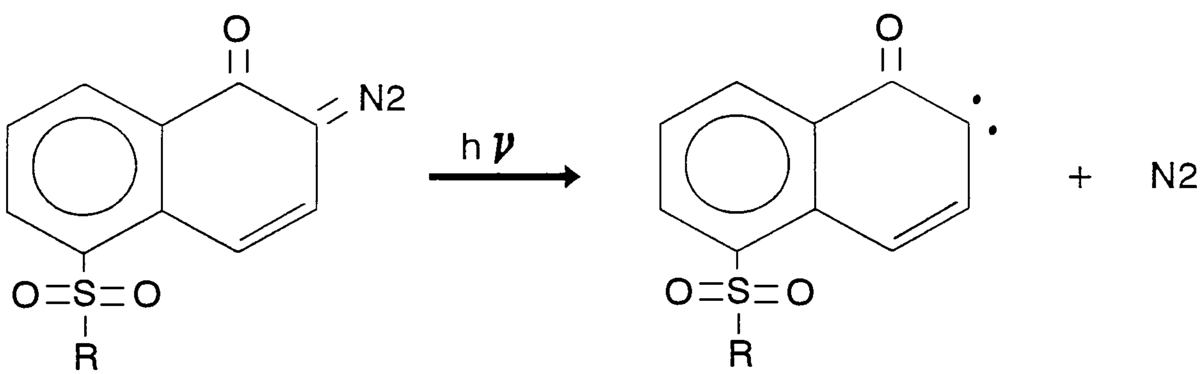

From the intermediate carbene, the molecule then undergoes a Wolff rearrangement to produce a ketene. The ketene then combines with water residing within the resist to form a base soluble indene carboxylic acid as below.

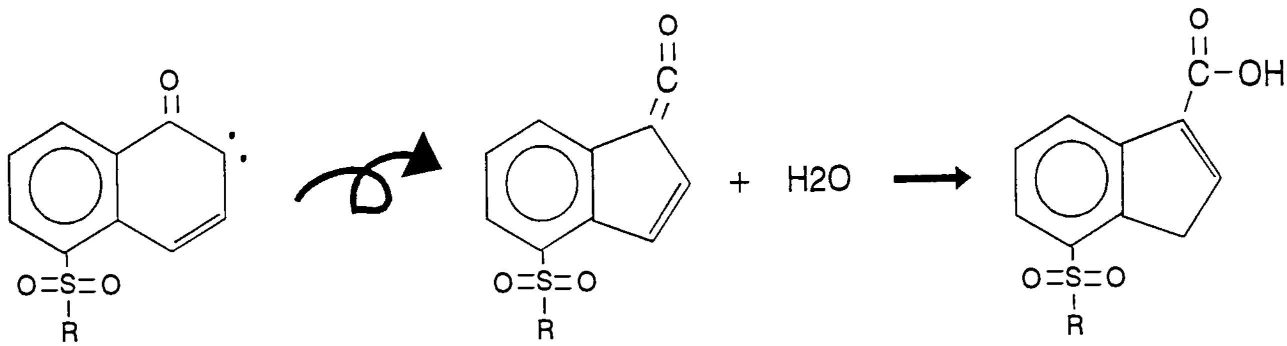

The DNQ/novolac combination is enhanced by two important effects. The first of these is a synergistic effect between the novolac binding material and the DNQ sensitizer. When the novolac binder is in close proximity to an unexposed DNQ molecule, the two form a material that far less soluble in the base developer than is otherwise observed for either of the two molecules alone. On the other hand, the novolac binder in combination with the exposed DNQ leads to a material that is far more soluble in the base developer than either of the two materials alone. Hence the solubility differential is enhanced on both sides of the exposure spectrum.

The second effect is known as bleaching. As a result of the resist exposure, the imaginary component of the refractive index of the resist decreases in magnitude so as to become less attenuative to the exposing light as the exposure progresses. At the beginning interval of time during the exposure, the top most portions of the resist receive the most energy on average while the exposure energy near the bottom of the resist is less on average due to the attenuation of the impinging light. However, as time progresses, the uppermost layers of resist become more transparent due to the bleaching effect and an effective aperture is formed at the top of the resist. The bottom layer of resist now encounters a larger percentage of the impinging light than it did at the beginning of the exposure. Hence, an enhanced sidewall in a positive resist line is observed.

Inherent to all transmissive thin film materials is the formation of standing waves due to constructive and destructive interference throughout the thin film during exposure. In the case of photoresist, this phenomenon has become known as the standing wave effect. This is an undesirable effect since the instantaneous development rate exhibits an oscillatory variation and as a result, the resist sidewalls after development are oscillatory in nature as a function of depth in the resist. In order to combat this effect Walker [19] has proposed the implementation of a post-exposure / pre-development bake (PEB). In theory, this bake allows the PAC to diffuse from areas of high concentration to areas of lower concentration. Although there are some second-order chemical reactions that result from this bake, the result by and large is to smooth over the sinusoidal nature of the resist sidewall.

At this point the resist is ready for development. Developers for DNQ/novolac resist are alkaline based. For areas of higher exposure, the concentration of the PAC has lowered from its original quantity and is replaced by the indene-carboxylic acid (ICA). Hence the dissolution rate in this area is enhanced in comparison to the unexposed or partially exposed regions and the desired pattern is resolved.

In order to prepare the resist for subsequent process steps such as wet chemical etches, dry plasma etches, or ion implantation, the wafer is baked once again. This bake is the most intense of the three bakes. The bake is intended to drive off much of the remaining solvents, to flow the resist surface, reducing pinholes and to form a thermoset network through thermal crosslinking.

3.2 Photolithography Modeling

3.2.1 Introduction

In general, modeling of exposure must include the light intensity calculations for all three dimensions. In the case of projection printing, the three dimensional image may be suitably approximated by the product of the aerial intensity and the intensity as a function of depth in the resist thin film [20]. Numerically stated,

$$I(x,y,z) \approx I(x,y)\,I(z) \quad \text{EQN 1}$$

where

I = the light intensity,

x and y = orthogonal axes parallel to the resist surface, and

z = the axis into the resist.

This allows for the convenient separation of models. I(z) is a function of the photoresist chemistry, the optical properties of the resist, and the development chemistry. I(x,y) on the other hand, primarily depends on imaging factors such as the imaged geometry, the exposing wavelength, the numerical aperture of the objective lens, the defocus distance and the degree of coherence.

In this thesis, the topic of concern was the parameter extraction for the modeling of the image after development as a function of depth. Hence, models used to simulate I(z) and the development rate, R(z), were of primary interest. In addition, the modeling of the pre-exposure and the post exposure/pre-development bake must also be included.

3.2.2 Exposure modeling

The model used for the exposure of conventional positive photoresist was proposed by Dill et al. [1-3] and is generally accepted as being a valid description of the dynamics of the resist's optical behavior during exposure. This model is based on the absorption of the three major components of the photoresist: the photo-active compound (PAC), the indene carboxylic acid (ICA), and the novolac binder resin. The optical absorption of the casting solvent was neglected.

Dill describes the change in light intensity as a function of depth in the resist as,

$$\frac{\partial I(z,t)}{\partial z} = -I(z,t)\,[a_1 m_1(z,t) + a_2 m_2(z,t) + a_3 m_3(z,t)] \qquad \text{EQN 2}$$

where

I = the light intensity

z = the vertical distance in the resist

t = the time

a_1 = absorption coefficient for the PAC

a_2 = absorption coefficient for the ICA

a_3 = absorption coefficient for the novolac binder

m_1 = the molar concentration of the PAC

m_2 = the molar concentration of the ICA

m_3 = the molar concentration of the novolac binder.

The transition from the PAC to the ICA is described as a first order differential relationship, namely,

$$\frac{\partial m_1(z,t)}{\partial t} = -m_1(z,t)\, I(z,t)\, C \qquad \text{Eqn 3}$$

where

C = the fractional decay rate of the PAC per unit intensity of light.

The boundary conditions,

$I(0,t) = I_o$ = light intensity at the resist surface,

$m_1(z,0) = m_o$ = the initial pac concentration

$m_3(z,t) = m_3$ = the constant molar concentration of the novolac binder

$m_2(z,t) = m_o - m_1(z,t)$ ==> PAC transforms to ICA, are substituted into equation 2 to yield,

$$\frac{\partial I(z,t)}{\partial z} = -I(z,t)\,[m_1(z,t)\,(a_1-a_2)+a_3m_3+a_3m_o] \qquad \text{EQN 4}$$

For simplicity, the PAC concentration is normalized with respect to its initial value and is defined with the variable, M(z,t). In addition the "a" parameters are redefined as follows,

$A=(a_1-a_2)m_o$ = the dynamic component of the extinction coefficient,

$B=(a_3m_3+a_2m_o)$ = the static component of the extinction coefficient,

C=C.

This allows equations 2 and 3 to rewritten as,

$$\frac{\partial I(z,t)}{\partial z} = -I(z,t)\,[AM(z,t)+B] = -I(z,t)\,\alpha \qquad \text{EQN 5}$$

and

$$\frac{\partial M(z,t)}{\partial t} = -I(z,t)\,M(z,t)\,C \qquad \text{EQN 6}$$

where

α = the dynamic attenuation coefficient.

Equations 5 and 6 become the working equations from which positive photoresist is simulated. Both A and B have units of inverse distance and C has units of area per energy. It is instructive to note the initial conditions,

$$\frac{\partial I(z,t)}{\partial z}=-I(z,t)\,[AM(z,t)+B] \qquad \text{EQN 7}$$

$$\frac{\partial M(z,t)}{\partial t}=-I(z,t)\,M(z,t)\,C \qquad \text{EQN 8}$$

and the boundary conditions at the resist surface,

$$I(0,t)=I_o \qquad \text{EQN 9}$$

$$M(0,t)=\exp(-I_oCt) \qquad \text{EQN 10}$$

The attenuation coefficient, α, is directly related to the imaginary component of the refractive index by the relationship,

$$k=\frac{\alpha\lambda}{4\pi} \qquad \text{EQN 11}$$

where

k = the attenuation coefficient,

lambda = the wavelength of the impinging light.

Babu and Barouch [21,22] propose a closed form solution for the case of a non-reflective substrate, however, in terms of simulation, equations 5 and 6 cannot be placed into a convenient closed-form.

However, with the aid of a computer, a numerical solution can be computed with relative ease by replacing equations 5 and 6 with their difference equation equivalents,

$$I(z_i,t_j)-I(z_{(i-1)},t_j)=-I(z_{(i-1)},t_j)\,[AM(z_{(i-1)},t_j)+B] \qquad \text{EQN 12}$$

$$M(z_i,t_j)-M(z_i,t_{(j-1)})=-I(z_i,t_j)M(z_i,t_j)C \qquad \text{EQN 13}$$

where

i = the integer count in the depth increment and

t = the time increment.

The approach used in the numerical approximation assumed that the photoresist thin film is comprised of many individual layers of photoresist, each having a unique complex refractive index that is constant within the layer. The primary restriction with this approximation is that the thickness for each of the layers must be much less than one half of the wavelength of the exposing light within the resist layer or,

$$z_i - z_{(i-1)} << \frac{\lambda}{2n} \qquad \text{EQN 14}$$

where

n = the magnitude of the refractive index of the photoresist.

Restrictions on the separation of the time increments needed to be quantitatively evaluated.

3.2.3 Development modeling

Three models for the development of conventional positive photoresist were examined. The first of these was developed by Dill [3] and accompanied the photoresist exposure model. This model was simply an quadratic empirical fit with a log transform of the rate data that allowed Dill to realize some modeling ability. Since it was strictly an empirical relationship, the validity of this model outside of the explored regime is weak and it lends little to the physical understanding of the development mechanism.

A second model was proposed by Kim et al. [23] Kim recognized a retardation in the development rate of the photoresist near the surface. The model estimates both the bulk development rate as a function PAC concentration and depth, and a model that accounts for the surface development rate inhibition. The equation for the bulk development rate is,

$$R_{bulk}(z,t) = \frac{1}{\dfrac{1-M(z,t)\exp(-R_3(1-M(z,t)))}{R_1} + \dfrac{M(z,t)\exp(-R_3(1-M(z,t)))}{R_2}}$$

EQN 15

where

R_1 = the development rate for fully exposed photoresist (M=0.0)

R_2 = the development rate for unexposed photoresist (M=1.0)

R_3 = a sensitivity parameter.

The units for R_1 and R_2 are distance per time and R_3 is unitless. The bulk development rate is then modified near the surface such that the overall development rate becomes,

$$R(z,t)=R_{bulk}(z,t)\,[1-(1-R_5+(R_5+R_6)M(z,t))\exp(\frac{-z}{R_4})] \qquad \text{EQN } 16$$

where

R_5 = the ratio of the surface development rate to the bulk development rate for fully exposed resist (M=0.0)

R_6 = the ratio of the surface development rate to the bulk development rate for no exposure (M=1.0)

R_4 = the characteristic length for the surface development rate inhibition.

The units for R_4 are inverse distance and R_5 and R_6 are unitless.

A third model, developed by Mack, [24] is a less empirical, physically based relationship. Very similar to an etch model, this model is based upon three mechanisms. The first mechanism is the diffusion of the unreacted developer in the bulk solution to the developer/resist interface and is described by a diffusion rate equation. The second mechanism is the reaction of the developer to the resist and is described by a reaction rate equation. A third mechanism, the diffusion of reacted developer away from the developer/resist interface is considered to be negligible.

Setting the rates of the two mechanisms equal to each other, the relationship,

$$R_{bulk,MACK}(z,t)=R_{max}\frac{(\alpha+1)\,(1-M(z,t))^{n'}}{\alpha\,(1-M(z,t))^{n'}}+R_{min} \qquad \text{EQN 17}$$

is realized, where

R_{max} = the maximum development rate,

R_{min} = the minimum development rate,

n' = the developer selectivity.

α' is simplification parameter which is defined as,

$$\alpha=\frac{(n'+1)\,(1-M_{th})^{n'}}{(n'-1)} \qquad \text{EQN 18}$$

where M_{th} is the point of inflection on the development rate versus PAC concentration curve or simply,

$$\frac{\partial^2 R}{\partial M^2}\Big|_{M_{th}}=0.0 \qquad \text{EQN 19}$$

Surface rate inhibition can be accommodated in the Mack development model in a manner similar to the Kim model by the insertion of an exponentially decaying function of the inhibition as a function of depth. The full Mack model that results is,

$$R(z,t) = R_{bulk,MACK}(z,t)\,(1-(1-R_{sb}\exp(\frac{-z}{L}))) \qquad \text{EQN 20}$$

where,

R_{sb} = the ratio of surface development rate to bulk development rate for fully exposed resist, and

L = the characteristic length of the surface development rate inhibition.

Together, equation 17, 18, and 20 form the Mack development rate model.

Other models such as the one proposed by Trefonas [16] and the one proposed by Robertson et al. [25] have not found the wide acceptance that aforementioned models have and hence were not considered.

For the purpose of this research, a process specific photolithography model was desired. As such, only the parameters for the Kim development model were extracted. However, one could readily extract the Mack development model parameters by substituting the Kim model with the Mack model.

3.2.4 Pre-exposure and post-exposure/pre-development bake modeling

A model for the pre-exposure bake (prebake) has been proposed by Mack [4]. In this model, the prebake conditions are viewed as being similar to an ultraviolet exposure where the exposure of the PAC to heat frees the nitrogen to form an intermediate ketene. It is hypothesized that the intermediate ketene then transfers into one of two possible molecules of which the selection between the two depends on the availability of water in the resist. The first product is the formation of the indene carboxylic acid discussed in section 2.2. As was shown, a water molecule is required for the formation of the ICA. In the absence of water, the second product is a crosslink of the ketene with the novolac binder to form an ester as below.

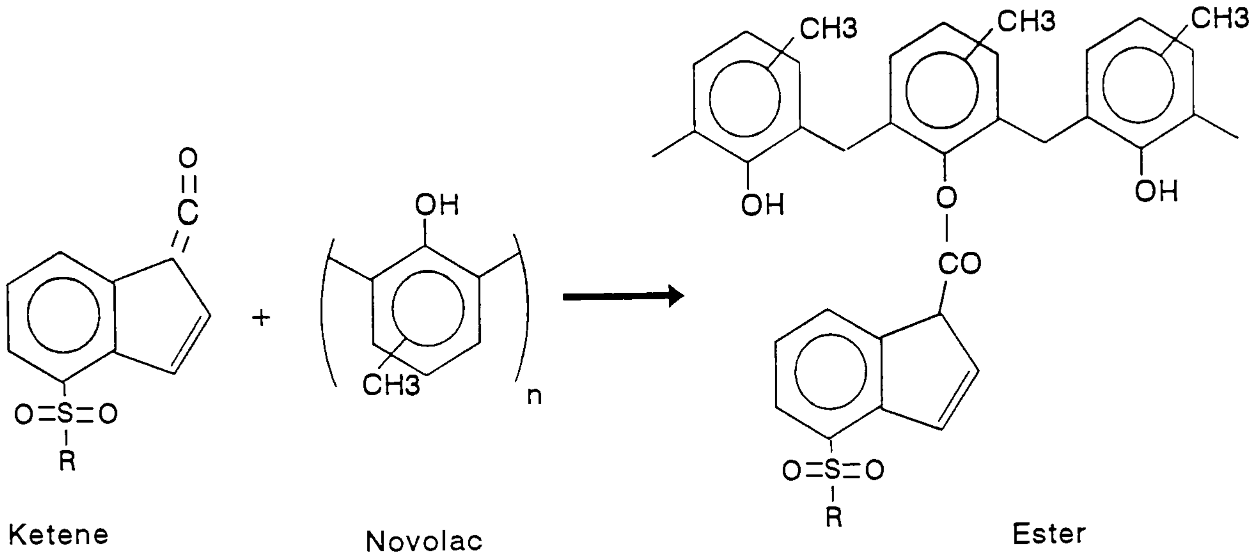

The reduction of photosensitivity due to prebake conditions is described as the first order differential equation,

$$\frac{\partial m'(z,0)}{\partial t} = -K_t m'(z,0) \qquad \text{EQN 21}$$

where

$m'(z,0)$ = the molar PAC concentration after prebake

K_t = a rate constant for a given temperature.

The solution to the first order differential equation above is the exponential,

$$m'(z,0) = m(z,0)\exp(-K_t t_b) \qquad \text{Eqn 22}$$

or equivalently,

$$M' = \exp(-K_t t_b) \qquad \text{EQN 23}$$

where

$m(z,0)$ = the molar PAC concentration before prebake

t_b = prebake time.

The rate constant, K_t, is related to the bake temperature via the Arrhenius equation,

$$K_t = A_r \exp(-E_a/RT) \qquad \text{EQN 24}$$

where

A_r = the Arrhenius coefficient,

E_a = the activation energy,

R = the universal gas constant,

T = the temperature.

In essence the bake modified PAC concentration alters the A and B parameters via the relationship,

$$A = A_{NB} M', \qquad \text{EQN 25}$$

$$B=B_{FB}-(B_{FB}-B_{NB})M' \qquad \text{EQN 25}$$

where the subscripts, NB and FB denote no-bake and full-bake respectively. Since the PAC concentration is normalized, the PAC concentration throughout the resist film prior to exposure but after the prebake remains at a value of 1.0.

The implementation of a post-exposure / pre-development bake (PEB) as an effective means to reduce the manifestation of the standing wave effect on the resist line integrity was first proposed by Walker [19]. A model based upon diffusion principles to describe the PEB has been proposed by Mack [5]. This model is essentially a smoothing of the PAC concentration profile after exposure. This model is presented without derivation as,

$$M^{*}(z)=\frac{1}{\sqrt{2\pi\sigma^{2}}}\int_{-\infty}^{+\infty}M(z')\exp\left(\frac{-(z-z')^{2}}{2\sigma^{2}}\right)dz' \qquad \text{EQN 27}$$

and

$$\sigma=\sqrt{2Dt_{PEB}} \qquad \text{EQN 28}$$

where

$M^*(z)$ = the modified PAC concentration after PEB,

σ = the PEB diffusion length constant, or equivalently, a smoothing factor,

z = the vertical position for which the PAC concentration is being computed,

z' = the interim depth for the integral,

D = the diffusion coefficient of the PAC in the resist at a given temperature,

t_{PEB} = the PEB time.

For numerical evaluation of equation 27, the resist layer may be divided into sublayers and the integral may be replaced by a summation,

$$M^*(z_j)=\frac{1}{\sqrt{2\pi\sigma^2}}\sum_{i=-\infty}^{\infty} M(z')\exp\left(\frac{-(z_i-z_j)^2}{2\sigma^2}\right)\Delta thick \qquad \text{EQN 29}$$

where

i = the count for the summation,

j = the count for the sublayer

and the restriction that (Δthick) < 3σ. The quantity (Δthick) is the thickness of each sublayer. $M^*(z)$ in equation 29 replaces M(z,t) in equations 15 and 16.

Just as the prebake rate constant, the diffusion coefficient, D, is related to the PEB temperature by the Arrhenius equation,

$$D=D_o\exp\left(\frac{-E_{PEB}}{RT}\right) \qquad \text{EQN 30}$$

where

D_o = the Arrhenius constant,

E_{PEB} = the activation energy,

R = the universal gas constant,

T = the temperature.

3.3 Conventional Parameter Extraction Techniques

3.3.1 Introduction

Much of the work on exposure modeling and parameter extraction was covered by Dill in 1975 [1-3]. However, the extraction of development model parameters has been questionable, given the technique used for the measurement of the development rates.

3.3.2 Exposure parameter extraction

The work performed by Dill and his coworkers that outlined the models for the exposure of conventional positive resist, also described a method by which the model parameters could be extracted [3].

Dill proposed that a specially prepared substrate be fabricated that was transparent but matched well optically (similar refractive index) with the resist so as to minimize the reflection of the resist substrate interface. After coating this substrate with the resist under investigation, the substrate is placed in the path of projection system with a calibrated incident light flux meter below the substrate. When the shutter of the projection system opens at t=0.0 sec., the transmitted light through the resist coated substrate is sampled at some frequency and the transmittance versus time is plotted. The plot of transmittance is fairly linear for small values of t but as time progresses, the transmittance asymptotically approaches some maximum value represented by $T_r(\infty)$.

The initial transmittance, at t=0.0 sec., is indicative of the attenuation of the incident light as it passes through the resist when M(z,t)=1.0 and α=(A+B). At t=∞, most of the resist has completely bleached and $\alpha \approx$B. Using the values of $T_r(\infty)$, $T_r(0)$, and the gradient of the transmittance with respect to time at t=0.0, Dill derived the equations,

$$A=\frac{1}{W\ln\left(\frac{T_r(\infty)}{T_r(0)}\right)} \qquad \text{EQN 31}$$

$$B=\frac{-1}{W}\ln(T_r(\infty)) \qquad \text{EQN 32}$$

$$C=\frac{A+B}{AI_oT_r(0)\,[1-T_r(0)]}\,\frac{\partial T_r(0)}{\partial t} \qquad \text{EQN 33}$$

for the computation of A, B, and C where

W = the resist thickness,

I_o = the light intensity at the resist/air interface.

3.3.3 Development parameter extraction

Most of the published work on the extraction of lithographic modeling parameters revolves around the Perkin-Elmer Development Rate Monitor (DRM) and its associated software, DREAMS [6-13]. Three of the faults that have plagued this tool are the required special wafer preparation, inherent noisy signals and the requirement that the wafer must be immersed in a developer bath in order to monitor the development mechanisms. DREAMS calculates the development rate versus time and depth. Model parameter extraction was not contained within, and therefore was left to be calculated by some post processing program.

The DRM requires a one dimensional array of open field exposure doses on a single wafer. This array of exposure doses requires special stepper programming and an open field exposure.

The noisy interference signals have be lessened by a couple of methods. Flanner [7] attributed much of the noise in the measured interference signals to the oscillatory swings in the development rate due to the standing wave effect. In order to combat this, a silicon nitride / tungsten / silicon dioxide sandwich was designed to act as an effective antireflective coating during exposure. This special wafer processing requires the access to a number of additional wafer processing tools and further complicates the process of extracting model parameters. Several authors [7,13] have removed some of the noise by removing anomalous spikes in the data and then smoothing over the curve by substituting a moving average for the interference curve data.

The third and most concerning problem of the DRM was the immersion development. Most lithography processing, and especially production processing, today is carried out on a "track". A track contains all of the chemical processing steps including resist deposition and development. Wafers are processed individually and serially, and receive a new batch of chemicals for each wafer. In addition, physical phenomenon, such as agitation are decidedly different. Hence, one has little reason to expect the model parameters extracted from the DRM to be much better than a first order estimation.

4.0 METHOD

4.1 A One-Dimensional Photolithography Simulator

4.1.1 Introduction

Paramount to the development of a parameter extraction technique is the knowledge that the proposed technique adequately converges on the appropriate set of values. Using the existing models for which the parameters are to be extracted along with an arbitrary, though realistic set of model parameters, the measured data may be artificially generated via simulation. Based upon this, the proposed parameter extraction technique should derive the original set of parameters or in the least should demonstrate the shortcomings of the parameter extraction technique under investigation. It is for this reason that a one - dimensional lithography simulator was written.

Commercially available simulators such as TMA's Depict, Finle Technology's Prolith, and SAMPLE through UC Berkeley can be used to generate the development rate and PAC concentration as a function of depth in the resist. However, in order to gain a full understanding of the simulation mechanisms and in particular, the treatment of boundary conditions, an independent one-dimensional photolithography simulator was developed, based upon existing models [1-3,4,5,23]. In addition, appropriation of numerical values of the PAC concentration versus depth can consume considerable post-processing time and effort when using the commercial software.

4.1.2 Model development

The development of the simulator was approached in two stages. The first was to implement the exposure models proposed by Dill. Since the simulation of the exposure DNQ resist is achieved through the two first order simultaneous differential equations in equations 5 and 6, a closed form, analytic solution for the exposure cannot be obtained.

However, if the resist thin film is divided into a number of individual resist thin films, each of which maintains a unique, yet constant PAC concentration, equation 5 can be suitably approximated by the equation,

$$I_j - I_{(j-1)} = (AM_j + B)\,(Z_j - Z_{(j-1)}) \qquad \text{EQN 34}$$

where j is the integer count of the resist sublayer. Similarly, equation 6 is approximated by

$$M_{(k-1)}(z,t)-M_k(z,t)=-I_k(z,t)M_k(z,t)C(t_k-t_{(k-1)}) \quad \text{EQN 35}$$

where

k = the count in the time increment.

The Mack prebake model manifests itself as a modification of the Dill A and B exposure parameters. As such, the prebake model requires no special consideration.

The Mack post-exposure / pre-development bake(PEB) model is essentially a smoothing function, the influence of which closely resembles a normal distribution centered about the sublayer under consideration. Numerical evaluation of the PEB model was obtained by summing over a large number of sublayers such that the influence of a given sublayer near the outer limits of the summation was relatively small.

Boundary conditions were an issue for those sublayers for which the PEB smoothing influence extended beyond the uppermost and lowermost sublayers. The smoothed PAC concentration for these layers were calculated by using the appropriate influence in combination with the PAC concentration for the sublayer under consideration.

Once the PAC concentration has been computed as a function of depth in the resist film, simulation of the development rate as a function of depth and time was straightforward. Both Mack's and Kim's development models are provided in a closed form. Given the sets of development parameters, for both respective models, calculation of the development rate was simply a matter of exercising the model equation.

Since the PAC concentration was only provided versus depth in the resist computation of the development rate versus time must depend on the development rate. Using the prior assumption that the development rate within each sublayer of resist film is constant, the time consumed for the development of each sublayer is simply the sublayer width divided by the sublayer development rate.

4.1.3 A two-port network approach

Calculation of the exposure in each individual sublayer was developed with a two port network (two light inputs and two light outputs) approach. It was assumed that the light was incident at a normal angle. Taking an individual sublayer, radiation is incident upon this layer from both sides as is shown in figure 2. On the left of this figure, represented by the label "E1", represents the initial light source, and from even numbers of reflections. The label "E" denotes the electric field at a given location. From the right side, the radiation enters the layer from odd numbers of reflections between sublayers and the substrate and is labeled with "E2". Similarly, light is output from the layer on both the left and right sides as is shown by labels "E3" and "E4". It was assumed that the optical properties, in specific, the refractive index of each sublayer was constant throughout the sublayer but was allowed to vary between sublayers. In this manner, variation in the light intensity due to the standing wave effect and attenuation of the light source as a function of depth in the resist thin film were properly accommodated as the thickness of the sublayer decreases.

Using a two port network approach, one can solve for the two inputs and the two outputs for all of the sublayers simultaneously. It was known from the Fresnel equations for normal incidence, that the reflection coefficient and the transmission coefficients for a given interface are related to the refractive indices [26] as,

$$r_i = \frac{n_{(i-1)} - n_i}{n_{(i-1)} + n_i} \qquad \text{EQN 36}$$

$$t_i = \frac{2n_{(i-1)}}{n_{(i-1)} + n_i} \qquad \text{EQN 37}$$

where

r = the reflection coefficient

t = the transmission coefficient

n = the complex refractive index

i = the increment of the sublayer.

As is shown in figure 3, the sublayers may be placed together in series, with an ambient or air interface to the left and the substrate interface to the right. Based upon the initial values of A and B in equations 5 and 11 we can find the refractive index of all of the sublayer prior to exposure. The electric field at the resist/air interface may be calculated from the exposure dose and the length of the time increment. The dose, given in units of energy per area was divided by the length of the time increment to give the intensity. The intensity is related to the electric field via the relation,

$$E = \sqrt{\frac{2I}{c\epsilon_o}} \qquad \text{EQN 38}$$

where

E = the electric field

I = the light intensity

c = the speed of light = 3.0e8 m/s

ϵ_o = the dielectric constant = 8.85e-14 F/cm.

Coupled with the complex refractive index of the silicon substrate[1], the refractive index of the air[2], and the electric field intensity at the resist/air interface, the electric field entering the substrate may be computed for the first increment of time. It was assumed that the substrate was sufficiently thick and the attenuation constant sufficiently large in the substrate so that the electric field entering the bottom resist sublayer from the substrate was negligible. Since the value of the electric field in the substrate is known for both directions, these values may be used to calculate the electric field for each of the sublayers in succession.

Once all four components of the electric field are known for a given sublayer, they may be added and the magnitude calculated for that sublayer. The electric field is converted

---

[1]The complex refractive index for silicon at G-line (435.8nm) is 4.73-j0.138.

[2]The refractive index for the ambient was assumed to be 1.0+j0.0.

back to intensity using equation 38 since the Dill exposure model in equations 5 and 6 use intensity. Using equation 34, the change in the PAC concentration for the sublayer may be calculated and used for the subsequent time increment calculation.

The simulation of the prebake and PEB are also added to the simulation by placing equations 23, 24, 25, 26 and 29 into their appropriate chronological locations. After having calculated the PAC concentration for the entire exposure, the development rate and time for development may be calculated by direct placement into equations 15 and 16 or equations 17, 18 and 20.

See appendix A for the computer source code in "C" for the one dimensional simulation of the prebake, exposure, PEB, and development of DNQ resist.

4.1.4 Approximation Adequacy Check

At this point it was necessary to determine what increments of time and of depth were adequately small to maintain validity in the approximations of equations 34 and 35. Clearly, as the number of sublayers increases, and as the number of time increments increases, the difference equations given in equations 34 and 35 should asymptotically approach the differential equations of equations 5 and 6. At the same time, as the number of time and depth increments increases, the demands of computer resources will increase geometrically. In order to maintain a sufficient compromise, a value of Δt and of Δx were chosen so as to adequately satisfy the approximation conditions and hence were assumed to be the true exposure conditions.

As a means of determining adequate increments of time and depth, excessively large values for the number of time increments and depth increments were chosen and simulated. The exposure time was divided into 500 increments and the thickness was divided into 2500 increments. This simulation is assumed to represent the true, continuous calculation of the PAC concentration. Next, replicate simulations were performed with the number of time increments and the number of depth increments varying independently from one to the true conditions. The sum of square errors(SSE) in the PAC concentration were calculated and plotted versus the respective increment factor for some of the simulated conditions as is shown in figures 4 and 5. Clearly, as the number of increments increase, the SSE asymptotically approaches zero and may be considered to represent the true condition. Since the computational expense was small, the number of time increments were chosen to be 50 and the number of depth increments were chosen to be 250, both well in excess of the minimum requirements.

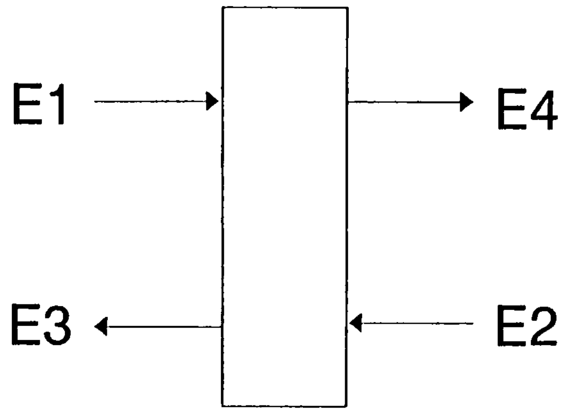

Figure 2 : Two - port electric field diagram.

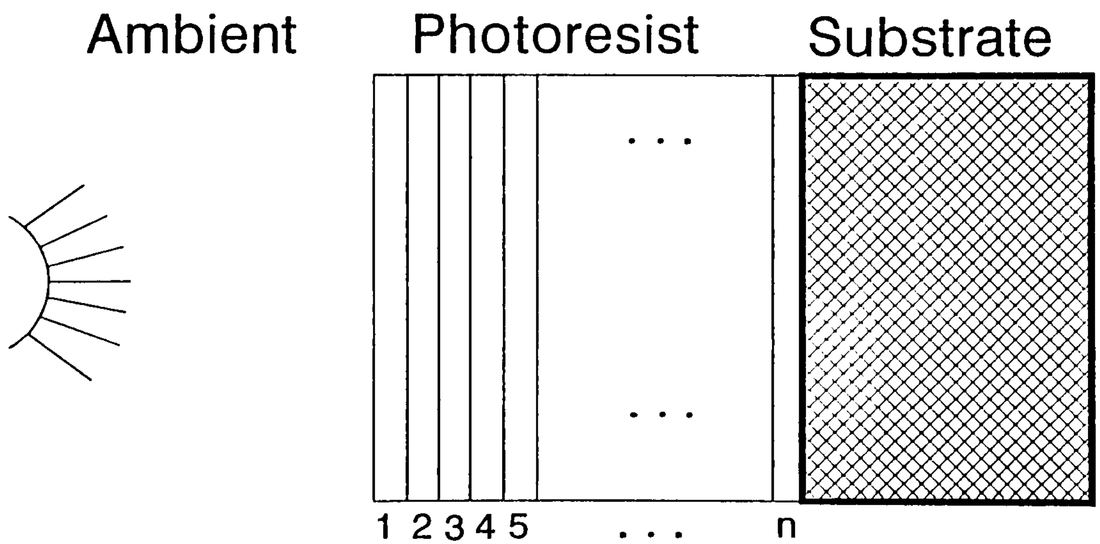

Figure 3 : Two - port network with resist sublayers.

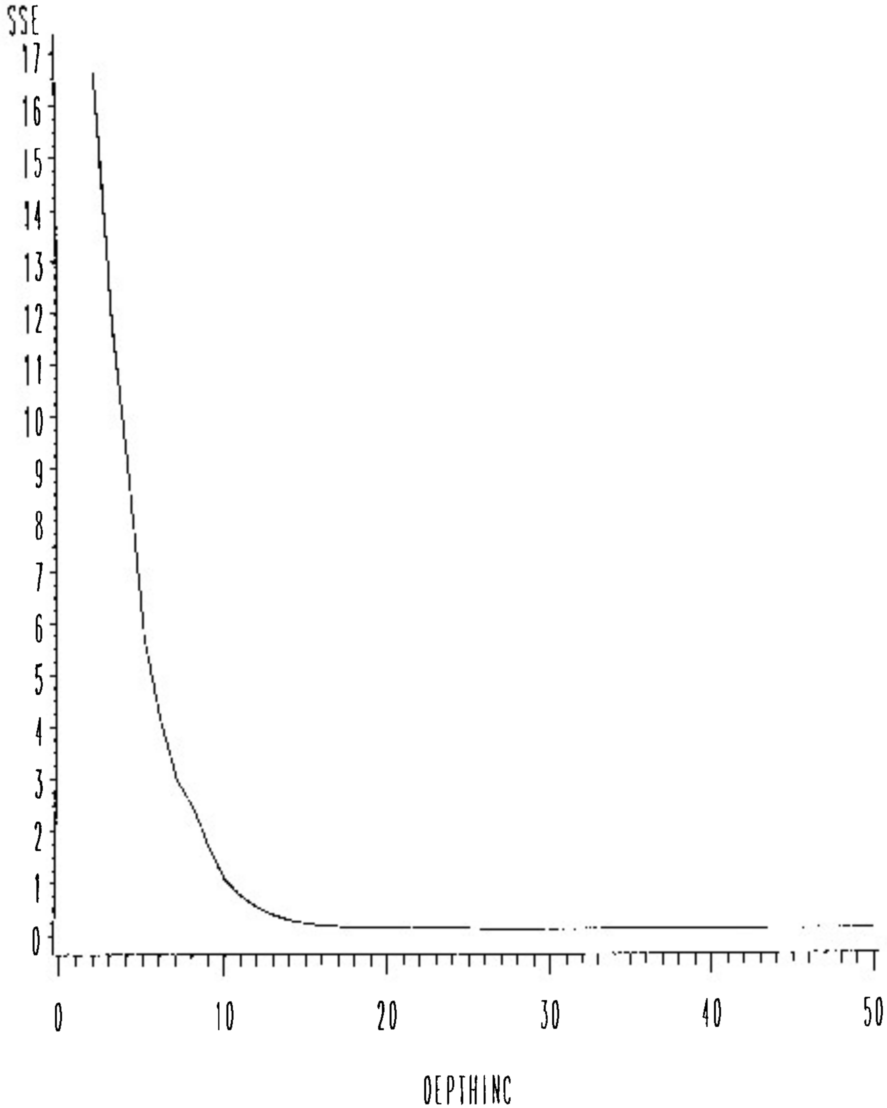

Figure 5 : Error in simulation versus the number of sublayers in the simulation.

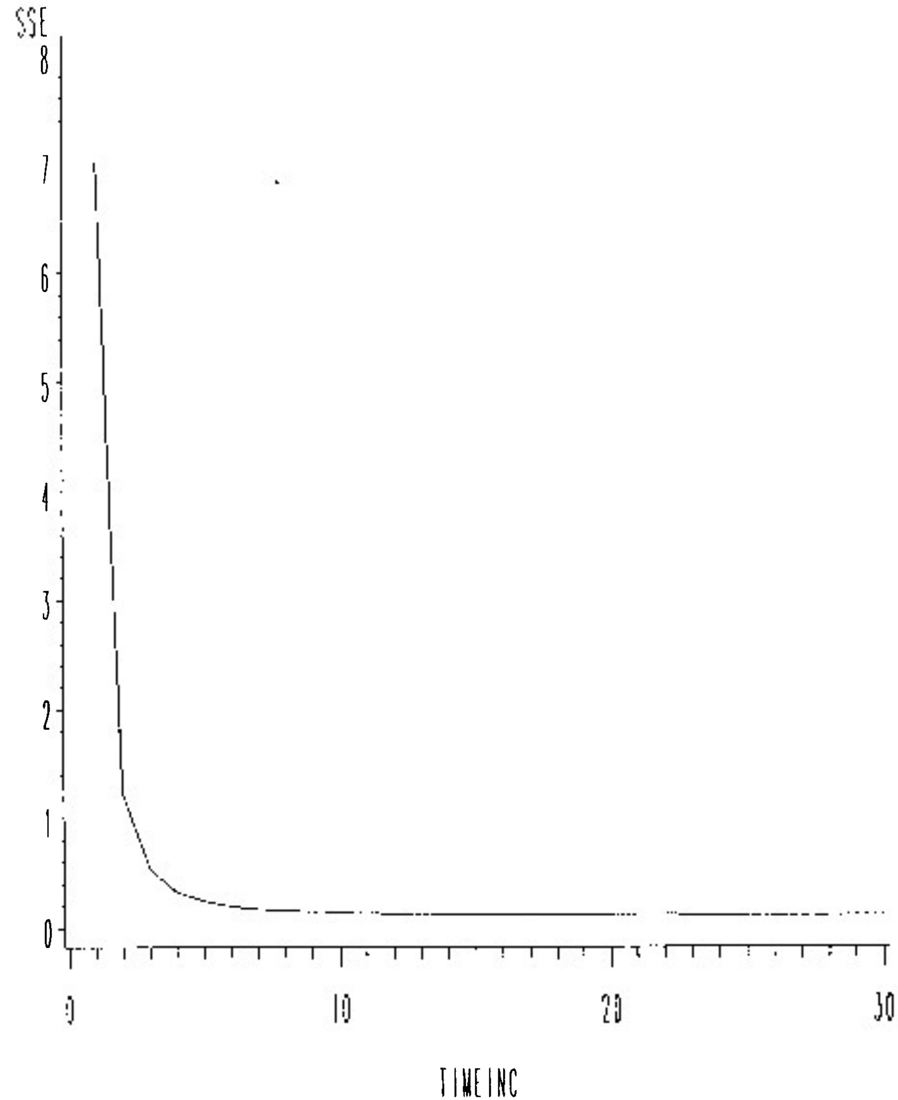

Figure 4 : Error in simulation versus the number of time increments in the simulation.

4.2 Model parameter extraction from simulation

4.2.1 Introduction

The extraction of photolithography model parameters presents a challenging predicament since there are four models serially contained within. Measurement the PAC concentration is not obtainable on the microscopic level, however, the PAC concentration can be obtained for the bulk resist using the resist transparency technique proposed by Dill [2]. This allows the exposure parameters to be extracted but unfortunately the effect of the pre-bake and PEB parameters on the PAC cannot be determined from this approach. Because the development models are provided in a convenient, closed form, the extraction of these parameters can be straightforward to obtain via non-linear regression algorithms. In order to do so, the PAC concentration as a function of depth in the resist must be known. Since the bake model parameter are not known, the PAC concentration is not available.

4.2.2 Correlation among model parameters

It was theorized that the development parameters were highly correlated with the exposure parameters in terms of the developed image. Given the development rate of the resist as a function of depth, an arbitrarily selected set of exposure parameters can be used to generate the PAC concentration as a function of depth in the resist. Then, the development rate parameters can be extracted using non-linear regression by iteratively searching for the appropriate parameters to match the calculated PAC to the measured development rate. In terms of the resist image after development, inaccurate exposure parameters are of little consequence since the development parameters have suitably compensated for them.

In order to substantiate this theory, the development rate versus depth in the resist was generated with the one dimensional simulator developed in this research. The first test examines the situation of an exposure and development but without either of the two bake simulations. The second test accommodates the pre-bake and PEB models in the parameter extraction approach.

Using the arbitrarily selected, though realistic parameters listed in table 1, the rate versus depth was simulated for three values of exposure (66, 90, and 114 mJ/cm^2) in order to obtain a larger range of development rates and to demonstrate the correlation of exposure and development parameters across a range of exposure doses.

Table 1: Parameters used to generate simulated development rate versus depth.

Parameter	**Value**
A	0.5198 μm^{-1}
B	0.2700 μm^{-1}
C	0.014 cm^2/mJ
Resist thickness	1.10 μm
Refractive index magnitude	1.68

In the same way that development rate data would be gathered from wafers subsequently in this research, the development rates were simulated as a function of depth in the resist for three different exposure doses. Three doses were chosen to accumulate a wide range of PAC concentrations, and although there already exists a range of PAC concentrations within a single wafer, three wafers guaranteed a wider range of values.

Extraction of the modeling parameters was pursued via nonlinear regression techniques. Among these techniques is the Marquardt-Levenberg technique [27-30] which uses a compromise of two separate techniques; steepest descent and a linearization.

The steepest decent approach begins with a set of initial guesses for the parameters to be estimated. For each set of guesses, the algorithm solves the proposed model for the entire set of factor and response values. For instance, if the development rate parameters of the Kim development model were desired, the algorithm would take the initial guesses of R_1 through R_6 and solve the development model for each combination of PAC concentration and depth that is provided. Then the SSE between the model solutions and the measured data could be computed. Since there are a number of guesses for R_1 through R_6, a plane of the SSE in terms of R_1 through R_6 could be established. In this manner, in whatever direction of this plane that has the steepest slope, R_1 through R_6 could be changed in order to lower the SSE between the model solutions and the measured data. This path is pursued until the SSE begins to increase. Then a new direction is calculated and pursued just as before.

Steepest descent is reliable way to find a minimum and does not require any derivatives. Unfortunately, after some initial gains in the fit of the model, this method tends to slow considerably. At this point, the Marquardt-Levenberg algorithm makes a transition to the linearization technique.

The linearization uses the first partial derivatives of the proposed model to find the first two terms of the Taylor series expansion. For each new combination of R_1 through R_6, a new linear approximation of the non-linear model is established and operated on. As such, the first partial derivative with respect to each of model parameters to be extracted are required. Since the Dill exposure model is not in a closed, analytic form, it cannot be inserted into the development model or in the bake models. This prevents nonlinear regression being used to extract these parameters, but this is of little consequence.

However, non-linear regression can be used to extract the parameters of the development models. Using the Kim development model, the first partial derivative with respect to the development model parameters are,

$$\frac{\partial R(z,t)}{\partial R_1} = \frac{R_{inhibit} * \dfrac{1-M(z,t)\exp[-R_3(1-M(z,t))]}{R_1^2}}{\{\dfrac{1-M(z,t)\exp[-R_3(1-M(z,t))]}{R_1} + \dfrac{M(z,t)\exp[-R_3(1-M(z,t))]}{R_2}\}^2}$$

EQN 39

$$\frac{\partial R(z,t)}{\partial R_2} = \frac{R_{inhibit} * \dfrac{M(z,t)\exp[-R_3(1-M(z,t))]}{R_2^2}}{\{\dfrac{1-M(z,t)\exp[-R_3(1-M(z,t))]}{R_1} + \dfrac{M(z,t)\exp[-R_3(1-M(z,t))]}{R_2}\}^2}$$

EQN 40

$$\frac{\partial R(z,t)}{\partial R_3} = \frac{R_{inhibit}\dfrac{-M(z,t)\,(1-M(z,t))\exp[-R_3(1-M(z,t))]}{R_2}}{\{\dfrac{1-M(z,t)\exp[-R_3(1-M(z,t))]}{R_1} + \dfrac{M(z,t)\exp[-R_3(1-M(z,t))]}{R_2}\}^2}$$

$$+ \frac{R_{inhibit}\dfrac{-M(z,t)\,(1-M(z,t))\exp[-R_3(1-M(z,t))]}{R_1}}{\{\dfrac{1-M(z,t)\exp[-R_3(1-M(z,t))]}{R_1} + \dfrac{M(z,t)\exp[-R_3(1-M(z,t))]}{R_2}\}^2}$$

EQN 41

$$\frac{\partial R(z,t)}{\partial R_4} = -\{[1-(R_5-(R_5-R_6)M(z,t))] * [\frac{z}{R_4^2}\exp(\frac{-z}{R_4})]\} * R_{bulk}(z,t)$$ EQN 42

$$\frac{\partial R(z,t)}{\partial R_5} = (1-M(z,t))\exp[-R_3(1-M(z,t))] * R_{bulk}(z,t)$$ EQN 43

$$\frac{\partial R(z,t)}{\partial R_6} = M(z,t)\exp(-z/R_4) * R_{bulk}(z,t)$$ EQN 44

where

$$R_{inhibit} = [1-(1-(R_5-(R_5-R_6) * M(z,t)))\exp(\frac{-z}{R_4})]$$ EQN 45

The development rate parameters were extracted using a program similar to the one in Appendix B using a set of exposure parameters ($A=0.781\mu m^{-1}$, $B=0.082\mu m^{-1}$, and $C=0.013 cm^2/mJ$) that were different from the ones in table 1 but were assumed to be correct during the parameter extraction. The program used for this extraction did not extract the PEB diffusion length constant since neither of the bakes were included in the simulation data. The program listed in the appendix extracts the PEB diffusion length constant. The parameter extraction was able to converge, the ANOVA table for which is given in table 2. Judging by the residual sum of squares, the parameter extracted from this routine provide an excellent fit to the simulated data. The extracted development rate parameters are listed in table 3 along with 95% confidence intervals where appropriate.[3] Plots of the original simulated data and data simulated with the extracted set of parameters in figures 6 through 8 demonstrate the closeness of fit.

[3]The 95% confidence interval establishes a range for the "true" value of the parameter to be contained within, with 95% confidence.

Table 2: ANOVA table for the extraction of model parameters. Development rate data was simulated using the parameters in table 1.

Source	DF	Sum of Squares	Mean Square
Regression	6	13473.597275	2245.599546
Residual	744	2.721391	0.003673
Uncorr. Total	750	13476.318667	

Table 3: Extracted parameters for the simulated development rate versus depth data.

Parameter	Estimate	Asymptotic Std. Error	Asymptotic 95% CI Lower	Asymptotic 95% CI Upper
R_1 (μm/min)	13.914284	0.045504	13.824950	14.003618
R_2 (μm/min)	0.035789	0.000420	0.034965	0.036613
R_3	8.357614	0.024256	8.309995	8.405233
R_4	0.238234	0.003429	0.231503	0.244965
R_5	0.803234	0.006400	0.790670	0.815797
R_6 (μm)	0.487934	0.012305	0.463777	0.512091
A(μm^{-1})	0.781*			
B(μm^{-1})	0.082*			
C(cm^2/mJ)	0.013*			

* Assumed for extraction.

Next, it was necessary to incorporate the Mack pre-bake model and the Mack PEB model. With a closer look at the pre-bake model in equations 25 through 26, it was evident that the pre-bake model manifests itself as a modification of the Dill A and B parameters. Therefore, since the Dill parameters are highly correlated with the combination of development parameter, for a given set of pre-bake conditions, the pre-bake can be removed from consideration for the parameter extractions.

If the PEB conditions are fixed, only one parameter, the PEB diffusion length constant, is required for the PEB model. Equations 28 and 30 that describe the time and temperature effects of the PEB can be summarized into σ if time and temperature are constant. The extraction of σ is straightforward since it is the only parameter outside of the closed form of the development models in equations 15 and 16. A practical approach for the search on the value of σ was to perform a three point minimization of the develop model regression SSE.

The three point minimization was performed as follows. First upper and lower limits for the parameter to be estimated are established. The SSE for the two limits and for the median σ between the two limits are found. The range between a limit and the median is successively cut in half by finding the SSE for the fit of the development model when the mean of the two σ's is used. If the new SSE is lower than the SSE for the median σ, then the median σ was modified. Otherwise, the limit σ was modified. Eventually, the limits have been paired down to a reasonable tolerance which is the best estimate. In the case of σ, the lower limit can be taken to some very small value, slightly larger than zero.[4] An upper limit was selected based upon the spread of influence of σ. For the sinusoidal nature in the PAC concentration, the PAC concentration profile will invert if the value of σ is too large. It was found that a value of $0.1\mu m$ was a practical upper limit for σ.

Using the parameters listed in table 4, a simulation of development rates for three different exposures was performed as above, but this time it incorporated the pre-bake and PEB models.

[4]For a non-robust simulator, a value of zero could cause the simulation to halt execution or even crash.

Table 4: Simulation parameters for the generation of development rate data. Simulation included both the pre-bake and the PEB models.

Parameter	**Value**
A	0.5198 μm^{-1}
B	0.2700 μm^{-1}
C	0.014 cm^2/mJ
Resist thickness	1.1 μm
Refractive index magnitude	1.68
$E_{a-pre-bake}$	29.5 Kcal/mol
$\ln(A_r)$	35.3 $\ln(min^{-1})$
f_{PAC}	1.5
E_{a-PEB}	62.0 Kcal/mol
$\ln(D_o)$	87.5 $\ln(nm^2/min)$
Pre-bake time	1.34 min
Pre-bake temperature	373 Kelvin
PEB time	0.75 min
PEB temperature	373 Kelvin

A program, written in SAS, for the extraction of R_1 through R_6 and σ, is given in appendices B and C. This program assumed values for A, B, and C of 0.781μm^{-1}, 0.082μm^{-1}, and 0.013cm^2/mJ respectively. The exposure parameters used to generate the development rate data were intentionally different from the exposure parameters in the extraction to demonstrate that they may be selected arbitrarily. The ANOVA table for the non-linear regression of the development model is given in table 5. It was worth noting, the agreement in the fit of the data as is evident by the very small SSE. In figure 9, a plot of the development model regression SSE versus σ demonstrates how the fit of the development model varies with the value of σ. A value for σ of 0.02406μm was found with the extraction routine and is shown in figure 9 to be the minimum on this plot. The extracted values are listed in table 6 along with confidence intervals where applicable.

Table 5: ANOVA table for the extraction of model parameter from simulated data. Simulation included the pre-bake and PEB models.

Source	**DF**	**Sum of Squares**	**Mean Square**
Regression	6	6731.065291	1121.844215
Residual	744	2.065702	0.002788
Uncorr. Total	750	6733.130993	

Table 6: Extracted parameters from simulated development rate versus depth. Simulation included pre-bake and PEB models.

Parameter	**Estimate**	**Asymptotic Std. Error**	**Asymptotic 95% CI Lower**	**Asymptotic 95% CI Upper**
R_1 (μm/min)	13.531180	0.118355	13.298824	13.763536
R_2 (μm/min)	0.037330	0.000467	0.035925	0.038246
R_3	8.152274	0.029600	8.094163	8.210385
R_4	0.266616	0.007312	0.252262	0.280970
R_5	0.781953	0.013353	0.755737	0.804356
R_6 (μm)	0.709424	0.017686	0.670758	0.740200
A(μm^{-1})	0.781*			
B(μm^{-1})	0.082*			
C(cm^2/mJ)	0.013*			

* Assumed for extraction.

These extracted values were then used to simulate the development rate as a function of depth for comparison with the original development rate data. In figures 10 through 12, both plots of development rate versus depth are shown to demonstrate that although two completely different sets of parameters were used, the resist after development is virtually the same.

Hence, for the extraction of the modeling parameters of resist after development, given a proposed A, B, and C and a known refractive index for the resist, only the development rate parameters and the PEB diffusion length constant need to be extracted to sufficiently model the resist.

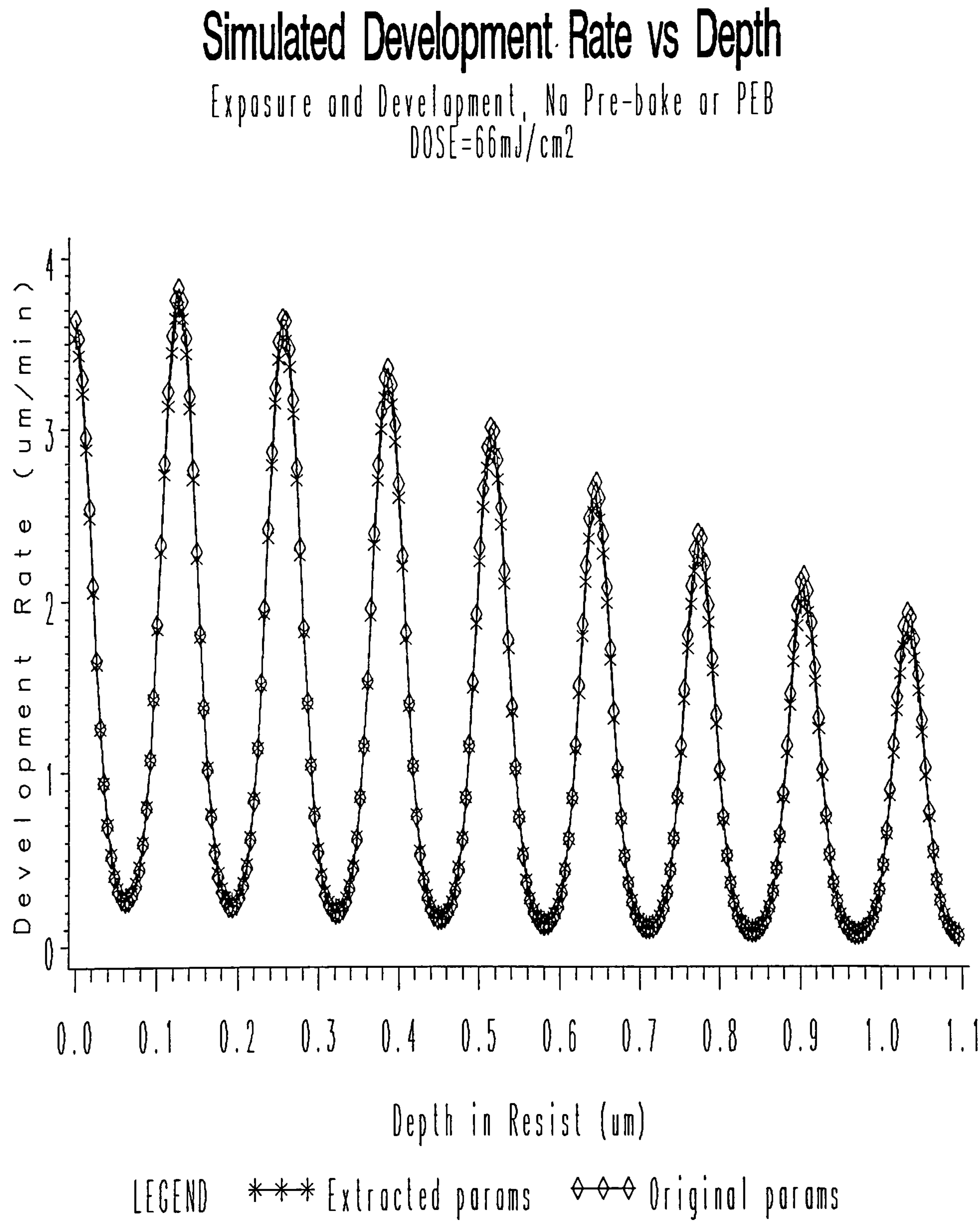

Figure 6 : Comparison of simulated development rate versus depth using original parameters and extracted parameters (no pre-bake or PEB, dose = 66mJ/cm^2).

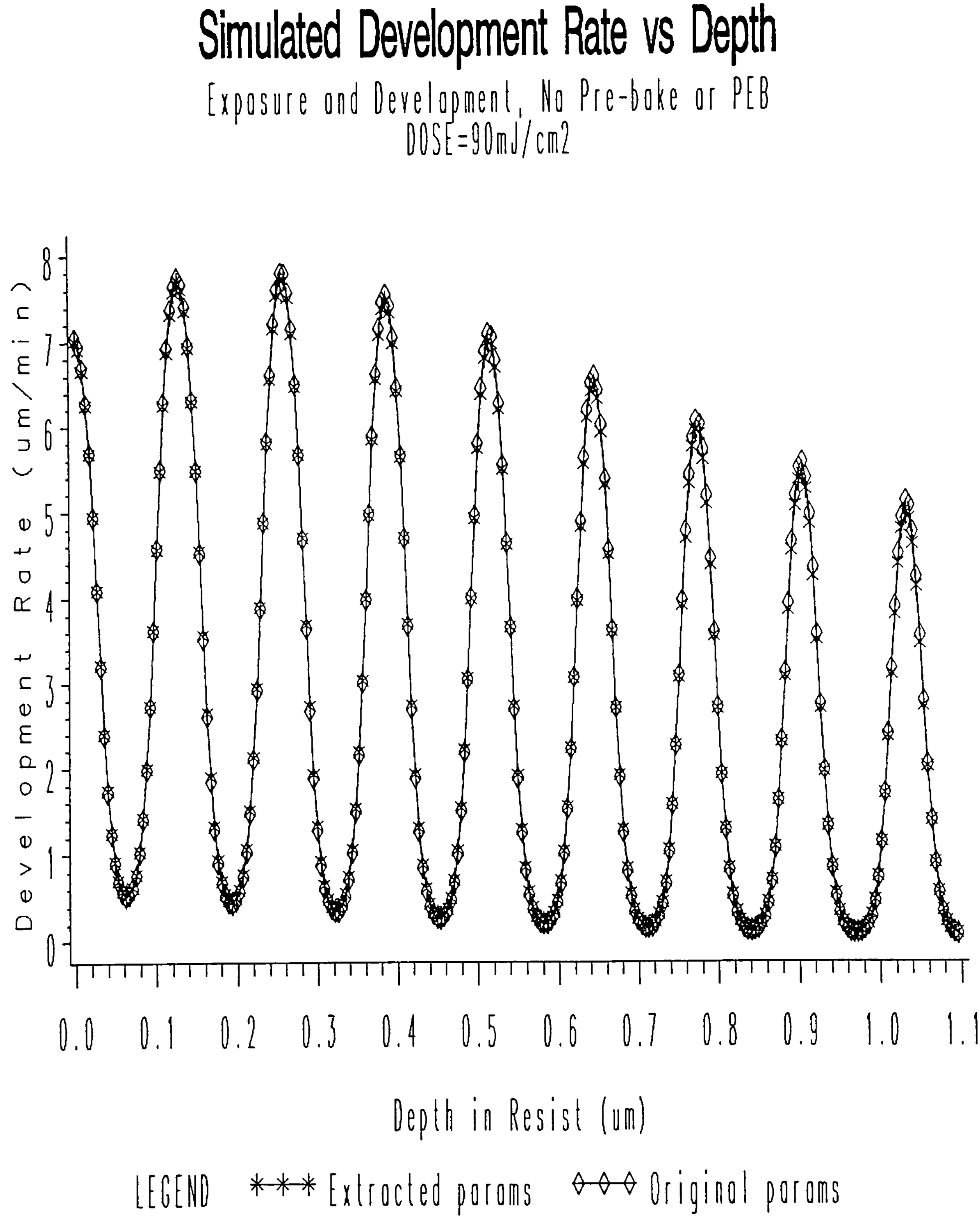

Figure 7 : Comparison of simulated development rate versus depth using original parameters and extracted parameters (no pre-bake or PEB, dose = 90mJ/cm^2).

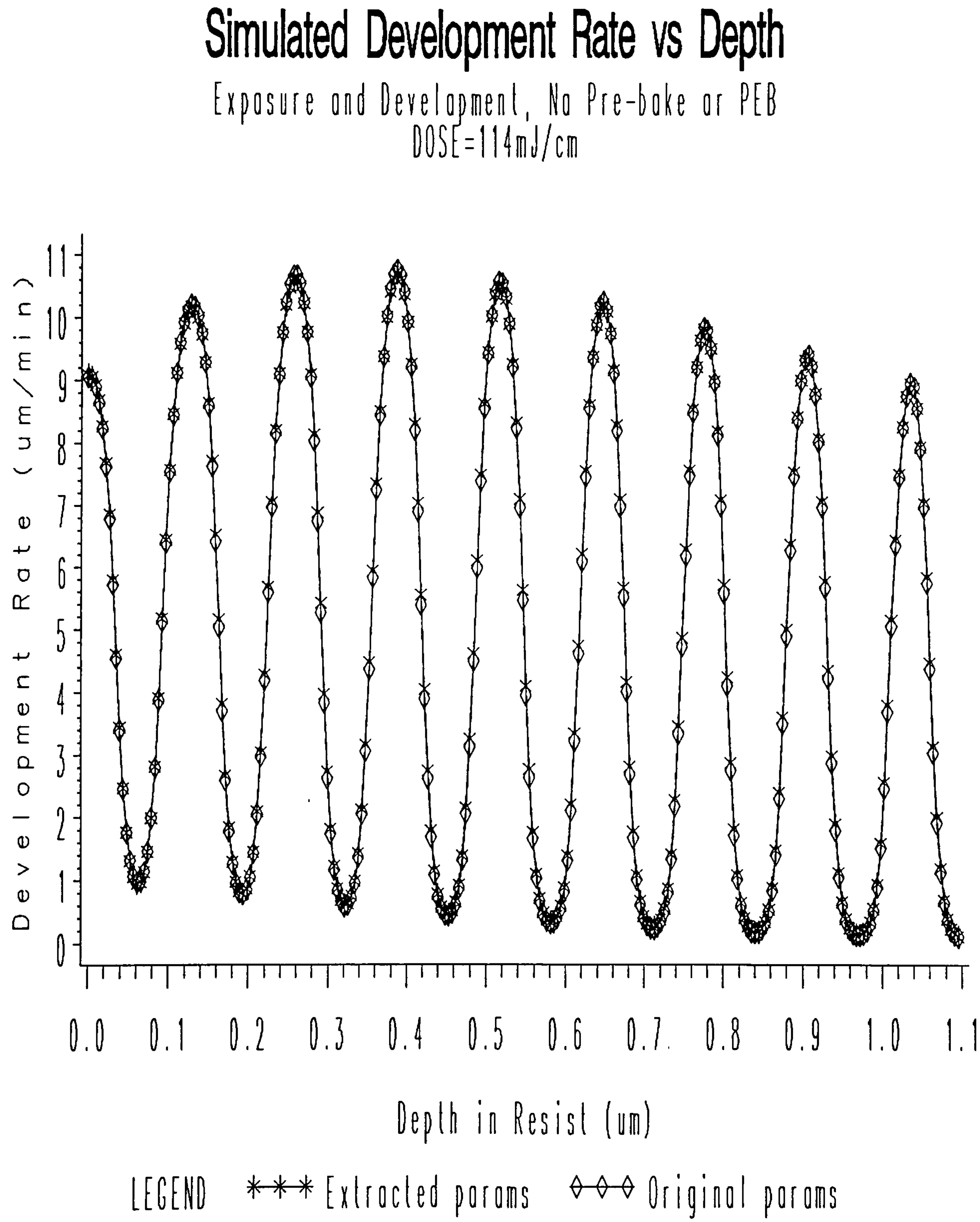

Figure 8 : Comparison of simulated development rate versus depth using original parameters and extracted parameters (no pre-bake or PEB, dose = 114mJ/cm^2).

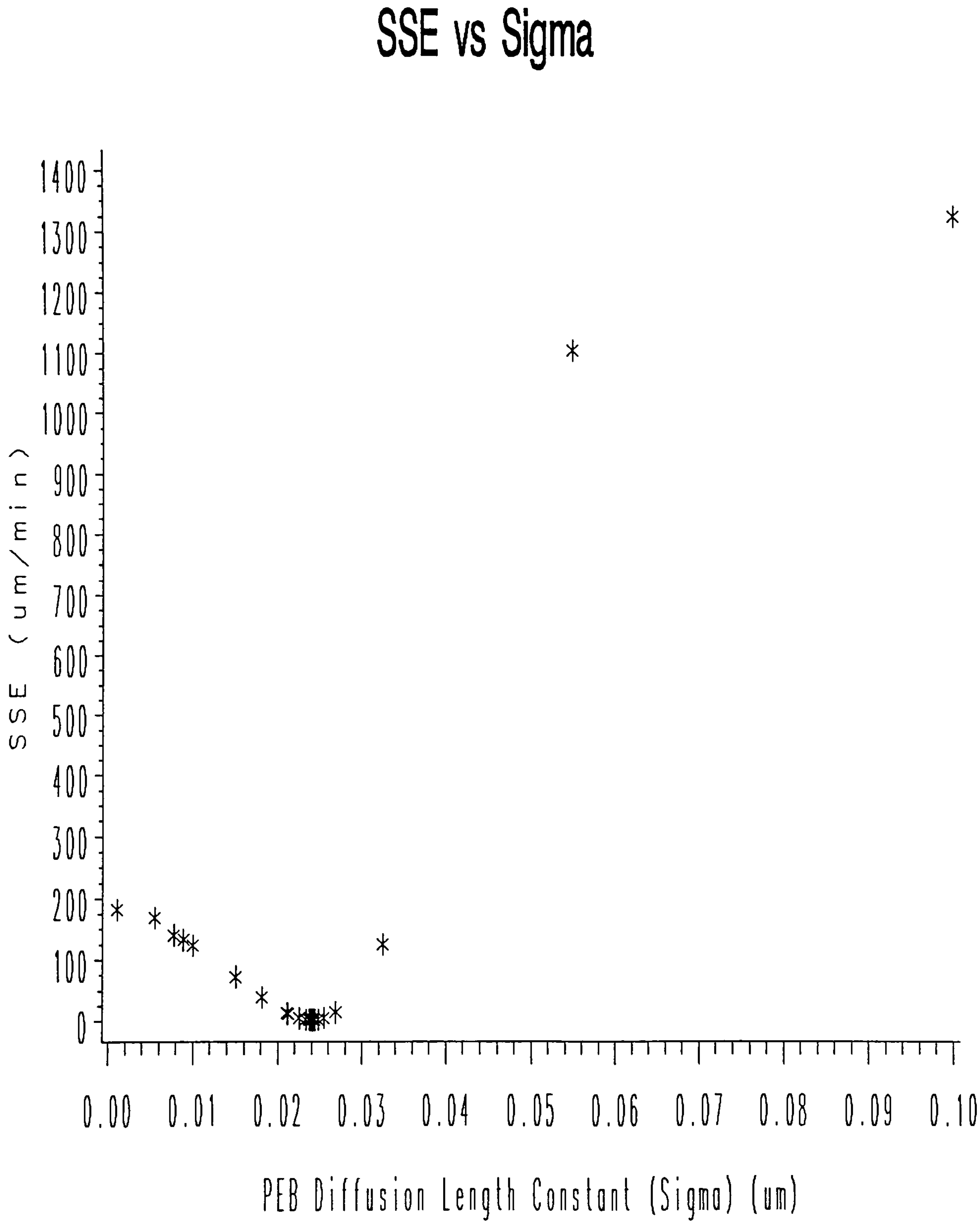

Figure 9 : Error in fit versus PEB diffusion length constant.

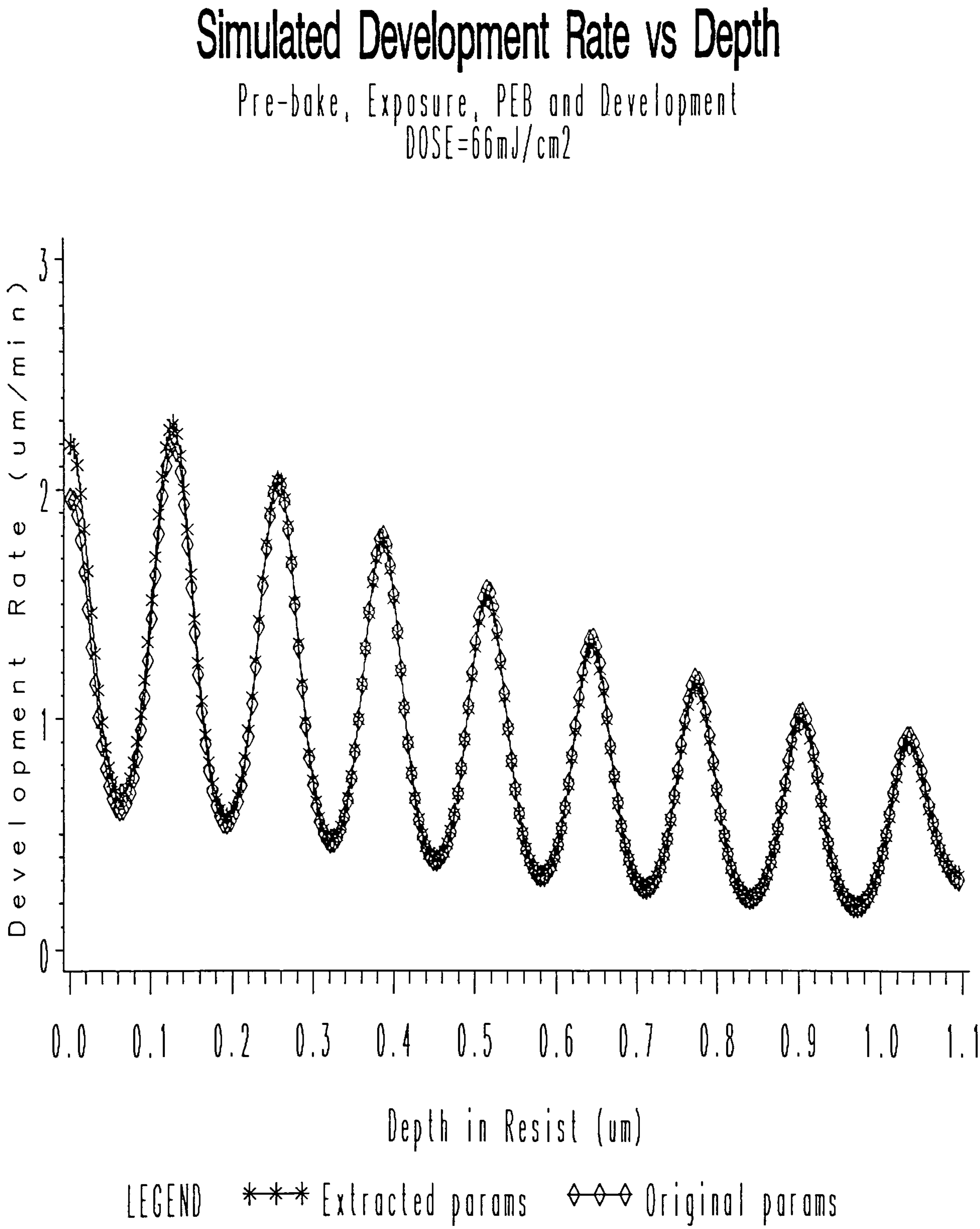

Figure 10 : Comparison of simulated development rate versus depth using original parameters and extracted parameters (dose = 66mJ/cm^2).

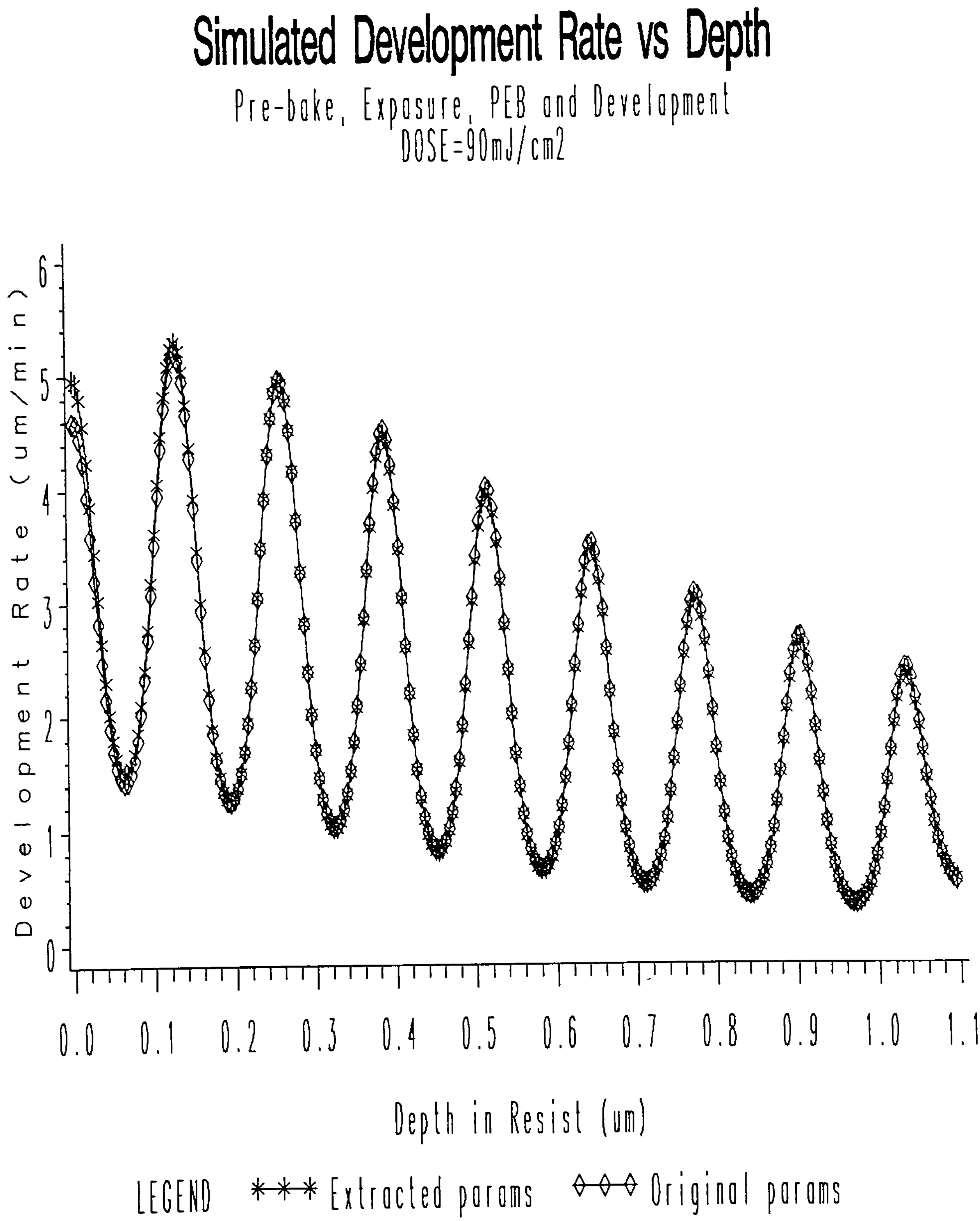

Figure 11 : Comparison of simulated development rate versus depth using original parameters and extracted parameters (dose = 90mJ/cm^2).

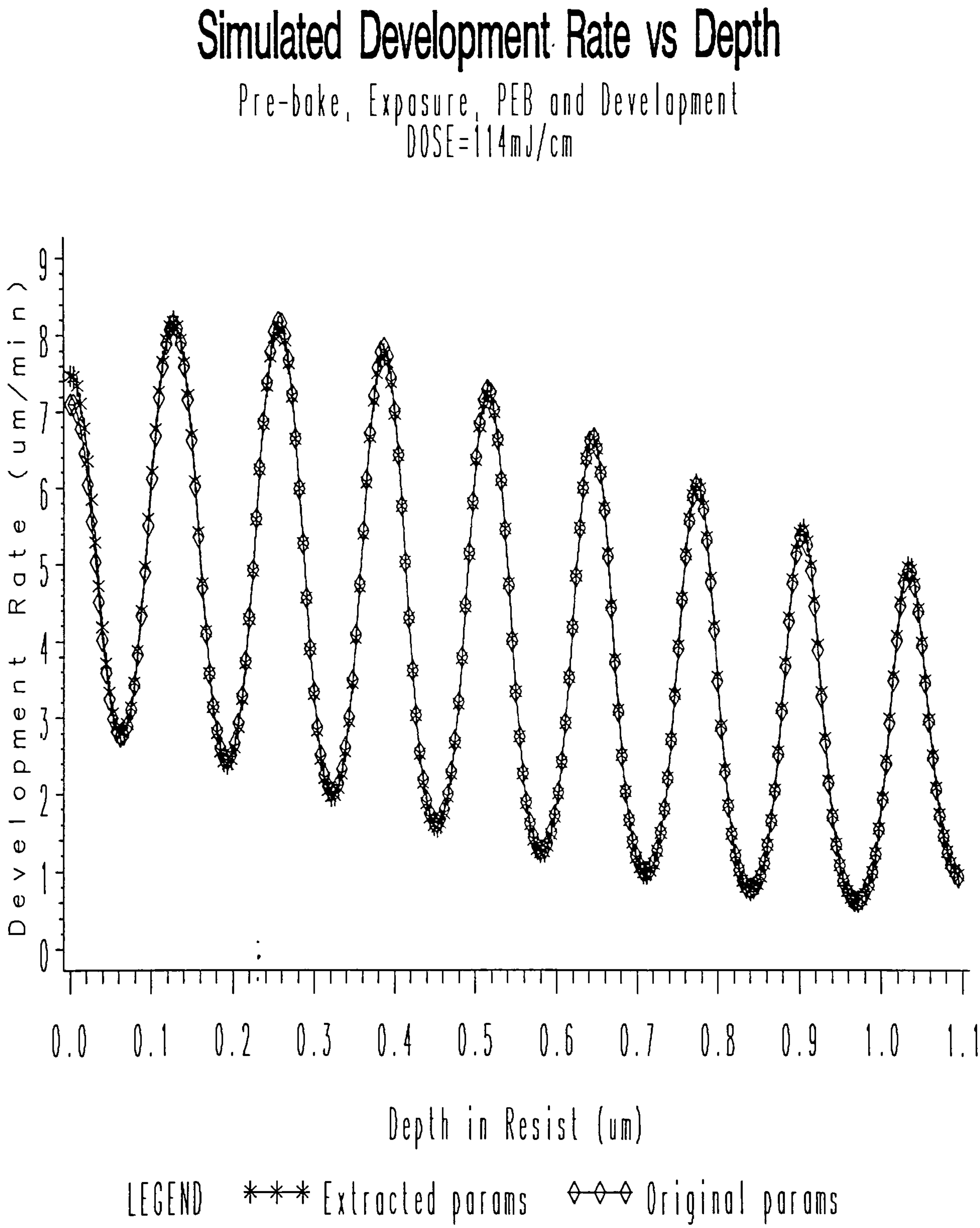

Figure 12 : Comparison of simulated development rate versus depth using original parameters and extracted parameters (dose = 114mJ/cm^2).

5.0 ANALYSIS AND DISCUSSION

5.1 Development Rate Extraction

5.1.1 Introduction

Fundamental to the extraction of process specific modeling parameters is the measurement of process specific responses. Previous work on model parameter extraction centered around the development rates as measured on the immersion-based Perkin Elmer DRM. Perhaps a good first order indicator, the DRM lacked any of the development nuances such as development agitation due to the centripetal forces of the development spinner and the development spray, the exact development time, and dynamic microscopic developer composition. If possible, one would naturally prefer to extract the development rates from the development module, in-situ.

In this section, the approach employed for the extraction for the in-situ development rate is presented. Attractive to this technique is the independence of the extraction technique from the development mechanisms. This approach works equally well for many types of resists and with many types of lithography exposure (ie. optical, e-beam, x-ray; contact, refractive projection, reflective projection).

The true strength of this photolithography parameter extraction technique lies within the in-situ, passive measurement of the development rate over time. This allows the extracted parameters to be process specific.

5.1.2 Signal Detection

Signal acquisition was performed through the use of the Site Services DSM (development spray monitor) 100. Although initially developed as an endpoint detection system, this tool monitors the thin film interference signal of the resist thin film from a circularly polarized polychromatic light source which may be converted to development rate.

The DSM system is comprised of three distinct elements, as shown in figure 13: the optical processing head(OPH), the signal processing unit(SPU), and a personal computer. The OPH sits above the wafer within the development cup module on the wafer track. A fiber optic cable runs from the OPH to the SPU and is multifurcated into eight cables before entering the SPU. From the SPU, converted data is loaded into the PC for data processing and operator interaction.

The OPH consists of tungsten halogen light source that is collimated and passed through a polarizing beam splitter. The light is then circularly polarized by passing it through a quarter wave plate before it strikes the wafer surface. An approximate one inch diameter beam of circularly polarized light is reflected from the resist coated and pattern wafer, off axis from its circular motion. The reflected light intensity is periodic with development as the thickness of the resist patterned images causes moments of constructive and destructive interference as a function of time. The reflected light is again passed through the quarter wave plate which causes only the circularly polarized light to become linearly polarized. The polarizing beam splitter reflects only the linear polarized light through a condenser lens and is focused onto a fiber optic bundle. The fiber optic bundle is then split into eight separate bundles each having a separate bandpass filter detector in the SPU. Signals output from the detector are then processed within the computer using the Site Services Lithacon software. The signal for the patterned geometries is isolated from the total signal (which includes that non-exposed region signal) by use of a Fast Fourier Transform (FFT) algorithm in the Lithacon software. It should be noted that spectrum of light used in the OPH was chosen to be outside of the range of absorbing frequencies of the resist.

There are a number of attractive features built into this system. The first of these is the obvious in-situ measurement. With little, if any modifications, the OPH can easily be added to almost any development cup. For this work, the OPH was mounted on a GCA 9000 wafer track at a distance of about eight inches from the wafer surface. This flexibility allowed easy access to the dispense nozels and required no physical modifications of the development cup.

The second set of features are inherent to the circular polarization of the incident light and the isolation of that circularly polarized light before detection. Experimental results [31,32] indicated a robustness in measurements to ambient light effects, scatter from resist sidewalls, aerosol droplets, suspended particles, bubbles in the developer and, for the case of static development, the "red cloud" effect. Red cloud is that term used to describe the opacity in the developer solution due to the presence of reacted resist in the developer solution.

5.1.3 Conversion to development rate

In figures 14 through 21, the interference signal output from the Site Services DSM are provided for a wafer that was exposed with $90mJ/cm^2$. It is clear to see that each of these curves was periodic in nature. However, the magnitudes of the peaks and valleys within a curve and between curves tended to be non-systematic. In order to implement a commonality between curves and within curves, peaks and valleys for each curve were identified or tagged and the signals were normalized with respect to their closest peak and valley to a value between -1.0 and +1.0. In this manner, a maximum could always be identified by a value of +1.0 and a minimum by a value of -1.0. The values of -1.0 and +1.0 were chosen such that a cosine function could readily be used in the subsequent development rate extraction. The corresponding normalized curves for figures 14 through 21 are shown in figures 22 through 29 respectively.

It was known from the superposition of the incident and reflected light that the resultant light should behave as a sinusoid. Specifically, the interference curve will oscillate as,

$$S=\cos\left(\frac{4\pi n}{\lambda}\,thickness\right) \qquad \text{EQN 46}$$

where

S = the interference signal

thickness = is the instantaneous thickness of the resist.

Since the range of lambda is relatively narrow, the refractive index was assumed to be constant.

In lieu of the absolute thickness, the instantaneous development rate and the thickness prior to Δt is inserted into equation 46, yielding

$$S_i=\cos\left(\frac{4\pi n}{\lambda_i}(rate\Delta t+d_o)\right) \qquad \text{EQN 47}$$

where

Δt = the inverse of the sampling frequency,

d_o = the thickness of the resist before Δt.

Using equation 47, for each increment of time, the rate that was required to produce the eight measured signals detected can be calculated beginning at the bottom of the resist/substrate interface where d_o=0.0.

This approach maintained the form of equation 47 and the minimized sum of square errors (SSE) of signal data. The Marquardt-Levenberg non-linear regression algorithm was used to compute the instantaneous development rate while minimizing the SSE in the signal data. The partial derivative of equation 47 with respect to the development rate is,

The SAS (Statistical Application Software) source code for the

$$\frac{\partial S}{\partial rate}=\frac{-4\pi^2 n\Delta t}{180\lambda}\sin\left(\frac{4\pi n}{\lambda}*(rate*\Delta t+d_o)\right) \qquad \text{EQN 48}$$

Marquardt-Levenberg approach to the development rate calculation is given in Appendix D.

For each increment in time, the instantaneous development rate was calculated. The added thickness in the resist for that increment in time was then added to d_o. The development rate versus time plot is given in figure 30 for the non-linear technique discussed. In this manner, the development rate versus development time was readily extracted from the signal data. This plot was then numerically integrated with respect to time to produce the thickness of the photoresist at each of the sampled times as in figure 31. This was converted to the development rate versus thickness and development rate versus depth in the resist in figures 32 and 33 respectively, which is the form of the development models given in equations 15 and 16.

In figures 30 through 33, the standing wave effect is not only apparent but is obvious. Although the in-situ development rate calculation made no assumption about nature of the development rate as time progressed, the algorithm clearly was able to discern the subtleties in the thickness versus time plot.

It should be noted that the accuracy of the instantaneous development rate near the bottom of the resist can be questionable. Looking at the interference plots in figures 22 through 29, all eight interference curves have a maximum at the resist/substrate interface. As the resist thickness increases, or the depth decreases, all eight curves remain nearly in phase until the resist is about 0.4μm thick. Because these interference curves are in phase, if one were look at the interference signals across the wavelengths at a given instant, one would see a fairly constant value. Since there is little sensitivity looking across the wavelengths, the cosine function in equation 47 has difficulty in extracting the instantaneous development rate.

This point is evident in figures 34 through 39. In figure 34 a plot of the normalized interference signal as a function of wavelength is relatively flat. As development time decreases, and the resist thickness increases, in figures 35 through 39 it is clear to see that the cosine function becomes more apparent, making it easier to extract the instantaneous development rate.

Inaccuracies in the cumulated thickness calculation are always compensated. When the interference reaches a maximum or a minimum, the cosine equation must have a given thickness in order to satisfy equation 47. Hence if development rate has been successively underestimated, when the calculations reach a minimum or a maximum, equation 47 must compensate and will tend to overestimate to make up the difference.

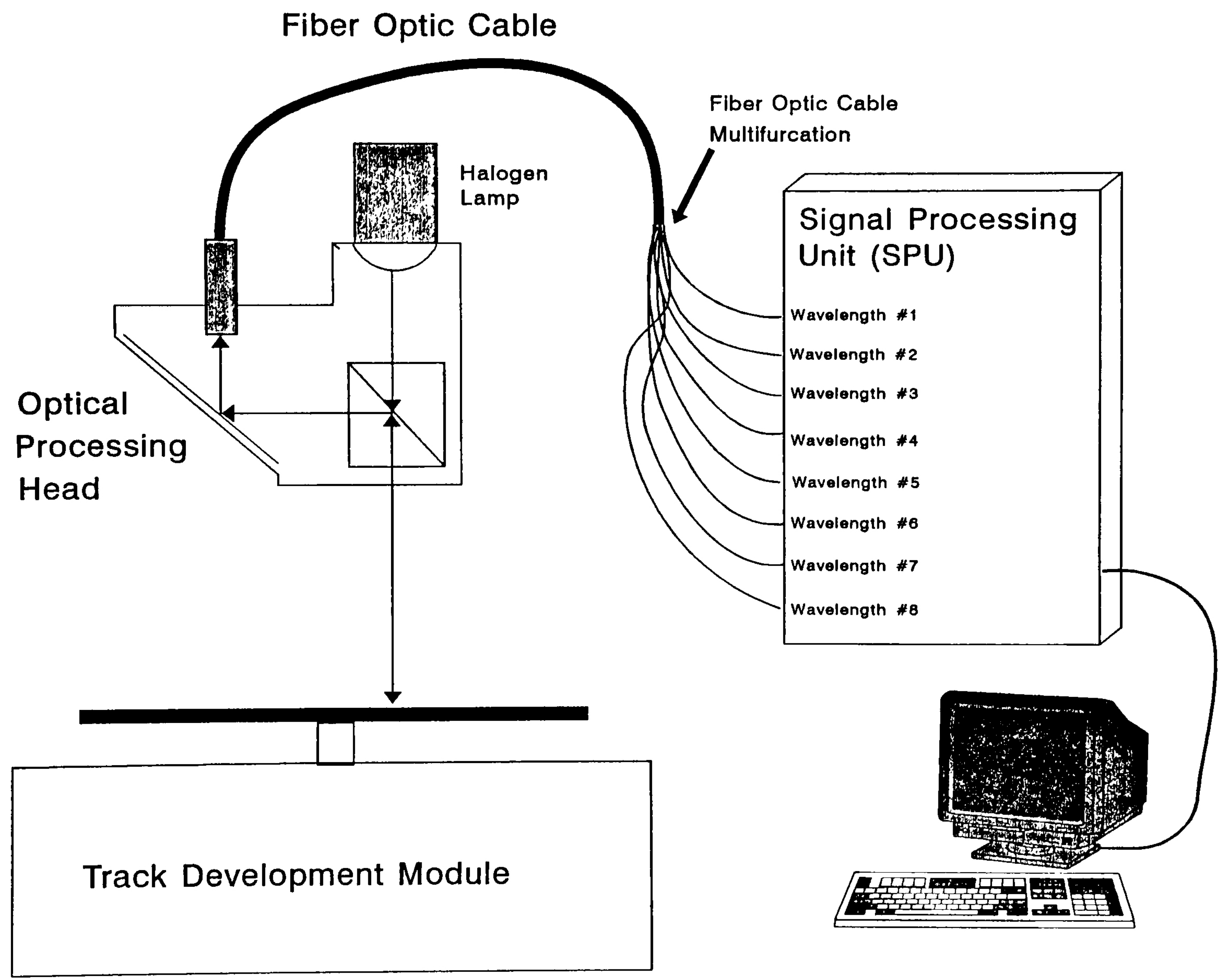

Figure 13 : Schematic diagram of Site Services DSM 100.

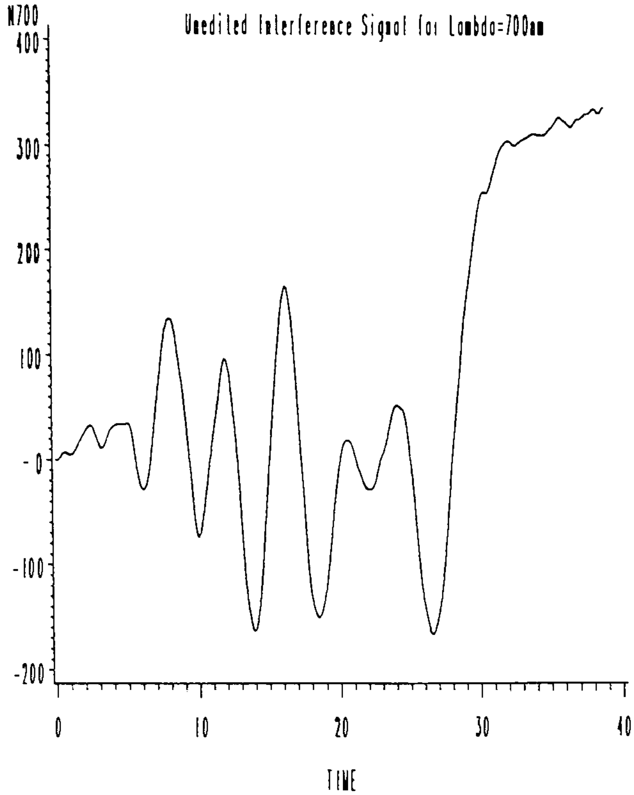

Figure 14 : Unedited interference signal for lambda = 700nm.

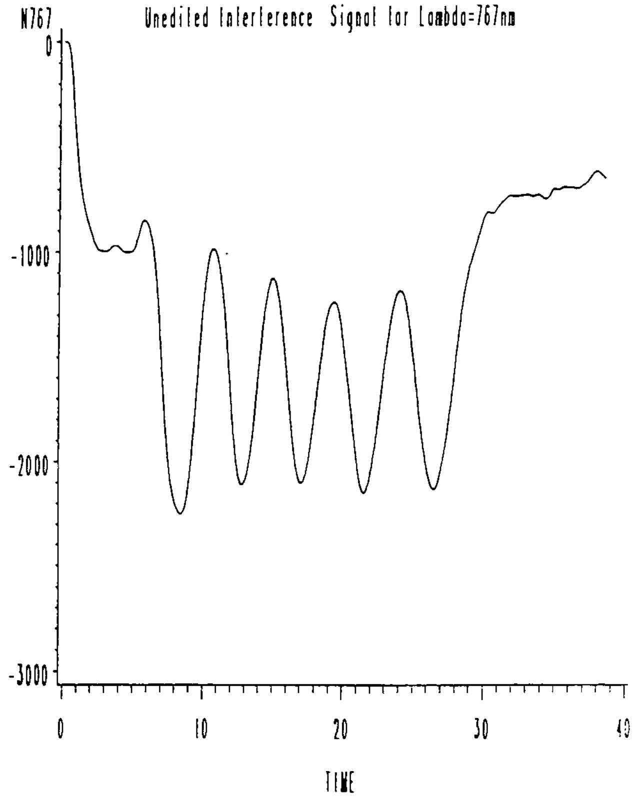

Figure 15 : Unedited interference signal for lambda = 767nm.

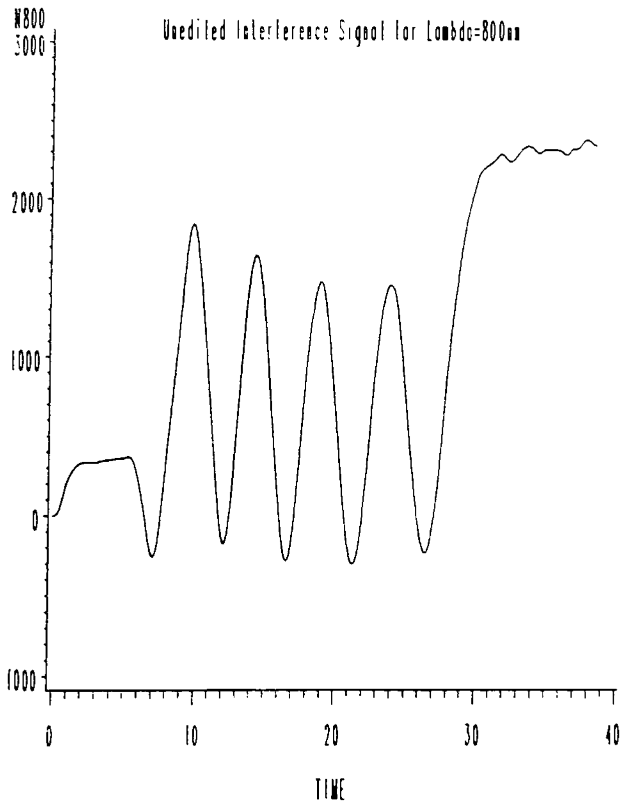

Figure 16 . Unedited interference signal for lambda = 800nm.

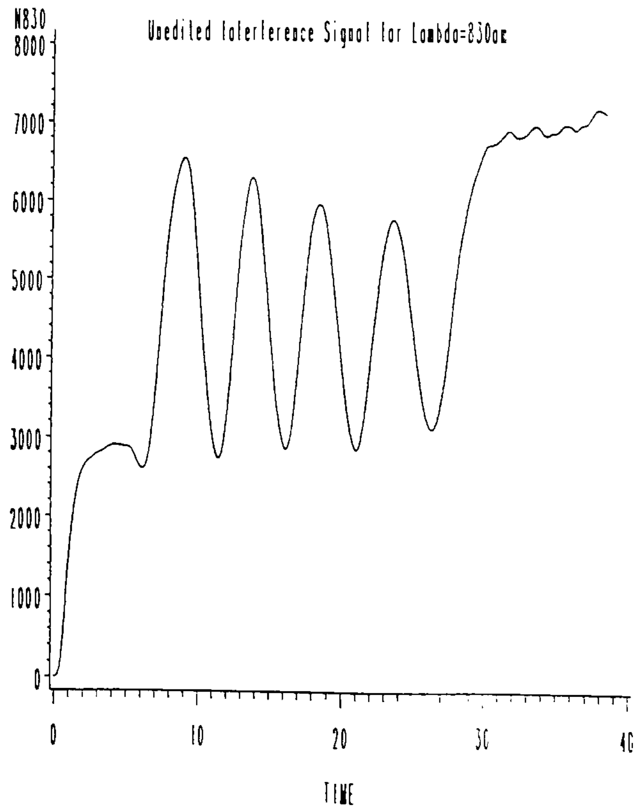

Figure 17 · Unedited interference signal for lambda = 830nm.

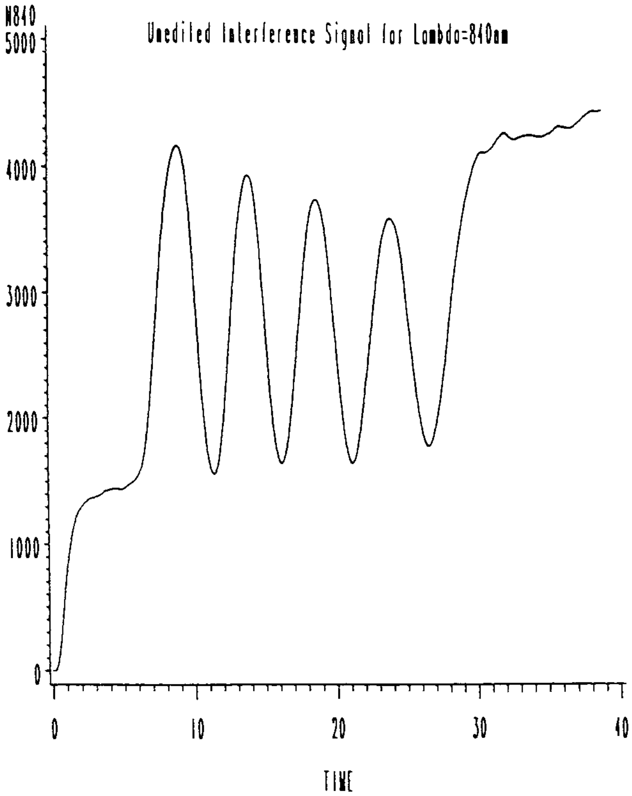

Figure 18 : Unedited interference signal for lambda = 840nm.

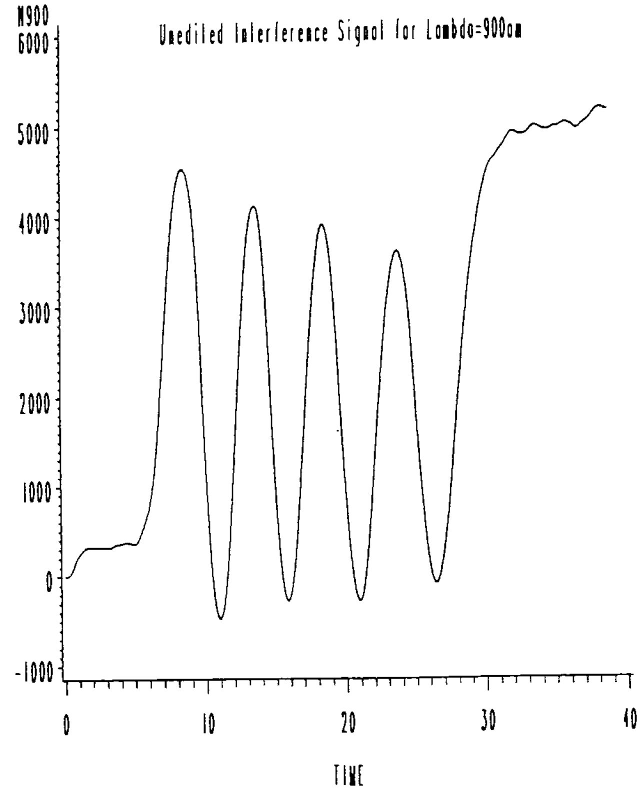

Figure 19 : Unedited interference signal for lambda = 900nm.

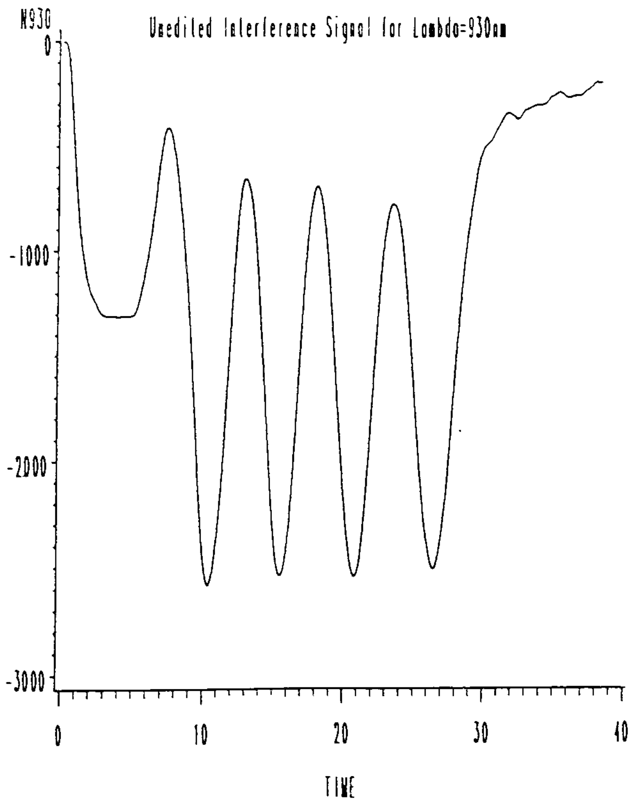

Figure 20 : Unedited interference signal for lambda = 930nm.

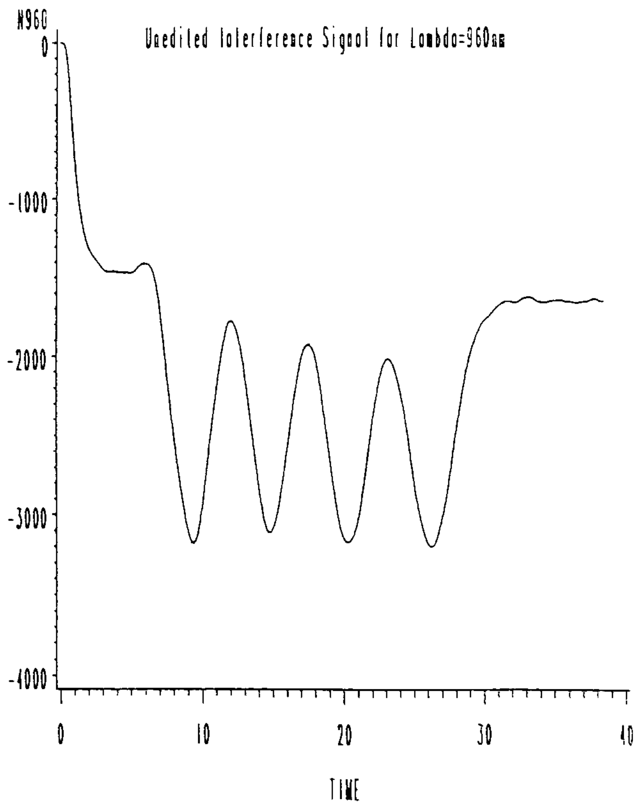

Figure 21 : Unedited interference signal for lambda = 960nm.

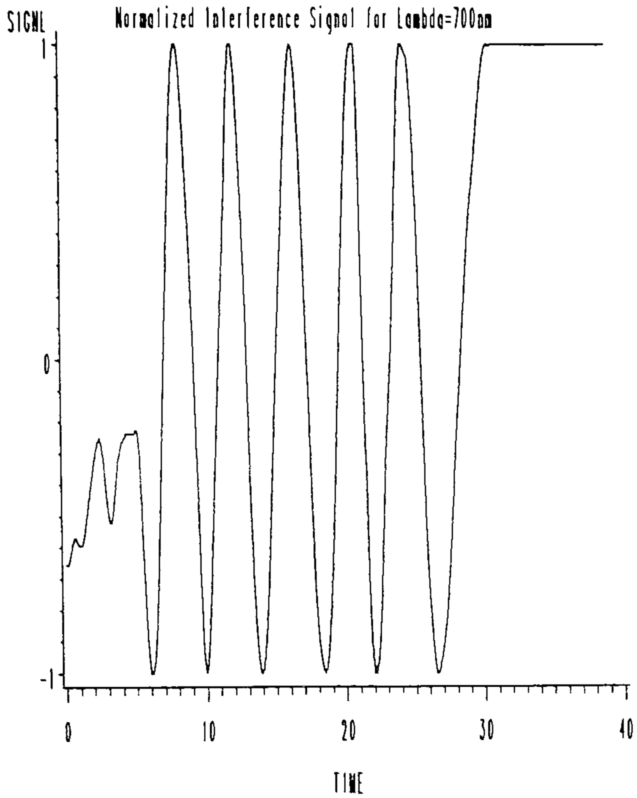

Figure 22 : Normalized interference signal for lambda = 700nm.

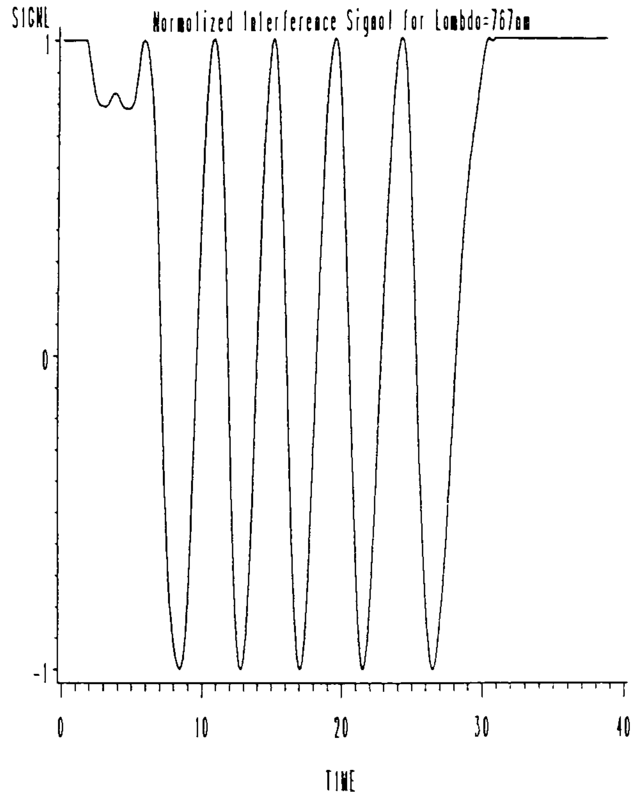

Figure 23 : Normalized interference signal for lambda = 767nm.

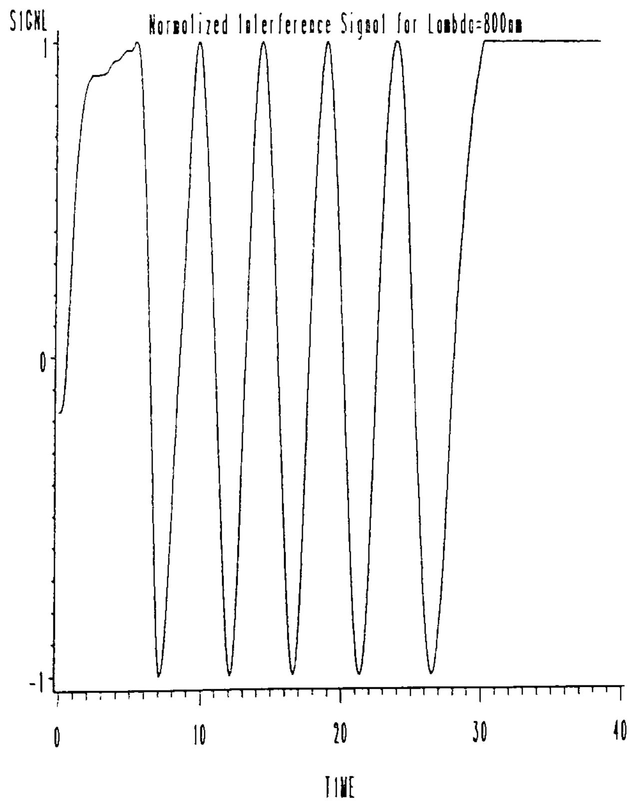

Figure 24 : Normalized interference signal for lambda = 800nm.

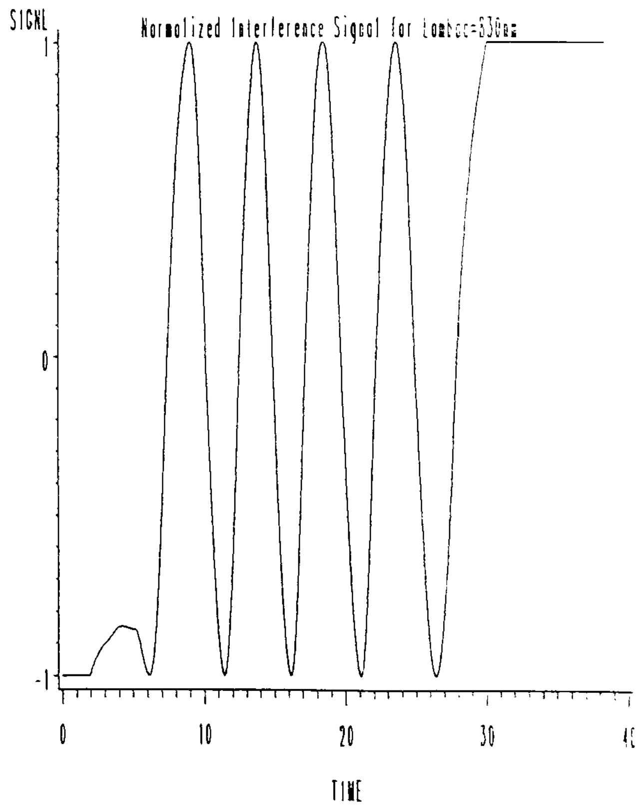

Figure 25 : Normalized interference signal for lambda = 830nm.

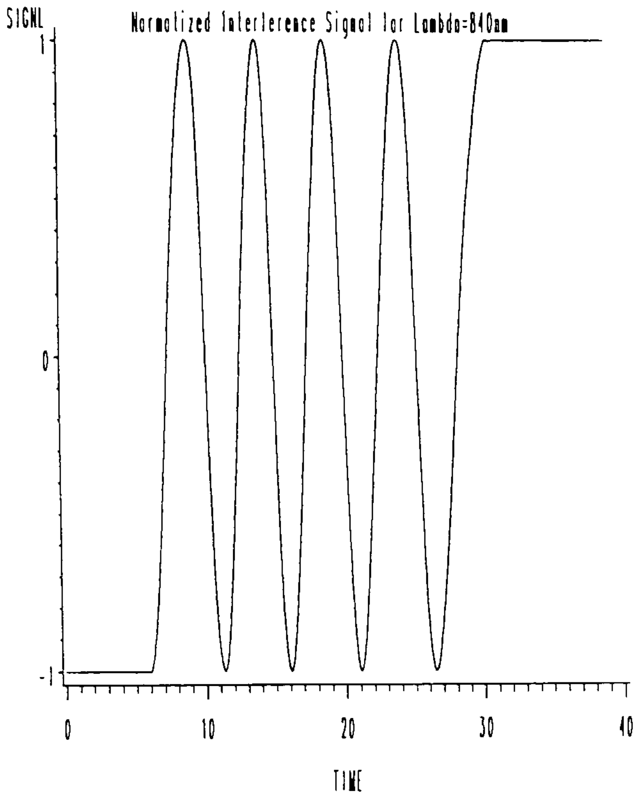

Figure 26 : Normalized interference signal for lambda = 840nm.

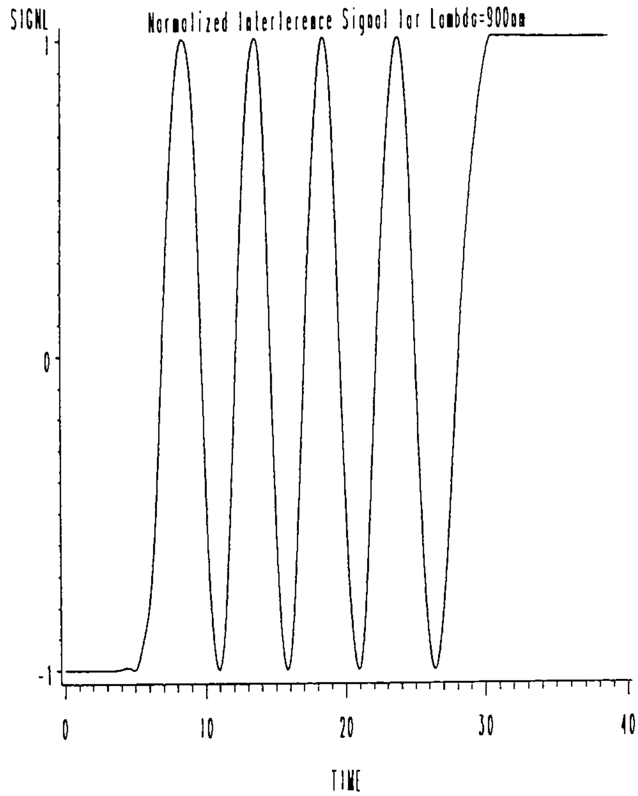

Figure 27 · Normalized interference signal for lambda = 900nm.

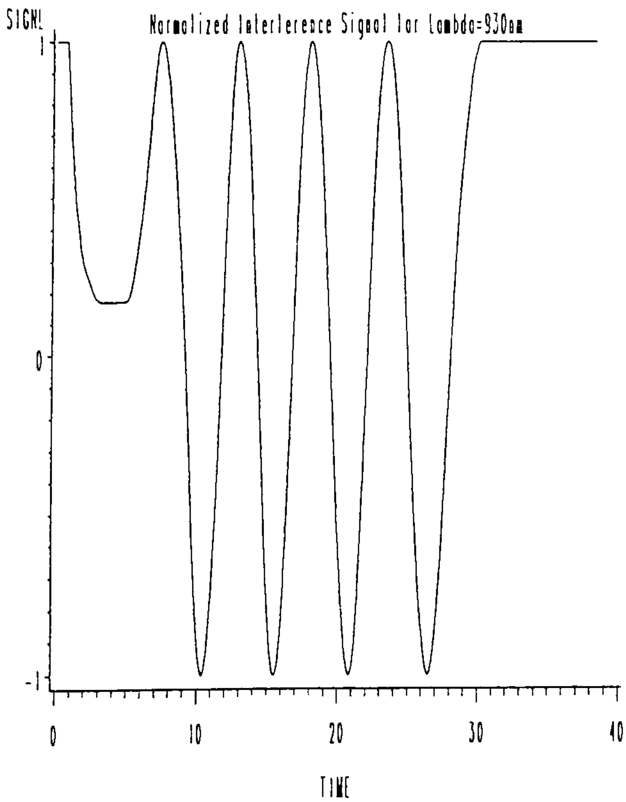

Figure 28 · Normalized interference signal for lambda = 930nm.

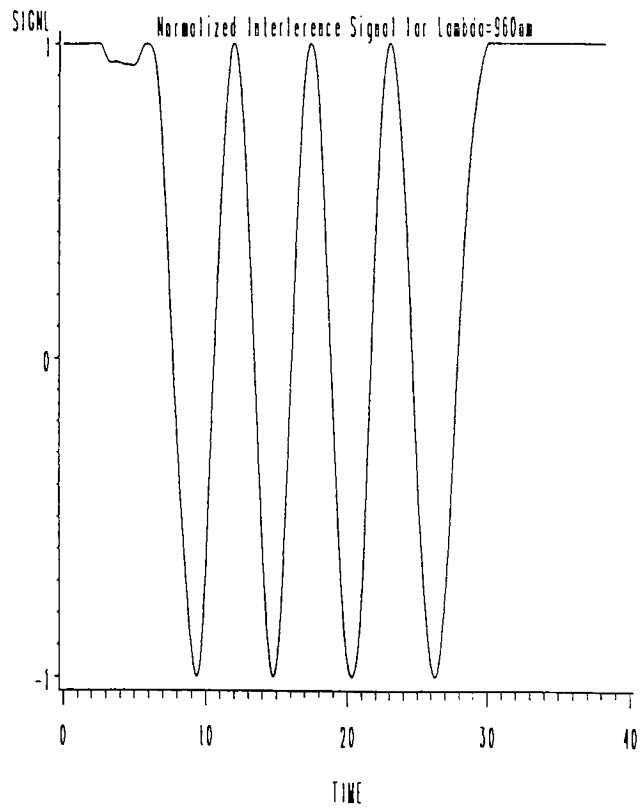

Figure 29 : Normalized interference signal for lambda = 960nm.

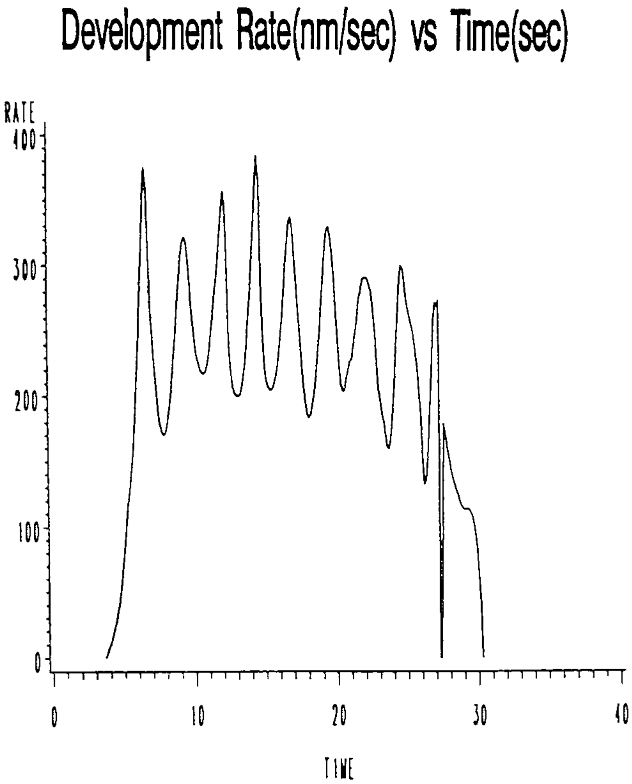

Figure 30 : In-situ development rate versus time (dose = 90mJ/cm^2).

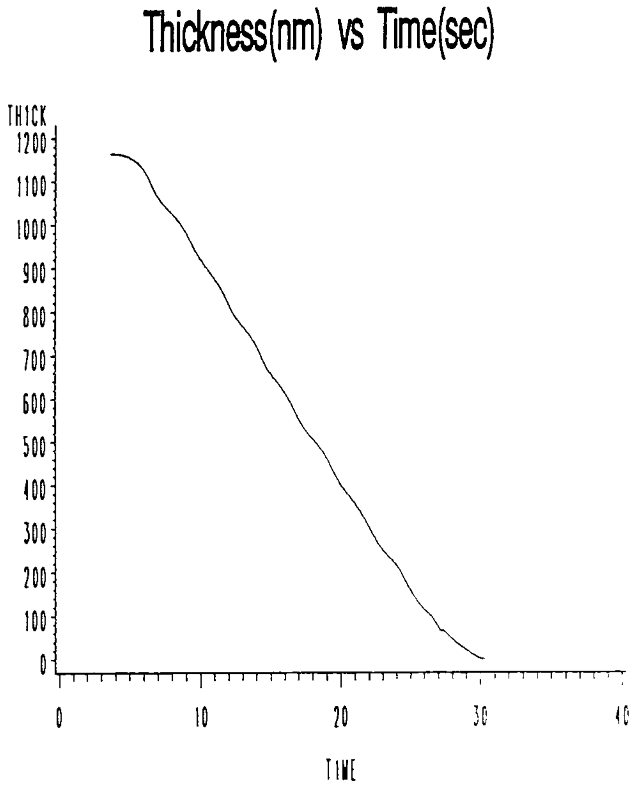

Figure 31 : In-situ resist thickness versus time (dose = 90mJ/cm^2).

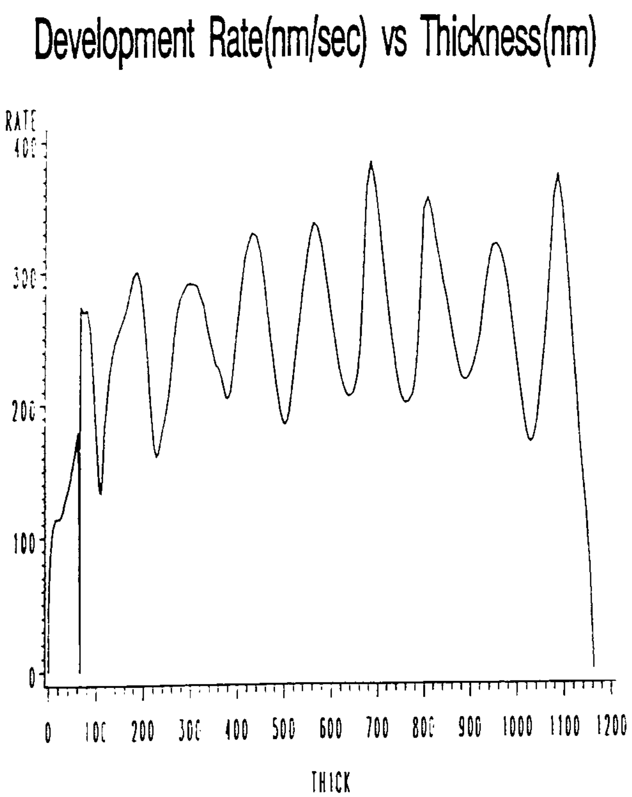

Figure 32 · In-situ development rate versus thickness (dose = 90mJ/cm^2).

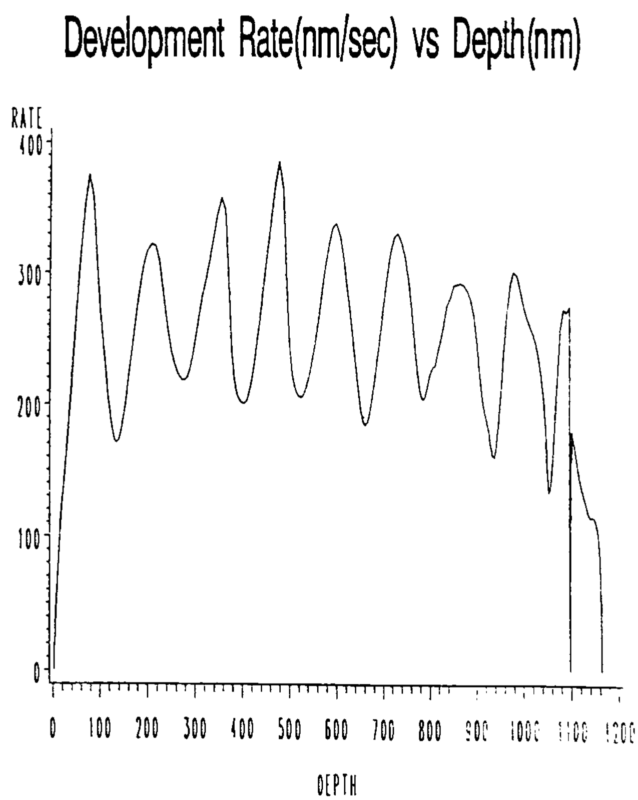

Figure 33 : In-situ development rate versus depth (dose = 90mJ/cm^2).

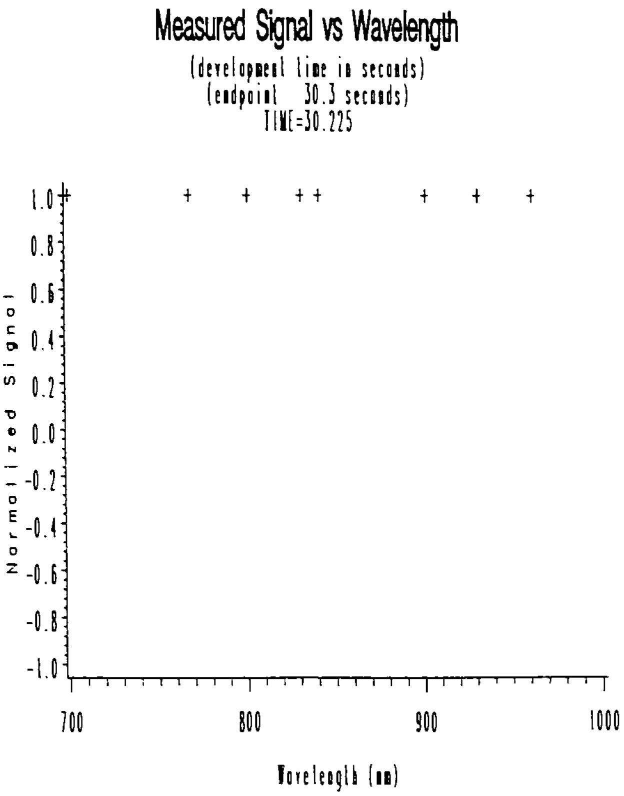

Figure 34 : Measured signal versus wavelength (time = 30.225 sec).

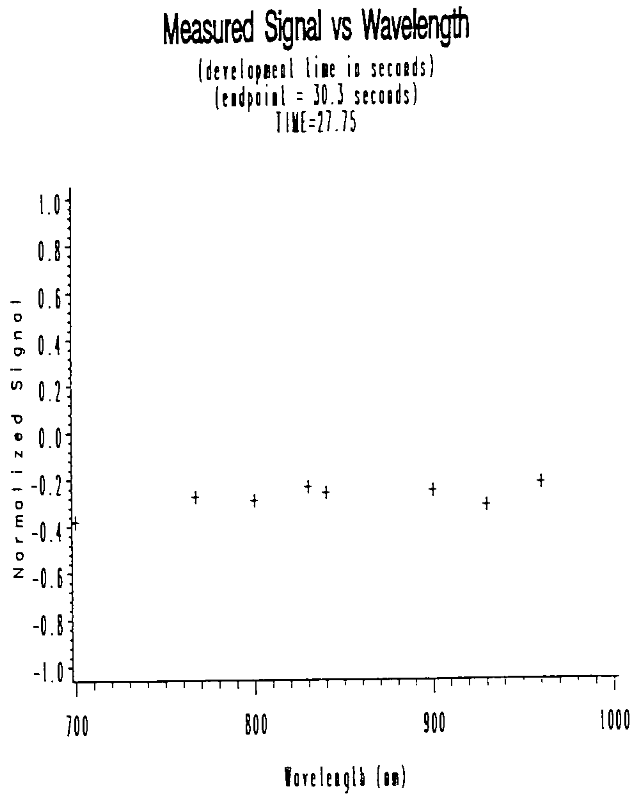

Figure 35 : Measured signal versus wavelength (time = 27.75 sec).

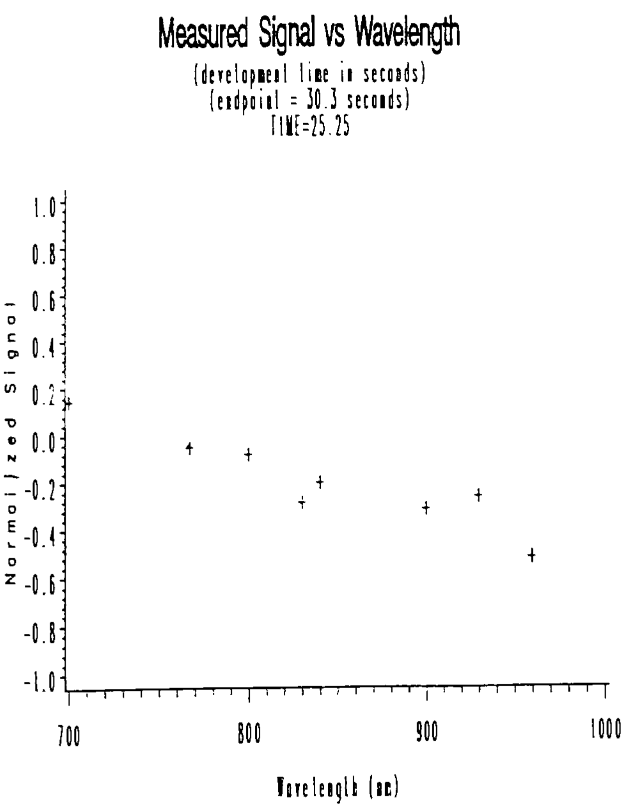

Figure 36 : Measured signal versus wavelength (time = 25.25 sec).

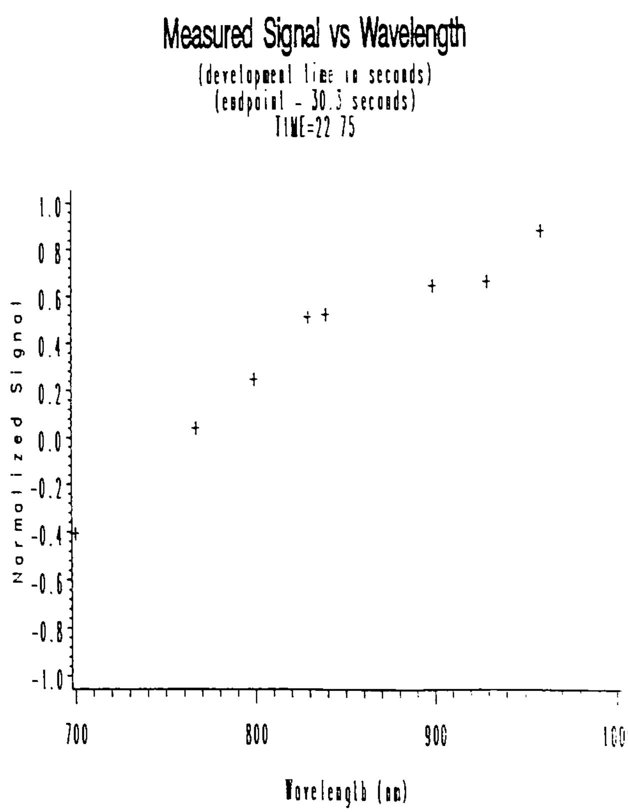

Figure 37 : Measured signal versus wavelength (time = 22.75 sec).

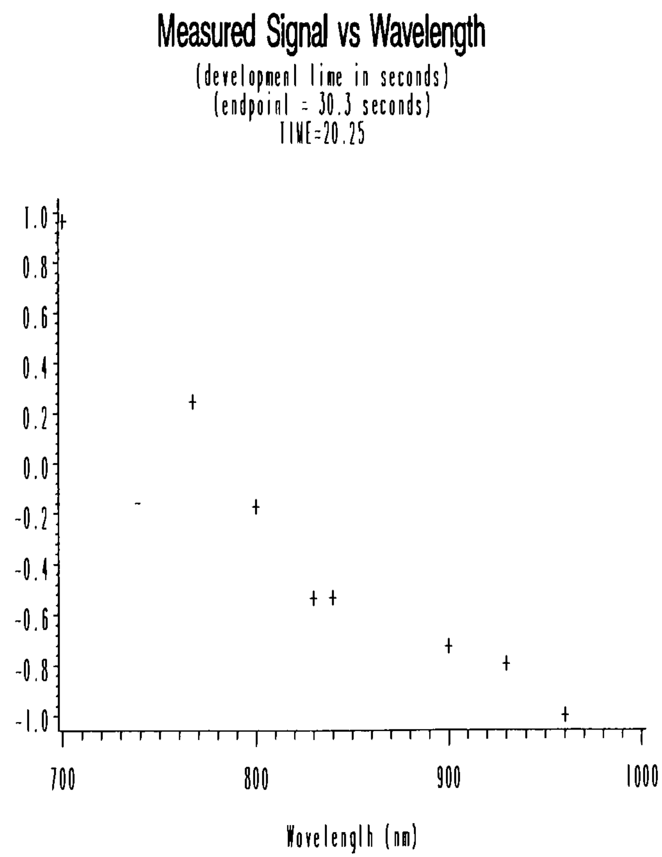

Figure 38 : Measured signal versus wavelength (time = 20.25 sec).

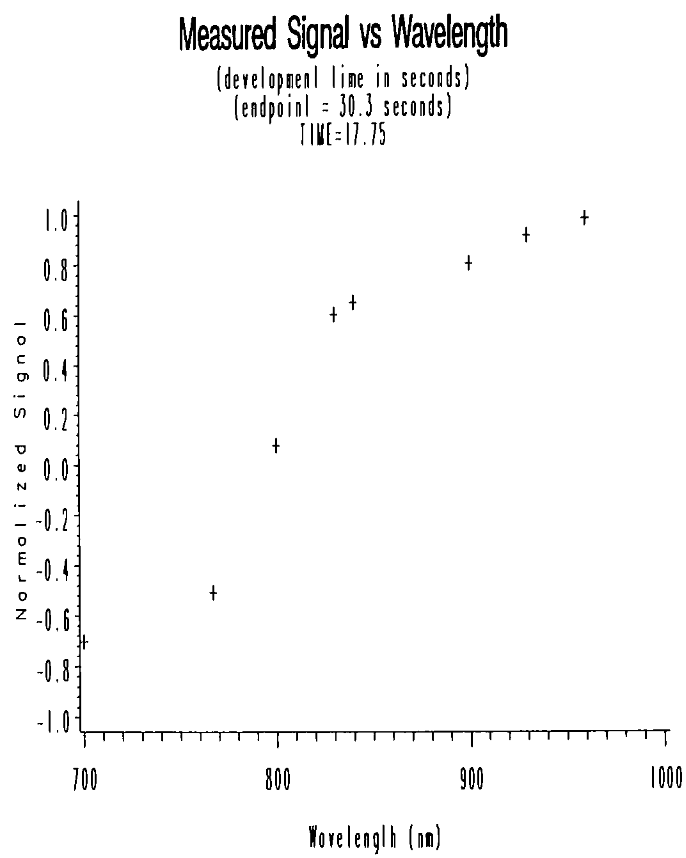

Figure 39 : Measured signal versus wavelength (time = 17.75 sec).

5.2 Model Parameter Extraction From Measured Data

5.2.1 Introduction

In order to examine the applicability of this technique to real-life photolithography, the model parameters for DNQ/Novolac positive Shipley System 812 resist with Shipley MF312 developer were sought.

5.2.2 Parameter extraction for Shipley 812 resist

Three wafers were prepared on a GCA 9000 Wafer track as follows in tables 7 through 11.

Table 7: Resist coat process steps.

Step	Time	Spin Speed
HMDS dispense	5 sec	500 RPM
Spin	25 sec	5000 RPM
Resist dispense	5 sec	500 RPM
Spin	25 sec	5000 RPM

Table 8: Pre-bake process steps.

Step	Time	Temperature
Hot plate pre-bake	45 sec	373 Kelvin

Table 9: Exposure process steps.

Wafer #	Exposure Dose	Exposure Time
1	66 mJ/cm^2	0.3143 msec
2	90 mJ/cm^2	0.4286 msec
3	114 mJ/cm^2	0.5429 msec

Table 10: Post exposure bake process steps.

Step	Time	Temperature
Hot plate PEB	45 sec	373 Kelvin

Table 11: Develop process steps.

Step	Time	Spin Speed
DI water dispense	5 sec	500 RPM
Developer spray	45 sec	500 RPM
DI water dispense	30 sec	500 RPM
Spin	30 sec	5000 RPM

Wafers were exposed with GCA 6700 G-line stepper with a 0.29 NA lens. An IL440 irradiance meter was used to measure to an irradiance of 210mW/cm^2 at the wafer surface. The reticle used for these exposures was an Exposure Test Matrix (ETM) which contains a number of test structures for focus and exposure optimization. A patterned reticle was chosen to demonstrate that the in-situ development rate can be measured from patterned resist.

If the DSM begins monitoring before the wafer surface is wet, the DSM software could detect an endpoint and erroneous measurements could have resulted. Hence, in order to gather measurements from the beginning of the development cycle, a 5.0 second DI water dispense prior to the development was added so as to provide a window of when the DSM development rate monitor could be turned on.

During the development, the interference signals were monitored for each of the three wafers and converted into plots of development rate versus depth in the resist. Crude development data for these is given in appendix E. Plots of the development rate versus time, development rate versus depth, and thickness versus time for each of the three wafers are given in figures 40 through 48. In all three cases the beginning thickness of the resist was calculated though the development rate measurement to be about 1.16μm.

Once the development rate curves were obtained, the modeling parameters could be extracted using the programs in appendices B and C. Exposure parameters used for the extraction were taken from Finle Technology's Prolith photolithography simulator for Shipley System 8 resist at 436nm. These parameters were $A=0.581\mu m^{-1}$, $B=0.082\mu m^{-1}$, and $C=0.013 cm^2/mJ$. The ANOVA for this regression is given in table 12. The algorithm in appendices B and C converged on the parameters listed in table 13.

Table 12: ANOVA table for the extraction of model parameters for Shipley 812 resist.

Source	DF	Sum of Squares	Mean Square
Regression	6	72280.498519	12046.749753
Residual	391	2412.489870	6.170051
Uncorr. Total	397	74692.988389	

Table 13: List of parameter estimates for Shipley 812 resist.

Parameter	Estimate	Asymptotic Std. Error	Asymptotic 95% CI Lower	Asymptotic 95% CI Upper
R_1 (μm/min)	25.559337	2.295053	21.047083	30.071591
R_2 (μm/min)	10.451110	0.311492	9.838692	11.063528
R_3	1.878882	0.477362	0.940351	2.817413
R_4	0.111717	0.013289	0.085590	0.137844
R_5	1.586487	0.136965	1.317203	1.855771
R_6 (μm)	0.000000	0.046279	-0.090989	0.090989
A (μm^{-1})	0.581**			
B (μm^{-1})	0.082**			
C (cm^2/mJ)	0.013**			
σ (μm)	0.0016			

** Estimates were taken from Finle Technology's Prolith software for Shipley System 8 resist at G-line exposure.

A plot of the SSE versus the PEB diffusion length constant, σ, is provided in figure 49. It was determined from this plot that a best fit (minimum SSE) could be achieved with a σ of 0.0016μm.

Using the extracted parameters in table 13 and the conditions used for processing the wafers, the development rates were simulated with the program in appendix A in order to verify the extraction routine. Plots of the development rates, simulated and measured are given in figures 50 through 52. All three plots appear to fit, particularly for the upper portions of the resist layer. It should be emphasized that only depths less than 0.7μm were used for the extraction since there is less confidence in the measured results for the bottom 0.4μm of resist.

It appears as if the models used for the simulation perhaps do not sufficiently describe the development mechanisms. For all three exposures, the predicted development rate does not seem to oscillate as far as the measured data. The predicted localized minima in the standing wave effect appears to be higher than the measured data. On the other hand the predicted maxima is lower than the measured data. Clearly, a more extensive analysis of the exposure , bake and development models needs to be performed in order to discern model inadequacies or bias from anomalous behavior.

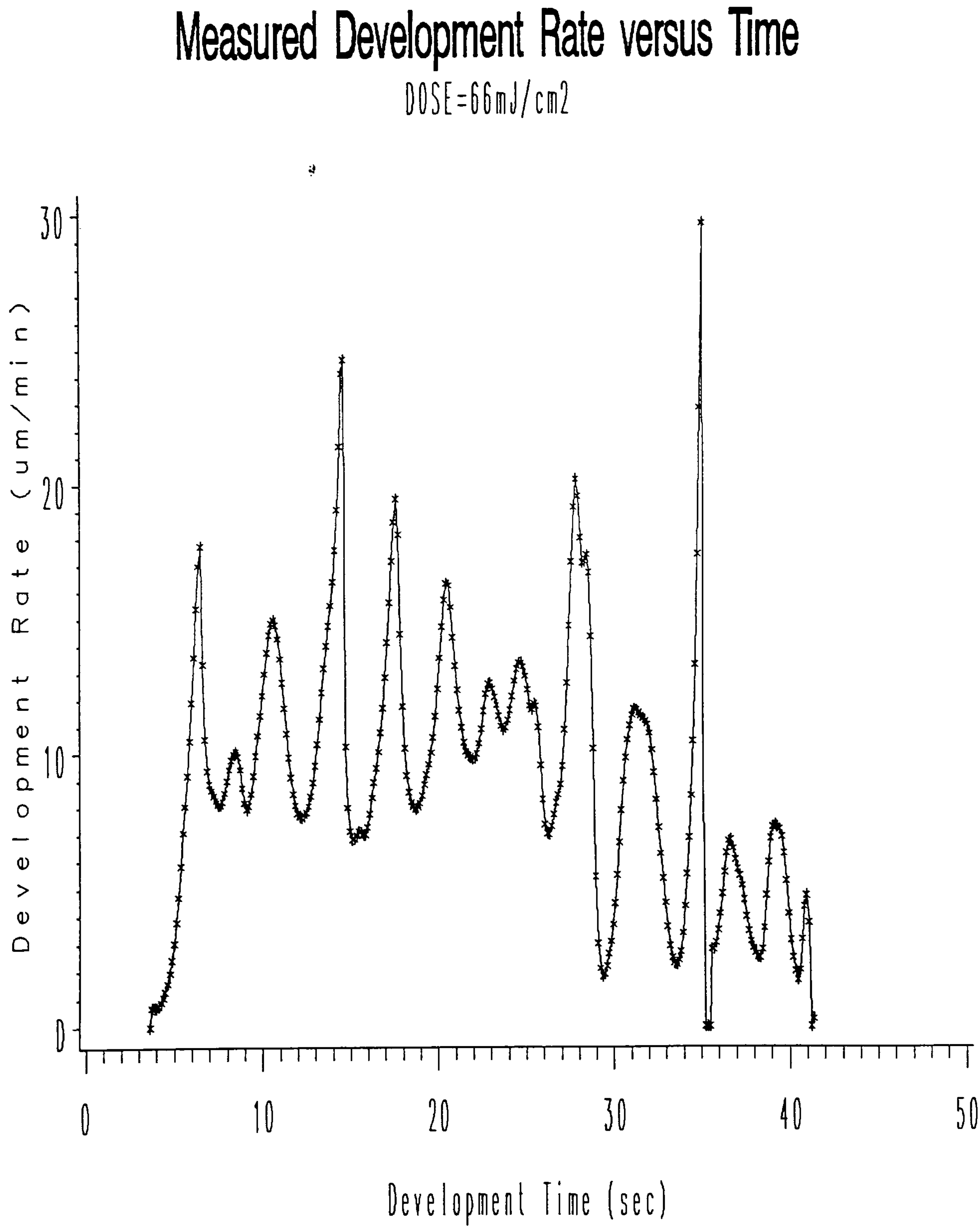

Figure 40 : In-situ development rate versus time (dose = 66mJ/cm^2).

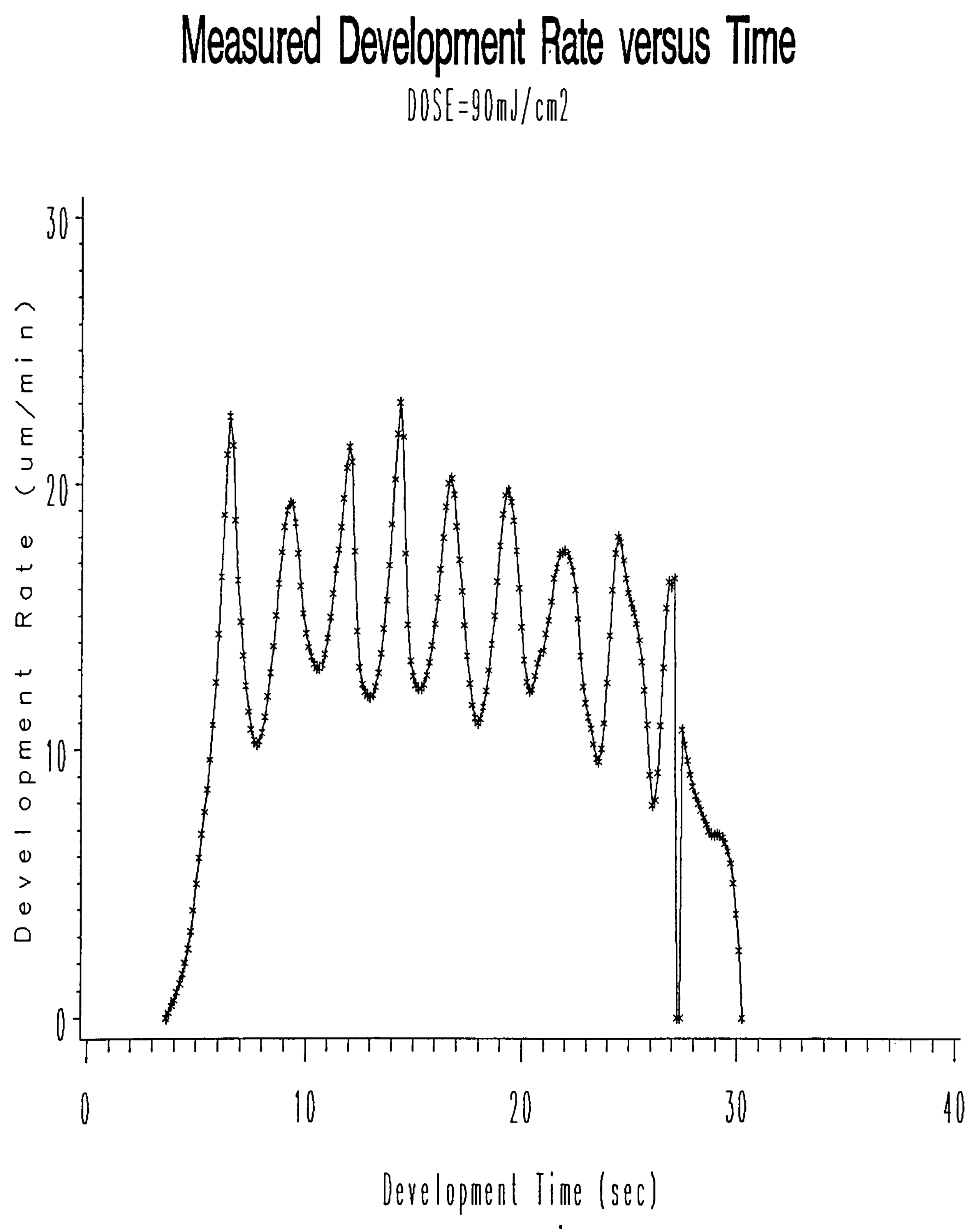

Figure 41 : In-situ development rate versus time (dose = $90mJ/cm^2$).

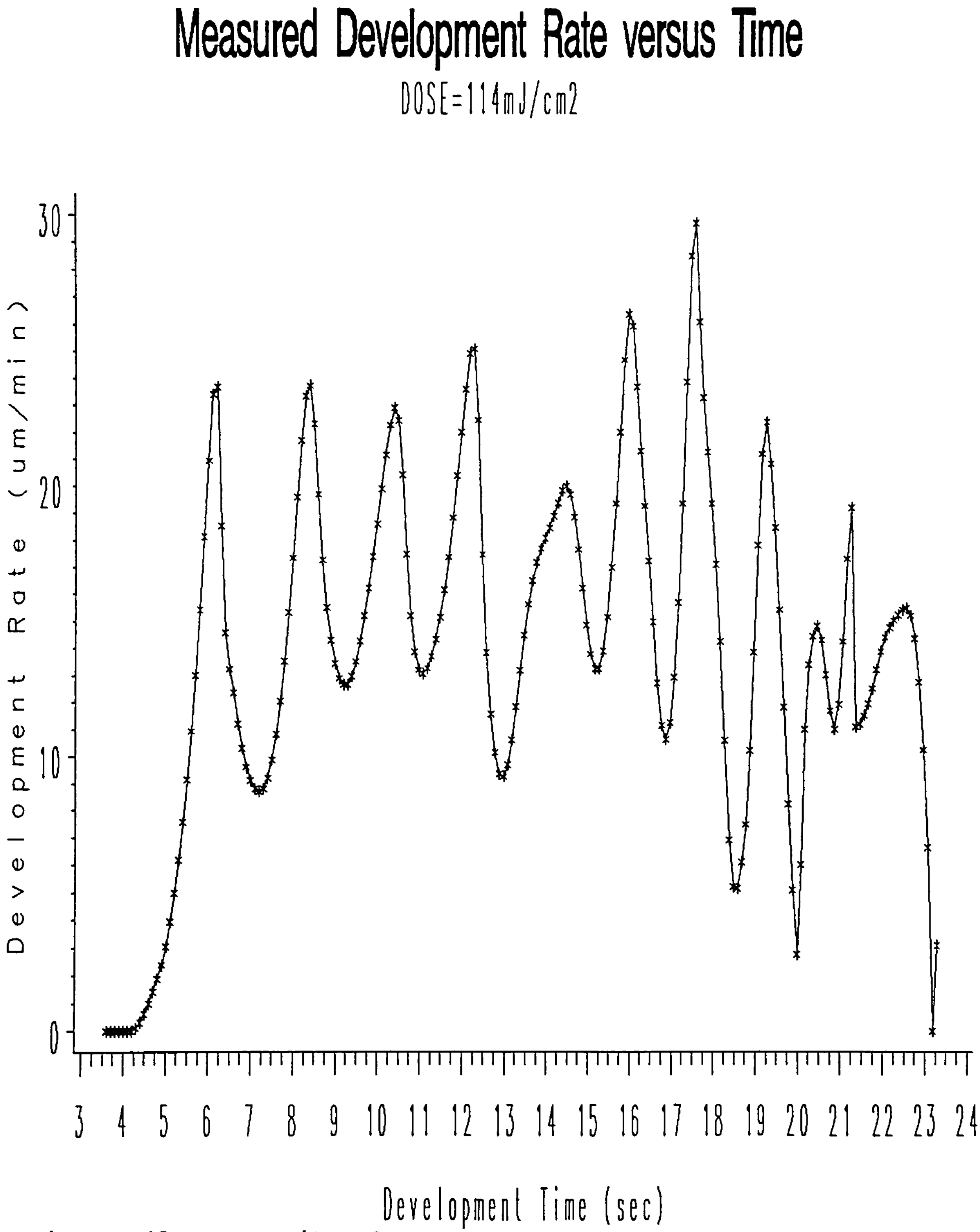

Figure 42 : In-situ development rate versus time (dose = 114mJ/cm^2).

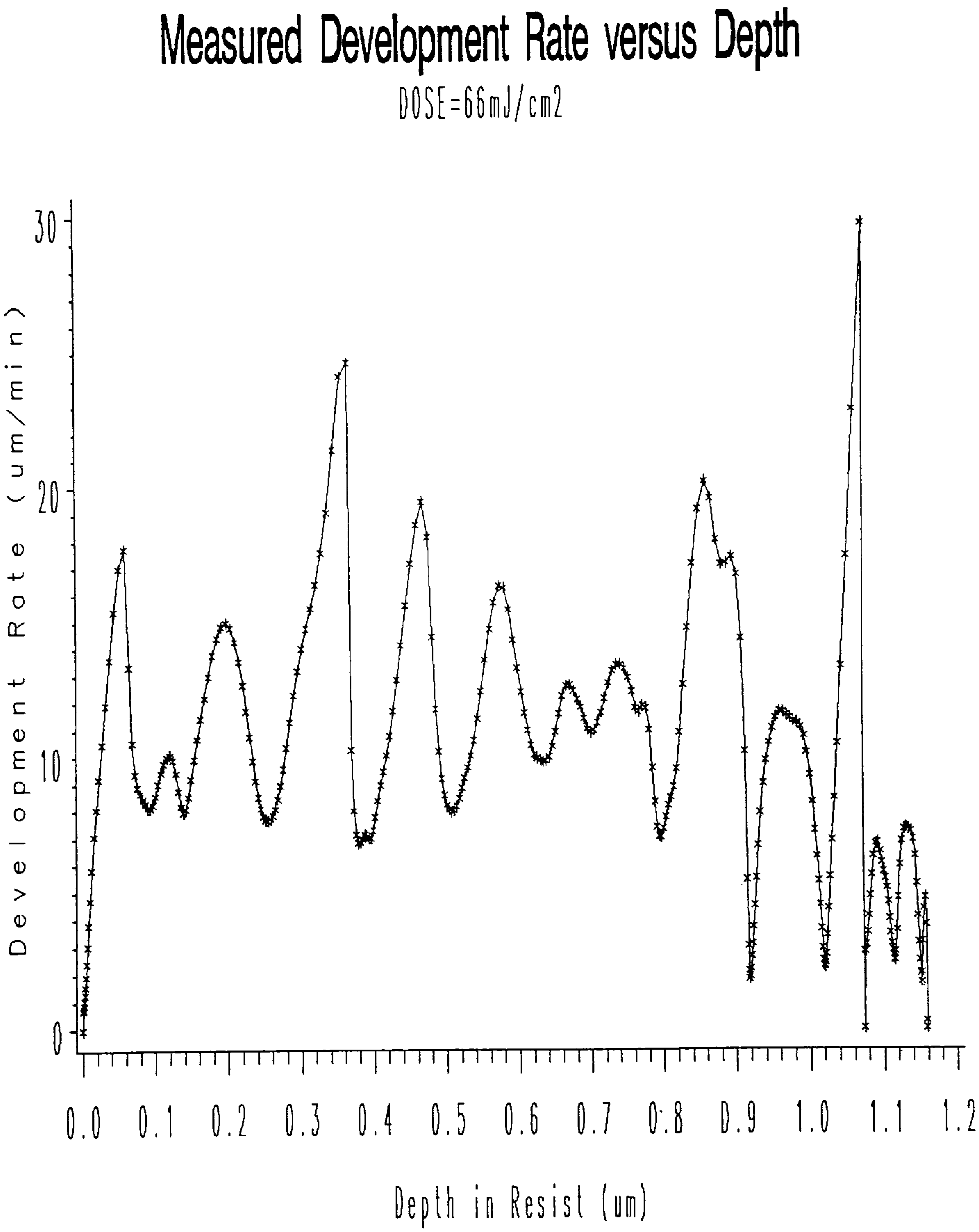

Figure 43 : In-situ development rate versus depth (dose = 66mJ/cm²).

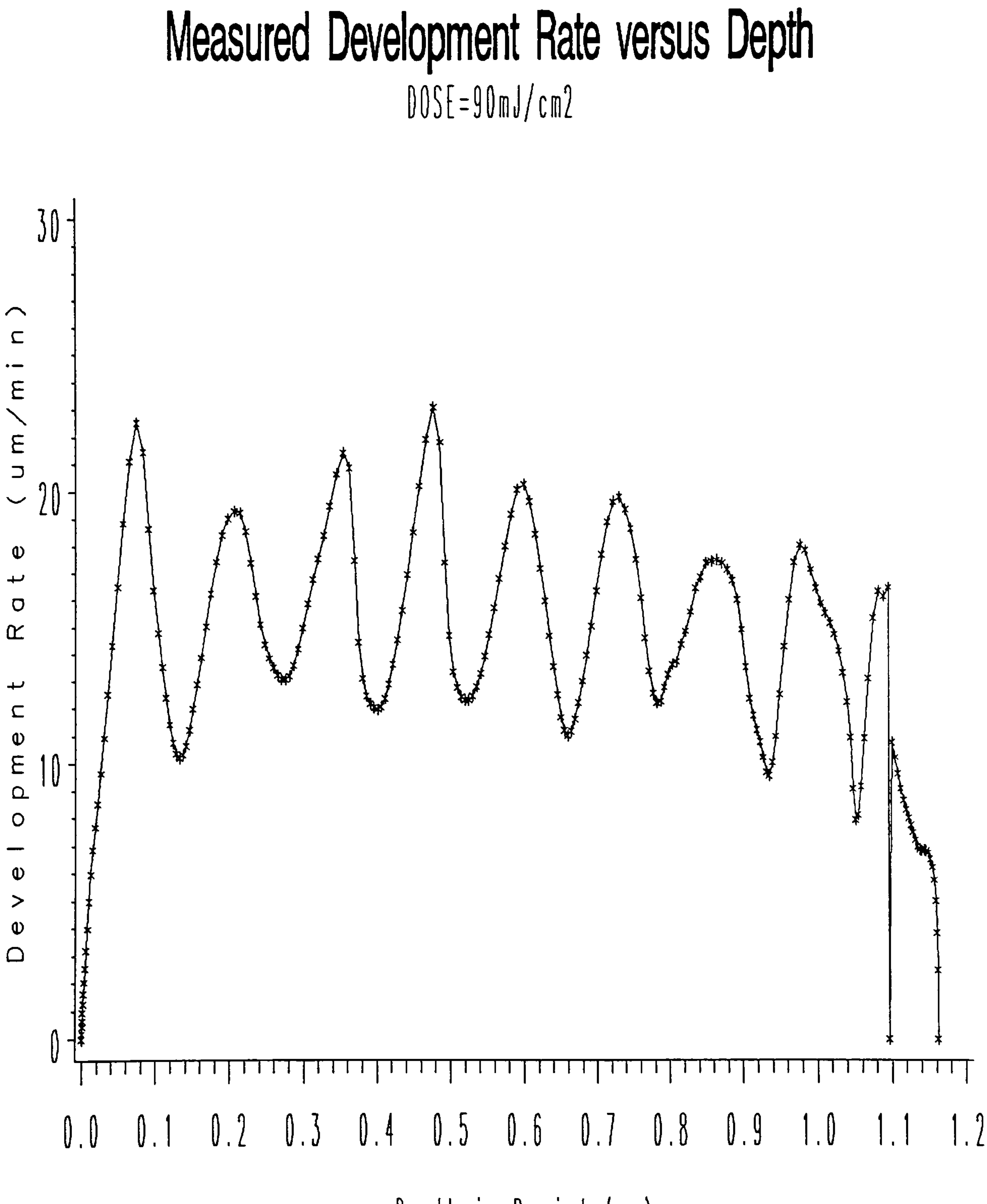

Figure 44 : In-situ development rate versus depth (dose = 90mJ/cm^2).

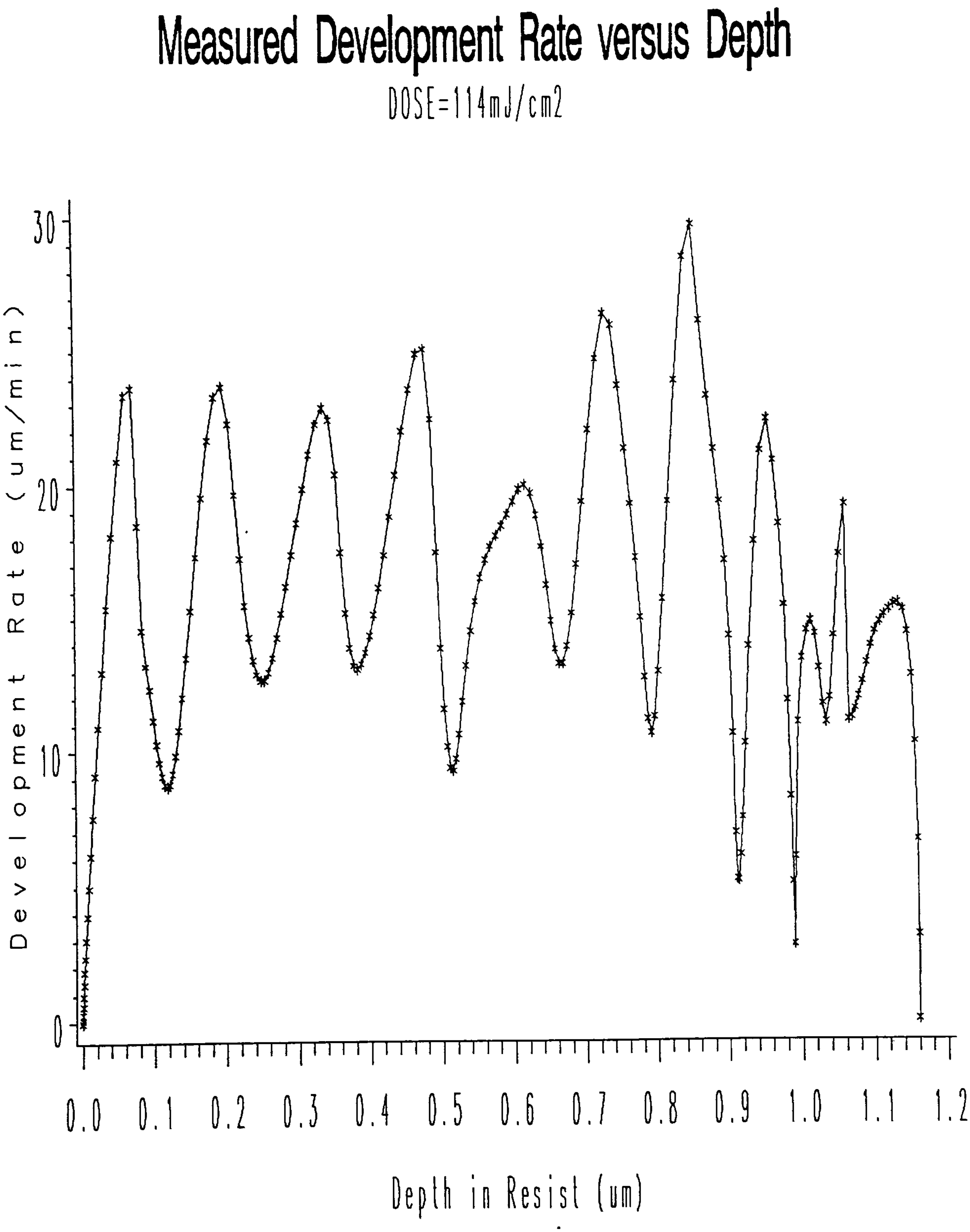

Figure 45 : In-situ development rate versus depth (dose = 114mJ/cm^2).

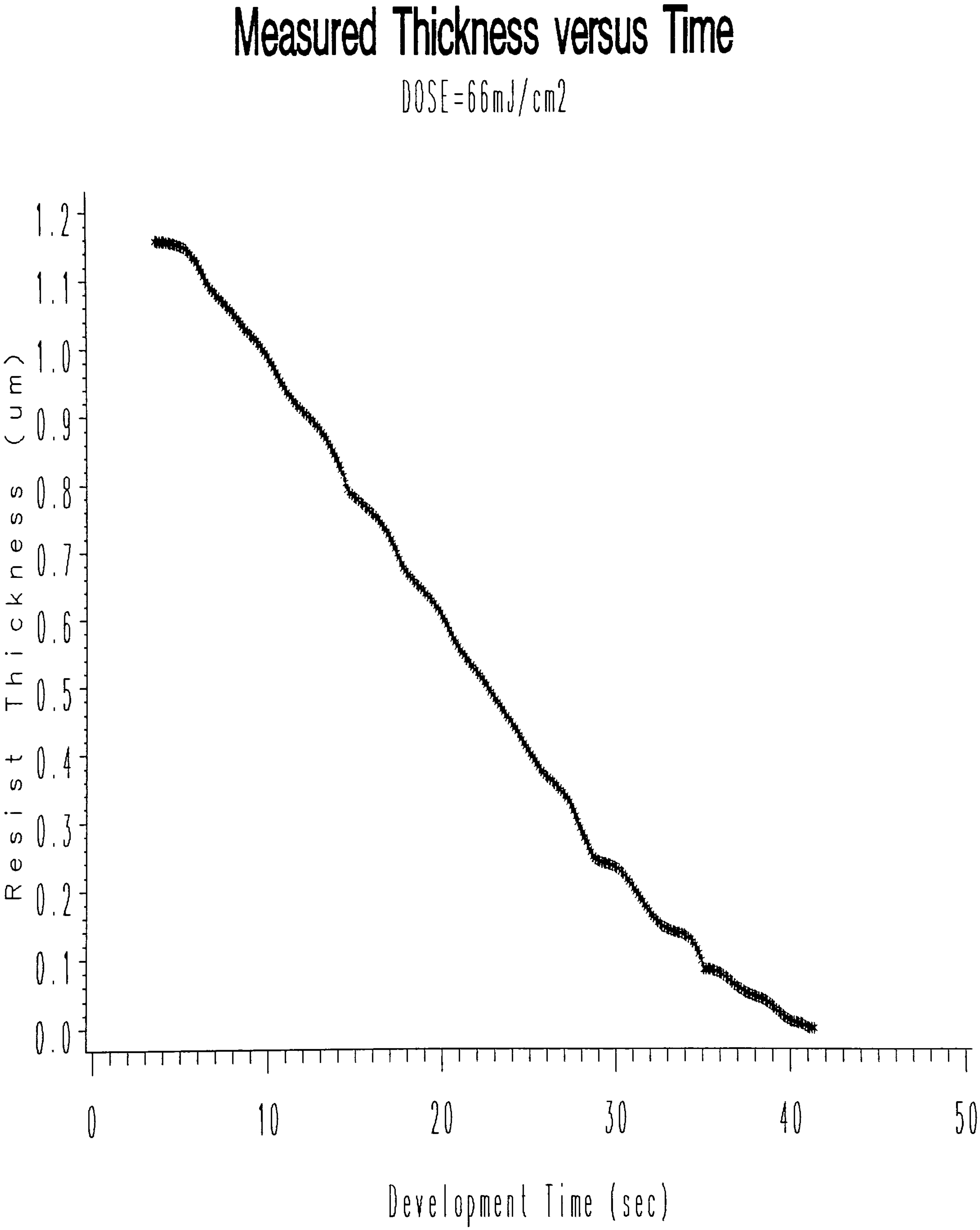

Figure 46 : In-situ thickness versus time (dose = 66mJ/cm^2).

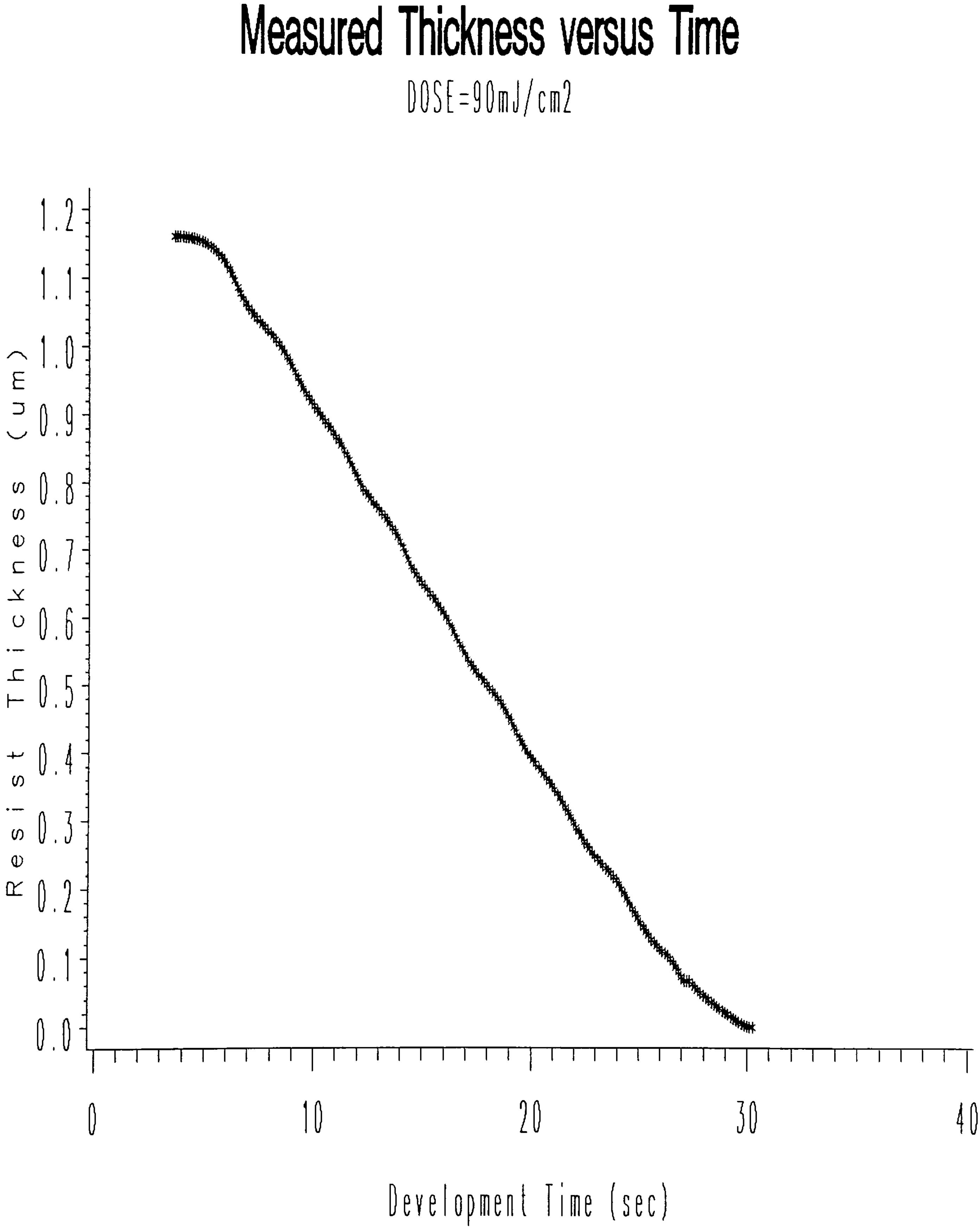

Figure 47 : In-situ thickness versus time (dose = 90mJ/cm^2).

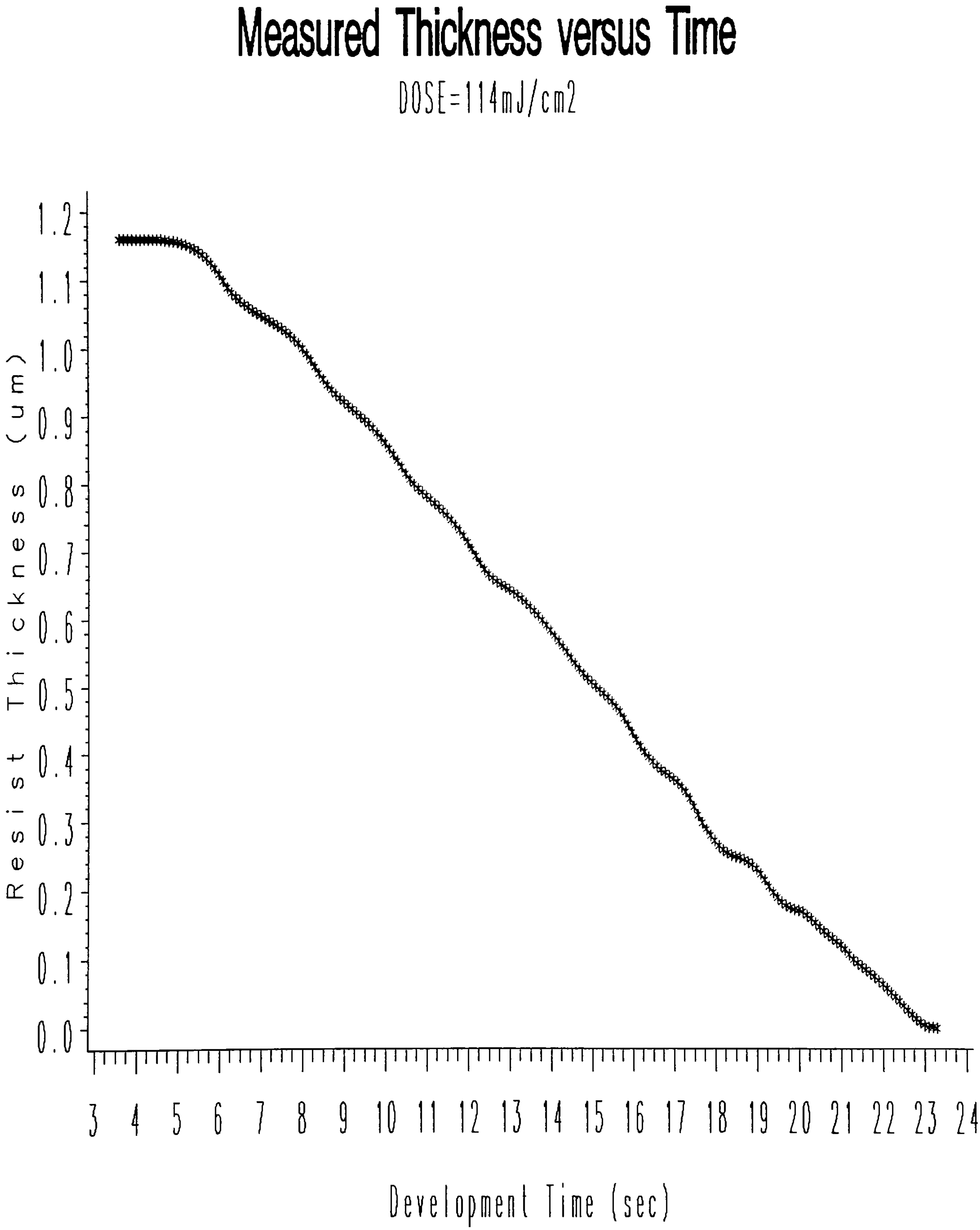

Figure 48 : In-situ thickness versus time (dose = 114mJ/cm^2).

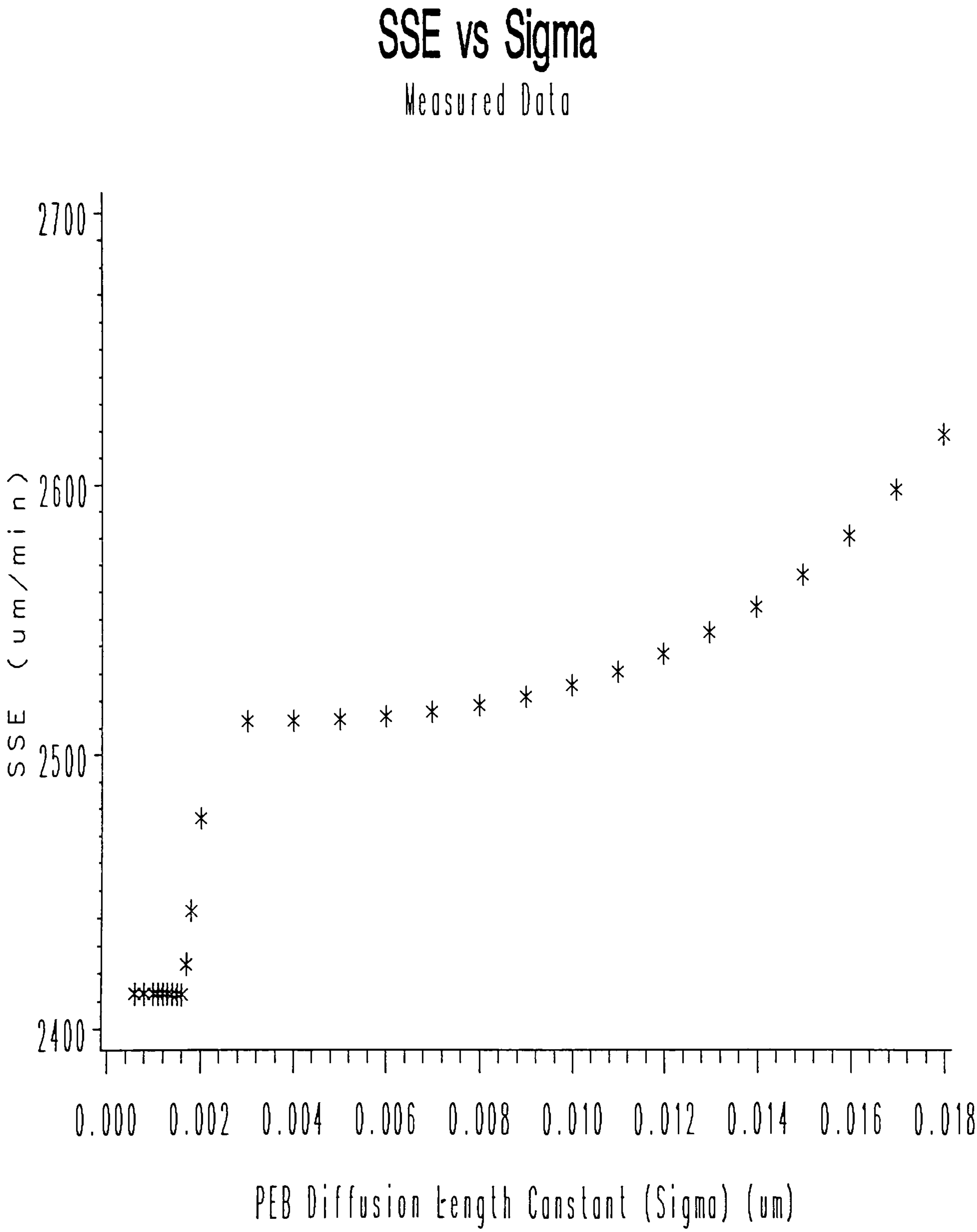

Figure 49 : Error in fit versus PEB diffusion length constant.

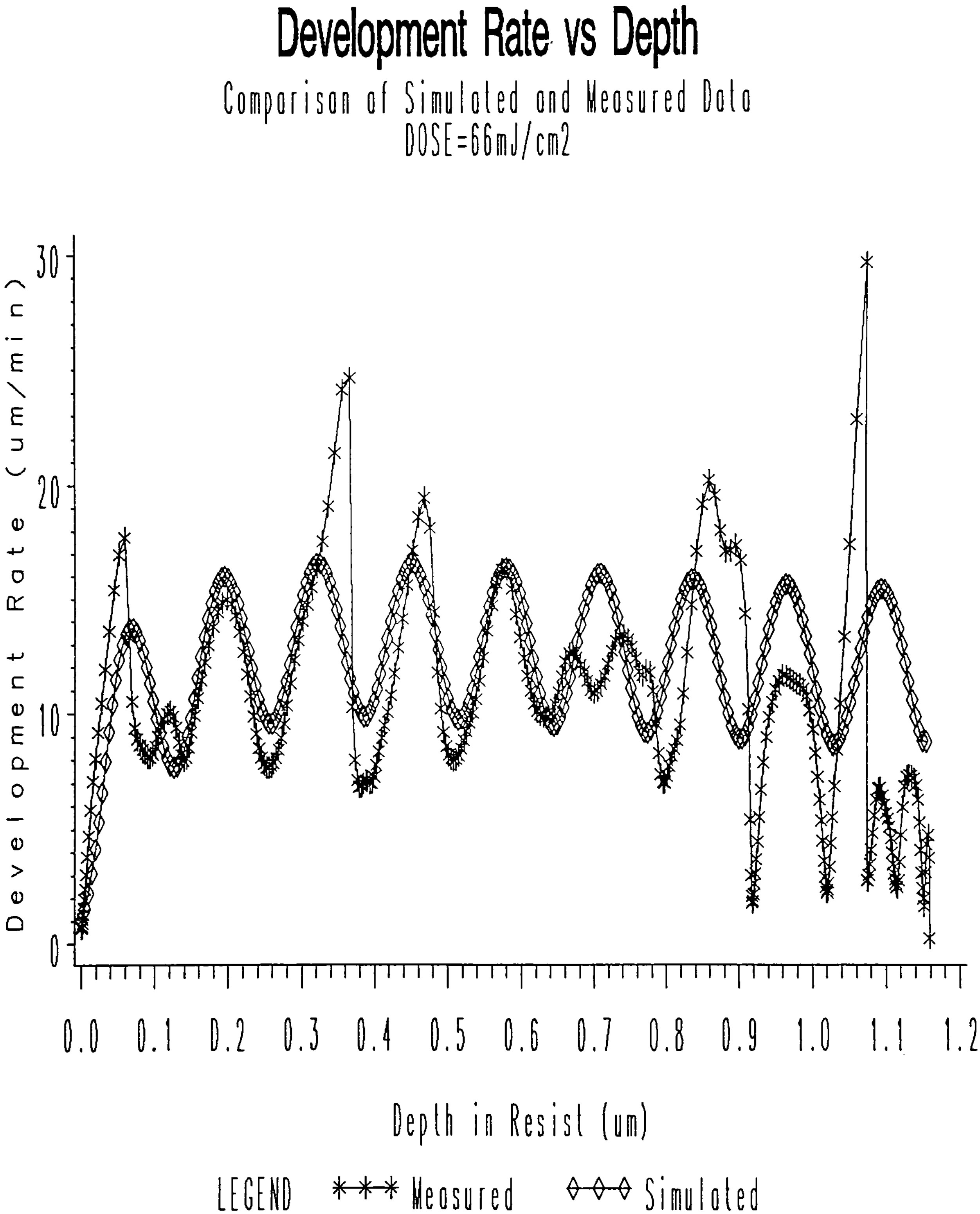

Figure 50 : Comparison of simulated and measured development rate versus depth in resist (dose = 66mJ/cm^2).

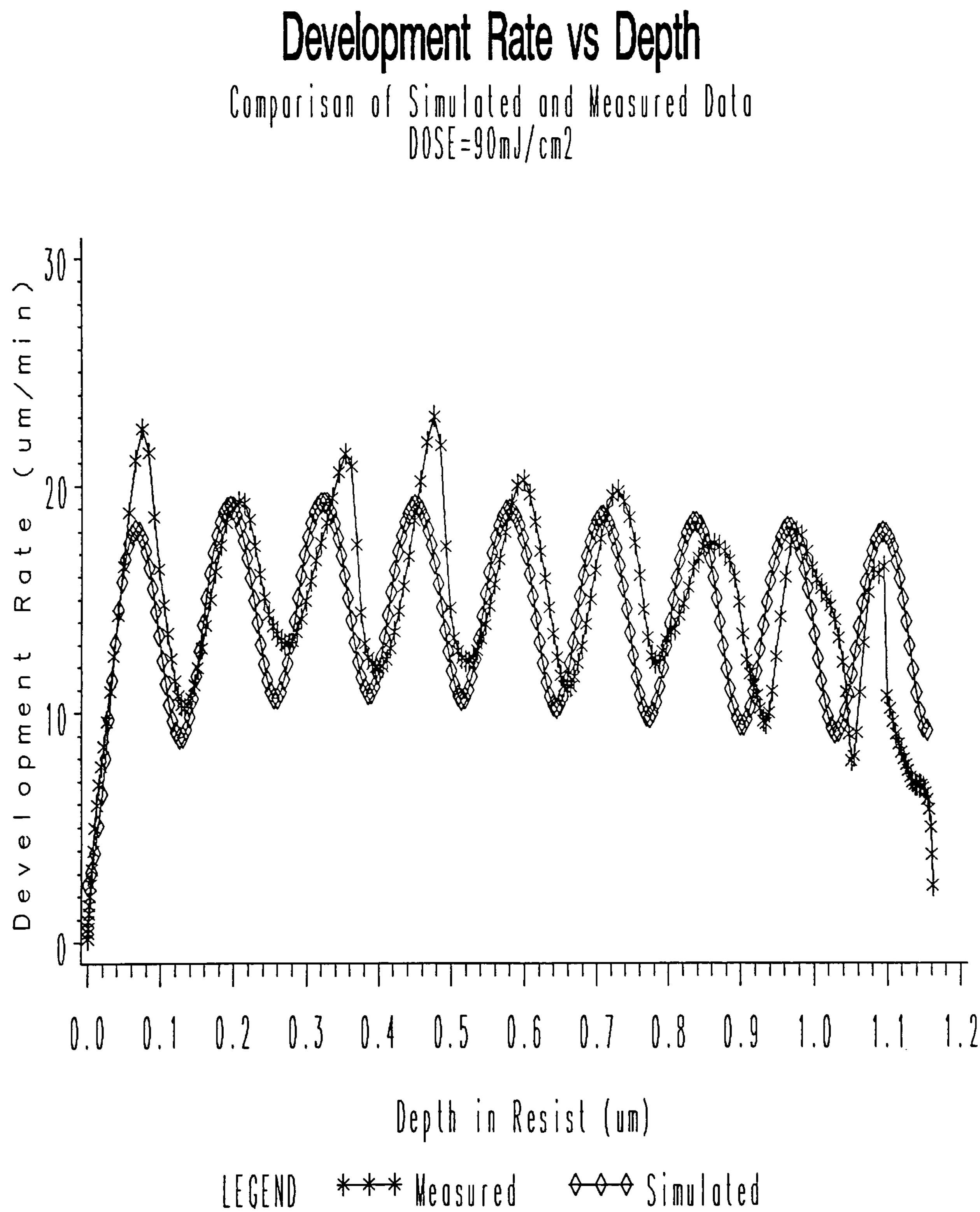

Figure 51 : Comparison of simulated and measured development rate versus depth in resist (dose = 90mJ/cm^2).

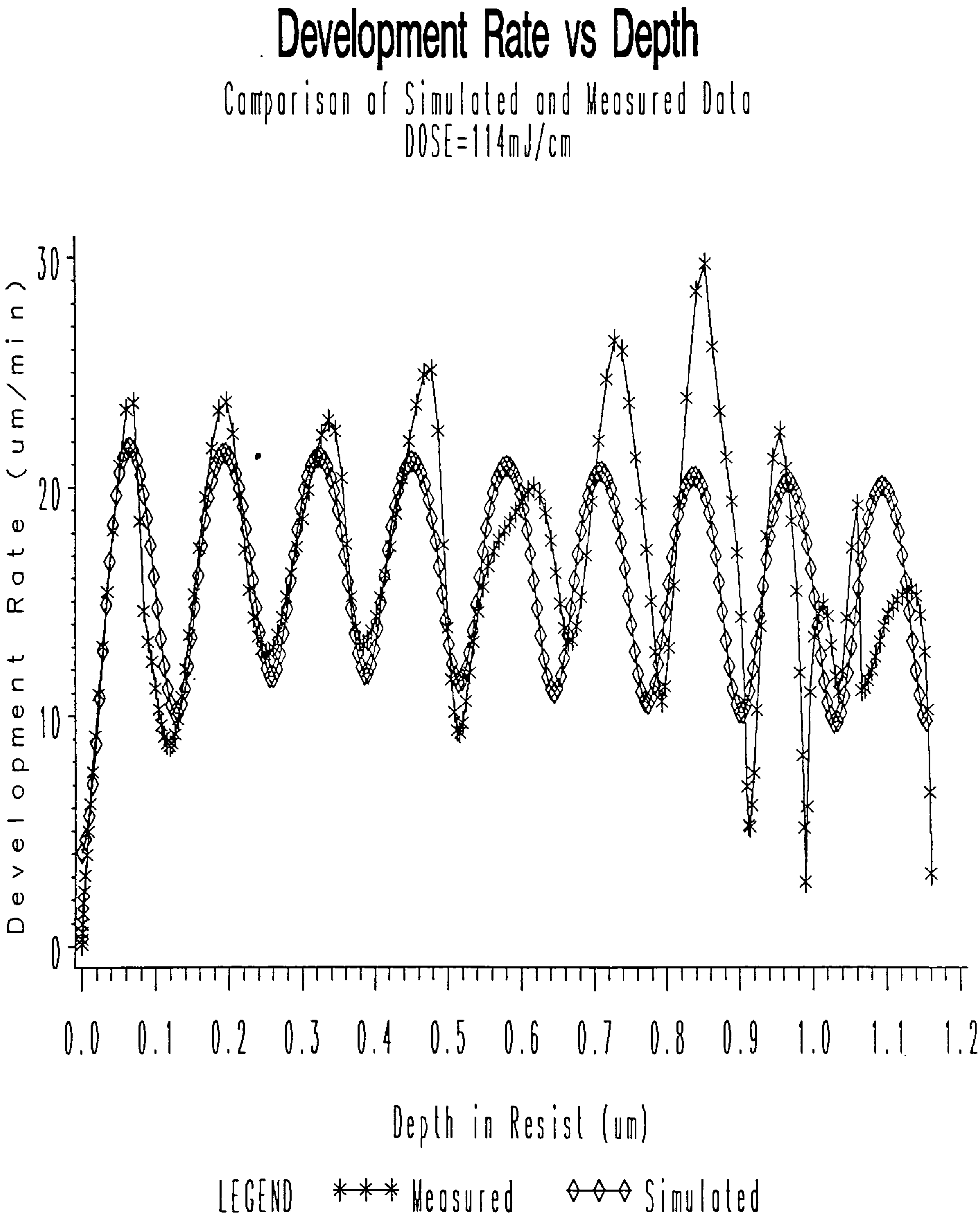

Figure 52 : Comparison of simulated and measured development rate versus depth in resist (dose = 114mJ/cm^2).

6.0 CONCLUSION

6.1 Conclusion

The value and convenience of a process specific simulation model is advantageous for timely process development. In this thesis, a method was proposed by which process specific modeling parameters can be extracted for photolithography modeling.

This approach began with an in-situ measurement of development rate versus depth in the resist, on a patterned wafer as it developed on a wafer track. Not only did the in-situ measurement demonstrate development nuances, such as surface rate inhibition and the standing wave effect, but it was also robust to ambient conditions as was demonstrated in the robust signal data of an independent study [14]. In addition, this measurement calculated the total resist thickness, resist thickness versus development time, and development rate versus development time.

Next a one-dimensional photolithography simulator was written in C to examine the relationship between model parameters. A difficult challenge was presented in how to extract the exposure parameters, but after simulation it was discovered that the set of exposure parameters were highly correlated with the development parameters. This meant that for a proposed set of exposure parameters, regardless of the accuracy, a set of development parameters could be extracted that would describe the resist profile after development.

With this extraction approach in mind, the parameters for Shipley 812 resist were extracted. It was found that for a proposed $A = 0.581\mu m^{-1}$, $B = 0.082\mu m^{-1}$, and $C = 0.013 cm^2/mJ$, the development parameters, $R_1 = 25.559\mu m/min$, $R_2 = 10.451\mu m/min$, $R_3 = 1.879$, $R_4 = 0.112$, $R_5 = 1.586$, $R_6 = 0.000\mu m$, and $\sigma = 0.0016\mu m$, were found. A plot comparison of measured and simulated development rate demonstrated the closeness of the simulation fit. It was concluded from this comparison that a more extensive model adequacy check should be performed in future analysis.

REFERENCES

[1] F. H. Dill, "Optical Lithography," Trans. Electron Dev., Vol. ED-22, No. 7, (July 1975) pp. 440-444.

[2] F. H. Dill, W. P. Hornberger, P. S. Hauge, J. M. Shaw, "Characterization of Positive Photoresist," Trans. Electron Dev., Vol. ED-22, No. 7, (July 1975) pp. 445-452.

[3] F. H. Dill, A. R. Neureuther, J. A. Tuttle, E. J. Walker, "Modeling Projection Printing Positive Photoresists," Trans. Electron Dev., Vol. ED-22, No. 7, (July 1975) pp. 456-464.

[4] C. A. Mack, "Modeling the Effects of Prebake on Positive Resist Processing," Kodak Microelec. Interface '85 (Nov. 1985) pp. 155-158.

[5] C. A. Mack, "A Diffusion Model for Post-Exposure Bake," source unknown.

[6] P. D. Flanner III, "Semi-automated Measurements of Photoresist Optical Parameters," Philips Research Laboratories, internal technical report.

[7] P. D. Flanner III, "Improved Methods of Photoresist Development Characterization," Philips Research Laboratories, internal technical report.

[8] M. Exterkamp, W. Wong, H. Damar, A. R. Neureuther, C. H. Ting, W. G. Oldham, "Resist Characterization: Procedures, Parameters, and Profiles," Optical Lithography, SPIE Vol. 334 (1982) pp. 182-187.

[9] C. Zee, W. R Bell, A. R. Neureuther, "Effect of Developer Type and Agitation on Dissolution of Positive Photoresist," Adv. in Resist Tech. and Processing V, Proc., SPIE, Vol. 920, (1988) pp. 154-161.

[10] W. R. Bell II, P. D. Flanner II, C. Zee, N. Tam, A. R. Neureuther, "Determination of Quantitative Resist Models from Experiment," Adv. in Resist Tech. and Proc. V, Proc., SPIE, Vol. 920, (1988) pp. 382-389.

[11] A. S. Chiu, et al., "Resist Parameter Extraction (PARMEX) with Graphical Interface in X," Adv. in Resist Tech. and Proc. VIII, Proc., SPIE, Vol. 1466, (1991) pp. 641-652.

[12] R. A. Ferguson, et al., " Modeling and Simulation of Multiple Chemical States in Photoresist Materials," Adv. in Resist Tech. and Proc. VI, Proc., SPIE, Vol. 1086, (1989) pp. 262-273.

[13] C. A. Spence, R. A. Ferguson, "Some Experimental Techniques for Characterizing Photoresists," Adv. in Resist Tech. and Proc. VIII, Proc., SPIE, Vol. 1466, (1991) pp. 324-335.

[14] K. M. Monahan, "Endpoint Detection of Photoresist Development Using Multiple Wavelengths and Polarized Light," Integrated Circuit Metrology, Inspection, and Process Control III, Proc., SPIE, Vol. 1087, (1989) pp. 322-331.

[15] H. M. Wadsworth, K. S. Stephens, A. B. Godfrey, **Modern Methods for Quality Control and Improvement**, John Wiley and Sons, New York, 1986, pp. 310-313.

[16] P. Trefonas III, "Positive Photoresist Development: A Multiple State Percolation Model," Adv. in Resist Tech. and Proc. VI, Proc., SPIE, Vol. 1086, (1989) pp. 484-494.

[17] S. Wolf, R. N. Tauber, **Silicon Processing for the VLSI Era: Volume 1 - Process Technology**, Lattice Press, Sunset Beach, CA, 1986.

[18] L. F. Thompson, C. G. Wilson, M. J. Bowden, **Introduction to Microlithography**, American Chemical Society, Washington, D. C., 1983.

[19] E. J. Walker, "Reduction of Photoresist Standing-Wave Effects by Post-Exposure Bake," Trans. Electron Dev., Vol. ED-22, No. 7 (July 1975) pp. 464-466.

[20] A. R. Neureuther and F. H. Dill, "Photoresist Modeling and Device Fabrication Applications," Optical and Acoustical Micro-Electronics, Polytechnic Press, pp. 223-247, 1974.

[21] S. V. Babu, E. Barouch, "Exact Solution of Dill's Model Equations for Positive Photoresist Kinetics," IEEE Electron Dev. Letters, Vol. EDL-7, No. 4, (April 1986) pp. 252-253.

[22] S. V. Babu, E. Barouch, "Exposure Bleaching of Nonlinear Resist Materials: Exact Solution," IEEE Electron Dev. Letters, Vol. EDL-8, No. 9, (Sept 1987) pp. 401-403.

[23] D. J. Kim, W. G. Oldham, A. R. Neureuther, "Development of Positive Photoresist," Trans. Electron Dev., Vol. ED-31,

No. 12, (December 1984) pp. 1730-1736.

[24] C. A. Mack, "Development of Positive Photoresist," Jour. Electrochem. Soc., Vol. 134, No. 1 (jan. 1987) pp. 148-152.

[25] S. A. Robertson, et al., "Photoresist Dissolution Rates: A Comparison of Puddle, Spray, and Immersion Processes," Integrated Cir. Metrology, Insp., and Proc. Control V, Proc., SPIE, Vol. 1464, (1991) pp. 232-244.

[26] E. Hecht, Optics, Addison-Wesley, Reading, MA, 1987, 94-104.

[27] N. R. Draper, H. Smith, **Applied Regression Analysis**, John Wiley and Sons, New York, 1981, pp. 458-517.

[28] G. A. F. Seber, C. J. Wild, **Nonlinear Regression**, John Wiley and Sons, New York, 1989.

[29] **SAS/STAT User's Guide**, Version 6, Fourth Edition, Volume 2, SAS Institute, Cary, NC, 1990, pp. 1135-1193.

[30] D. W. Marquardt, "An Algorithm for Least-Squares Estimation of Nonlinear Parameters," J. Soc. Indust. Appl. Math., Vol. 11, No. 2, (June 1963) pp. 431-441.

[31] M. R. Hannifan, D. C. DeBruin, "Measurement and Control Systems for In-Situ Development Processes: Technology Advancements and Application Capabilities," Site Services promotional documentation (June 1991).

[32] M. R. Hannifan, "Lithacon 808 Process Analyzer: Application Capabilities," Site Services promotional documentation (June 1991).

APPENDIX A

C SOURCE CODE FOR ONE DIMENSIONAL PHOTOLITHOGRAPHY SIMULATION

```
/*Program:simul.c
  Written by: Patrick G. Drennan
  Date:2/18/93

  This program simulates in 1-dimension, the pre-bake, exposure,
  post exposure bake (PEB) and development of conventional
  positive photoresist on Silicon. It uses the Dill model for
  exposure, the Mack pre-bake model, the Mack PEB model, and
  Kim development model. It simulates three different exposures
  (at 66mJ/cm2, 90mJ/cm2, and 114mJ/cm2) and outputs the
  development rates, the development times and depth in the
  resist in a file called "ccddata.out".

*/

#include <stdio.h>
#include <math.h>
#include "complex.h"

/*divide the resist into 250 sublayers and break up the
  exposure into 50 intervals to approximate the differential
  equations of the Dill model.*/

#define numpts 250
#define numtint 50
#define pi 3.14159265

/* G-line exposure */
#define lambda 0.4358

/* define the complex refractuve index for Silicon */
#define nSi Complex(4.73,-0.138)

/* The universal gas constant is in C/(mole*degreeK) */
#define R 1.987

/* speed of light in meters/second */
#define light 3.0e8

/* dielectric constant in F/m */
#define epsilon 8.85e-12

/* define the Kim development rate parameters */
#define R1 14.4
#define R2 0.03
#define R3 8.1
#define R4 0.24
#define R5 0.76
#define R6 0.55


void matmult();
void ccd();
```

```
main()
{
  FILE *fp2;
  float dilla,dillb,dillc,thick,refind,preea,prear,fpac,
    pebea,pebdo,dose,pretime,pretemp,pebtime,pebtemp;
  float tc,deltath,alpha,m[numpts],n,exparg,Kt,relm;
  float efield,inten,sigma,mnew[numpts],rate[numpts],time;
  fcomplex cumul[4],addon[4],ebotplus,nnow,nnext,ij,etopplus;
  int j,k;

  if ((fp2 = fopen("ccddata.out","w"))==NULL){
    printf("cannot open write file\n");
    exit(1);
    }


/* define the Dill exposure parameters, A, B, & C */
  dilla=0.5198;
  dillb=0.2700;
  dillc=0.014;

/* define the thickness of the photoresist in microns */
  thick=1.1;

/* define the magnitude of the refractive index of the resist */
  refind=1.68;

/* define the activation energy for the Arrhenius equation in
   the Mack pre-bake model */
  preea=29.5;

/* define the Arrhenius coefficient for the Mack pre-bake
   model */
  prear=35.3;

/* fpac is the ratio of the Dill B parameter after and before
   a long pre-bake. This is a parameter that is define by TMA
   for Depict II and is used here to define B-Fullbake for the
   sake of continuity. */
  fpac=1.5;

/* define the activation energy for the Arrhenius equation in
   the Mack PEB model */
  pebea=62.0;

/* define the Arrhenius constant for the Mack PEB model.*/
  pebdo=87.5;

/* define the exposure dose for the first simulation */
  dose=66.0;

/* define the  pre-bake time and temperature for the Mack
   pre-bake model */
  pretime=0.5;
```

```
  pretemp=373.0;

/* define the PEB time and temperature for the Mack PEB model */
  pebtime=0.75;
  pebtemp=383.0;

/* run the first simulation */
  ccd(1,dilla,dillb,dillc,thick,refind,preea,prear,fpac,pebea,
    pebdo,dose,pretime,pretemp,pebtime,pebtemp,fp2);

/* change the exposure for the second simulation */
  dose=90.0;
  pretime=0.5;
  pretemp=373.0;
  pebtime=0.75;
  pebtemp=383.0;
  ccd(2,dilla,dillb,dillc,thick,refind,preea,prear,fpac,pebea,
    pebdo,dose,pretime,pretemp,pebtime,pebtemp,fp2);

/* change the exposure for the second simulation */
  dose=114.0;
  pretime=0.5;
  pretemp=373.0;
  pebtime=0.75;
  pebtemp=383.0;
  ccd(3,dilla,dillb,dillc,thick,refind,preea,prear,fpac,pebea,
    pebdo,dose,pretime,pretemp,pebtime,pebtemp,fp2);

  fclose(fp2);
}


void ccd(tc,dilla,dillb,dillc,thick,refind,preea,prear,fpac,
  pebea,pebdo,dose,pretime,pretemp,pebtime,pebtemp,fp2)

float dilla,dillb,dillc,thick,refind,preea,prear,fpac,
  pebea,pebdo,dose,pretime,pretemp,pebtime,pebtemp;
int tc;
{
  float deltath,alpha,m[numpts],n,exparg,Kt,relm,rateb4;
  float efield,inten,sigma,mnew[numpts],rate[numpts],time;
  fcomplex cumul[4],addon[4],ebotplus,nnow,nnext,ij,etopplus;
  int j,k;

/* find the real component of the refractive index */
  n=sqrt(refind*refind-(dilla+dillb)*(dilla+dillb)*(lambda/
    4/pi)*(lambda/4/pi));

/* find the width of each sublayer */
  deltath=thick/numpts;

/* find the PEB diffusion length constant */
sigma=sqrt(2.0*pebtime*exp(pebdo-1000.0*pebea/R/pebtemp))
  /1000.0;
```

```
/* find the intermediate value Kt for the Mack pre-bake model */
  Kt=exp(prear-1000.0*preea/R/pretemp);
/* relm tells us how much to change Dilla and Dillb as a result
   of prebake */
  relm=exp(-1.0*Kt*pretime);

/* modify dilla and dillb parameters as a result of the
   pre-bake */
  dilla=dilla*relm;
  dillb=dillb*(fpac-relm*(fpac-1));

/* make sure that the PAC is 100% for each of the sublayers
   before we begin to simulate */
  for(j=0;j<numpts;j++) m[j]=1.0;

/* find PAC profile for each increment in time */
  for(j=1;j<=numtint;j++){
    alpha=(dilla*m[0]+dillb)*lambda/4/pi;
    cumul[0]=cumul[3]=Complex((1+n)/2,-1.0*alpha/2.0);
    cumul[1]=cumul[2]=Complex((1-n)/2,alpha/2.0);

/* simultaneously solve for the E-fields in each of the
   sublayers relative to the impinging E-field. We don't know
   the magnitude or phase of the E-field coming out of the
   resist so we can solve for each sublayer quite yet */
    for(k=0;k<numpts;k++){
      exparg=deltath*(dilla*m[k]+dillb)/2.0;
      addon[3]=Complex(exp(-1.0*exparg)*cos(-2.0*n*pi*deltath
        /lambda),exp(-1.0*exparg)*sin(-2.0*n*pi*deltath/lambda));
      addon[1]=addon[2]=Complex(0,0);
      addon[0]=Complex(exp(exparg)*cos(2.0*n*pi*deltath/lambda),
       exp(exparg)*sin(2.0*n*pi*deltath/lambda));
      matmult(cumul,addon,0);
      if(k<numpts-1){
        nnow=Complex(n,(-1.0*lambda*(dilla*m[k]+dillb)/4.0/pi));
      nnext=Complex(n,(-1.0*lambda*(dilla*m[k+1]+dillb)/4.0/pi));
        addon[0]=addon[3]=Cmul(Complex(.5,0),Cadd(Complex(1.0,
          0),Cdiv(nnext,nnow)));
        addon[1]=addon[2]=Cmul(Complex(.5,0),Csub(Complex(1.0,
          0),Cdiv(nnext,nnow)));
        }
        else{
        addon[0]=addon[3]=Cmul(Complex(.5,0),Cadd(Complex
          (1.0,0),Cdiv(nSi,nnow)));
        addon[1]=addon[2]=Cmul(Complex(.5,0),Csub(Complex
          (1.0,0),Cdiv(nSi,nnow)));
        }
      matmult(cumul,addon,0);
    }

/* OK. Now we know the E-field entering the silicon from the
   resist and we know that no light is coming back out of the
   silicon since it is so attenuative and thick. Therefore we
```

```
   can solve for the E-field phase and magnitude for each
   sublayer for this increment in time. */

    etopplus=Complex(sqrt(2.0*dose/numtint/light/epsilon),0.0);
    ebotplus=Cdiv(etopplus,cumul[0]);

    /* CALC PAC CONCENTRATION */

  for(k=numpts-1;k>=0;k--){
    nnow=Complex(n,(-1.0*lambda*(dilla*m[k]+dillb)/4.0/pi));
    if(k<numpts-1){
      nnext=Complex(n,(-1.0*lambda*(dilla*m[k+1]+dillb)/4.0/pi));
      addon[0]=addon[3]=Cmul(Complex(.5,0),Cadd(Complex(1.0,0),
        Cdiv(nnext,nnow)));
      addon[1]=addon[2]=Cmul(Complex(.5,0),Csub(Complex(1.0,0),
        Cdiv(nnext,nnow)));
      matmult(addon,cumul,1);
    }
    else{
      cumul[0]=cumul[3]=Cmul(Complex(.5,0.0),Cadd(Complex
        (1.0,0.0),Cdiv(nSi,nnow)));
      cumul[1]=cumul[2]=Cmul(Complex(.5,0.0),Csub(Complex
        (1.0,0.0),Cdiv(nSi,nnow)));
    }
    exparg=deltath*(dilla*m[k]+dillb)/2.0;
    addon[3]=Complex(exp(-1.0*exparg)*cos(-2.0*n*pi*deltath
        /lambda),exp(-1.0*exparg)*sin(-2.0*n*pi*deltath/lambda));
      addon[1]=addon[2]=Complex(0,0);
      addon[0]=Complex(exp(exparg)*cos(2.0*n*pi*deltath/lambda),
        exp(exparg)*sin(2.0*n*pi*deltath/lambda));
      matmult(addon,cumul,1);

/* add the components of the E-field coming into and out of
   the sublayer */
      efield=Cabs(Cmul(Cadd(cumul[0],cumul[2]),ebotplus));

/* convert E-field back to light intensity */
      inten=efield*efield*light*epsilon/2.0;

/* find out how much the PAC should decrease for this
   sublayer of resist */
      m[k]=m[k]-1.0*inten*m[k]*dillc;
    }
  }

/* Lets find the smoothing of from the PEB model. We look at
   50 sublayers above and 50 sublayers below the current
   sublayer */
  for(k=0;k<numpts;k++){
    mnew[k]=0;
    for(j=-50;j<=50;j++){
      if(((k+j)>=0) && ((k+j)<numpts)){
        mnew[k]=mnew[k]+m[k+j]*exp(-1.0*j*deltath*j*
          deltath/2.0/sigma/sigma)*deltath;
```

```
      }
      else{
 /* need to take into consideration what happens near the top
    and bottom of the resist */
    if((k+j)<0)
      mnew[k]=mnew[k]+m[-1*(k+j)]*exp(-1.0*j*deltath*j*
        deltath/2.0/sigma/sigma)*deltath;
    if((k+j)>numpts)
      mnew[k]=mnew[k]+m[2*numpts-k-j]*exp(-1.0*j*deltath*j
        *deltath/2.0/sigma/sigma)*deltath;
  }
}
/* find the new PAC after PEB */
    mnew[k]=mnew[k]/sqrt(2.0*pi)/sigma;
  }

/* solve for the Kim development equation and print out the
   development rate, PAC concentration, depth and exposure
   dose */
  time=0.0;
  for(k=0;k<numpts;k++){
    rate[k]=(1-(1-(R5-(R5-R6)*mnew[k]))*exp(-1*k*deltath/R4))*
      (1/((1-mnew[k]*exp(-1*R3*(1-mnew[k])))/R1+mnew[k]
      *exp(-1*R3*(1-mnew[k]))/R2));
    rateb4=(1-(1-(R5-(R5-R6)*m[k]))*exp(-1*k*deltath/R4))*
      (1/((1-m[k]*exp(-1*R3*(1-m[k])))/R1+m[k]
      *exp(-1*R3*(1-m[k]))/R2));
    time=time+deltath/rate[k];
    printf("tc=%d rate=%f pac=%f depth=%f\n",tc,rate[k],m[k],
      k*deltath);
    fprintf(fp2,"%d  %f %f  %f %f\n",tc,rate[k],rateb4,
      k*deltath,dose);
  }

}

/* routine for multiplying complex 2X2 matrices */
void matmult(mtra,mtrb,flag)
  fcomplex mtra[4],mtrb[4];

  int flag;
  {
    fcomplex temp[4]; int cnt1,cnt2;
    temp[0]=Cadd(Cmul(mtra[0],mtrb[0]),Cmul(mtra[1],mtrb[2]));
    temp[1]=Cadd(Cmul(mtra[0],mtrb[1]),Cmul(mtra[1],mtrb[3]));
    temp[2]=Cadd(Cmul(mtra[2],mtrb[0]),Cmul(mtra[3],mtrb[2]));
    temp[3]=Cadd(Cmul(mtra[2],mtrb[1]),Cmul(mtra[3],mtrb[3]));
    if(flag==0){
      for(cnt1=0;cnt1<=3;cnt1++){
        mtra[cnt1].r=temp[cnt1].r;
        mtra[cnt1].i=temp[cnt1].i;
      }
    }
    else{
```

```
    for(cnt1=0;cnt1<=3;cnt1++){
      mtrb[cnt1].r=temp[cnt1].r;
      mtrb[cnt1].i=temp[cnt1].i;
    }
  }
}
```

APPENDIX B

SAS SOURCE CODE FOR PARAMETER EXTRACTION USING MARQUARDT-LEVENBERG NON-LINEAR REGRESSION

```
options bufno=2 nonotes noxwait xsync ps=5000;

/* Program: MASTER1.SAS
   Written by: Patrick G. Drennan
   Date: 5/1/93

   This program calculates the Kim development model parameters
   through the use of Marquardt-Levenberg non-linear regression
   routine. PAC data as a function of depth in the resist was
   simulated using a program called PACGEN which is written in
   C. Development rates are read in from a data file. According
   to the doses specified in that data file and the parameters
   specified within this routine, the PAC is computed. These
   values of PAC are then interpolated for the depth in order
   to find the appropriate PAC concentration for the depth
   input from initial data file. These values are then input
   into the non-linear routine in order to iteratively solve
   for development rate parameters.

*/

/*filename thickdat 'c:\sas\rates.dat';*/
filename thickdat 'c:\sas\ratered.dat';
/*filename thickdat 'c:\thesis\array\ccddata.out';*/
filename pacdata 'c:\thesis\array\pacdata.out';
filename workdir 'c:\thesis\array';
filename pacdir 'c:\thesis\array';

/* Read in the development rate data. We know a priori that
   the beginning thickness of the resist is about 1.161um.
   The file that is read in contains data from three different
   wafers. Each wafer number is denoted by the variable "tc".
*/
data mastset;
  infile thickdat;
  input tc rate dummy depth dose;
  total=1.161;
  retain total;
  if rate>0.01 then output;
run;
/* Need to separate the three different wafers. Data is place
   in data sets called "rate1", "rate2", and "rate3".
*/
%macro rategen;
  %do select = 1 %to 3;
    data rate&select(keep=tc rate pac depth);
      set mastset(keep=tc rate depth);
      pac=.;
      if tc = &select then output;
      if tc > &select then stop;
    run;
  %end;
%mend;
%rategen;
```

```
/* Need.to separate the factor levels, in this case, its the
   three dose levels.
*/
data exper(keep=tc total dose);
  set mastset;
  if tcold=. then tcold=0;
  if tc^= tcold then output;
  tcold=tc;
  retain tcold;
run;
/* Get rid of the original data file to save memory.
   (file is ~ 1M for a sampling freq of 40 times/sec).
*/
proc datasets library=work;
  delete mastset;
run;

/* Define  macro for the interpolation of the PAC
   data that is read in from the simulator. This is just a
   simple linear interpolation. More  sophisticated methods
   are not needed since simulated PAC data is so closely
   spaced.
*/
%macro splinep;
  data pacdata;
    infile 'pacdata.out';
    input tc depthsim pac;
  run;
  data rtbase&ccdpt(keep=hatpac tc depth rate);
    set rate&ccdpt(keep=tc depth rate);
    retain depthsim depthold pac pacold;
    do i=1 to last1;
      set pacdata point=i nobs=last1;
      if (depth>=depthold & depth<depthsim) then do;
        percent=abs((depth-depthold)/(depthsim-depthold));
        hatpac=(percent*(pac-pacold)+pacold);
        /* throw out data near the bottom of the resist layer
           since confidence in these rates is very low*/
        if depth<0.7 then output;
      end;
      pacold=pac; depthold=depthsim;
    end;
  run;
%mend;

/* Here a macro is defined for the setup, execution and
   retrieval of the simulated PAC data */
%macro depict;
  proc datasets library=work;
    delete mastdat;
  run;
  %do ccdpt=1 %to 3;
    data _null_;
      file 'pactmp.in';
```

```
      j=&ccdpt;
      set exper point=j; /*contains tc,total,dose*/
      /* dill parameters may be arbitrarily selected since
         the combination of them is so highly correlated with
         the development rate parameters. */
      dilla=0.581; dillb=0.082; dillc=0.013;
      /* refractive index was found from the period in the
         sinusoidal plot of rate versus depth */
      refind=1.68;
      /* value sigtmp is the diffusion length constant for
         the Mack PEB model */
      sigtmp=&sigma;
      /* write everything to "pactmp.in" */
      put tc; put dilla; put dillb; put dillc;
      put total; put refind; put dose; put sigtmp;
      stop;
    run;
    /* execute pacgen which will calculate the simulated
       PAC profile for the set of parameters input into
       "pactmp.in" */
    X "c:\thesis\array\pacgen";
    /* execute interpolation macro. */
    %splinep;
    /* since we are doing this for three different exposure
       doses, we need to add the latest PAC calculations onto
       the list. This is the data set ("mastdat") that will be
       input into the non-linear regression routine.
    */
    proc append base=mastdat data=rtbase&ccdpt force;
    run;
  %end;
%mend;
%macro sigfind;
%depict;

/* Now to find the development rate parameters. We choose an
   initial array of guesses for the Kim model (R1-R6) for
   the non-linear regression routine to start out on.
*/
/*proc gplot data=mastdat;
  plot hatpac*depth rate*depth/
  overlay;
  by tc;
run;*/

proc nlin method=marquardt outest=nest maxiter=300
        convergeparm=1e-10
        data=work.mastdat(rename=(hatpac=m depth=z));
  parms R1=12.0,20.0
        R2=0.02,0.1
        R3=6.0,10.0
        R4=0.24
        R5=0.6
        R6=0.6;
```

```
  /* We know that all of the parameters are positive */
  bounds R1>0.0000001, R2>0.0000001, R3>0, R4>0.0000001,
    R5>0.0000001, R6>0;
  /* This is the Kim model for which we want to solve for */
  model rate=(1-(1-(R5-(R5-R6)*m))*exp(-1*z/R4))*
             (1/((1-m*exp(-1*R3*(1-m)))/R1+m*
             exp(-1*R3*(1-m))/R2));
  /* first partial derivative wrt R1 */
  der.R1=(1-(1-(R5-(R5-R6)*m))*exp(-1*(z/R4)))*
         ((1-m*exp(-1*(R3*(1-m))))/R1**2/
         ((1-m*exp(-1*(R3*(1-m))))/R1+
         m*exp(-1*(R3*(1-m)))/R2)**2);
  /* first partial derivative wrt R2 */
  der.R2=(1-(1-(R5-(R5-R6)*m))*exp(-1*(z/R4)))*
         (m*exp(-1*(R3*(1-m)))/R2**2/
         ((1-m*exp(-1*(R3*(1-m))))/R1+
         m*exp(-1*(R3*(1-m)))/R2)**2);
  /* first partial derivative wrt R3 */
  der.R3=(1-(1-(R5-(R5-R6)*m))*exp(-1*(z/R4)))
         *-1*((-1*(m*-1*((1-m)*exp(-1*(R3*(1-m))))/R1)+
         m*-1*((1-m)*exp(-1*(R3*(1-m))))/R2)/
         ((1-m*exp(-1*(R3*(1-m))))/R1+
         m*exp(-1*(R3*(1-m)))/R2)**2);
  /* first partial derivative wrt R4 */
  der.R4=-1*((1-(R5-(R5-R6)*m))*(z/R4**2*exp(-1*(z/R4)))*
         (1/((1-m*exp(-1*(R3*(1-m))))/R1
         +m*exp(-1*(R3*(1-m)))/R2)));
  /* first partial derivative wrt R5 */
  der.R5=(1-m)*exp(-1*(z/R4))*(1/((1-m*exp(-1*(R3*(1-m))))/R1+
         m*exp(-1*(R3*(1-m)))/R2));
  /* first partial derivative wrt R6 */
  der.R6=m*exp(-1*(z/R4))*(1/((1-m*exp(-1*(R3*(1-m))))/R1+
         m*exp(-1*(R3*(1-m)))/R2));
  run;
  /* search through the solution of the non-linear regression
     to find parameter estimates.*/
  data ssefind(keep=sse);
    if i=. then i=1;
    retain i;
    set nest(rename=(_SSE_=sse) keep=_TYPE_ _SSE_) nobs=last1;
    if _TYPE_ = "FINAL" then do;
      output;
      stop;
    end;
    if i=last1 then do;
      output;
      stop;
    end;
    i=i+1;
  run;
%mend;

/* Since the PEB manifests inself in a non-closed form, a
   binary search is performed to find the PEB diffusion
```

```
   constant. */

/* pick a high value */
%let sigma=0.1;
%sigfind;
data _null_;
  set ssefind;
  temp=&sigma;
  call symput('sigmax',left(temp));
  call symput('ssemax',left(sse));
  stop;
run;
%put sigma= &sigma &ssemax;
/* pick a low value */
%let sigma=0.001;
%sigfind;
data _null_;
  set ssefind;
  temp=&sigma;
  call symput('sigmin',left(temp));
  call symput('ssemin',left(sse));
  stop;
run;
%put sigma= &sigma &ssemin;
/* pick a middle value */
%let sigma=0.01;
%sigfind;
data _null_;
  set ssefind;
  temp=&sigma;
  call symput('sigcen',left(temp));
  call symput('ssecen',left(sse));
  stop;
run;
%put sigma= &sigma &ssecen;
/* Do a binary search to find the PEB diffusion constant.
   Usually converges within 10 iterations. */
%macro siglook;
  %do iteratn=1 %to 20;
    data _null_;
      signew=(&sigmin+&sigcen)/2;
      call symput('sigma',left(signew));
    run;
    %sigfind;
    data _null_;
      i=1;
      set ssefind point=i;
      temp=&sigma;
      call symput('temp2',(sse));
      if (sse < &ssecen) then do;
        call symput('sigcen',left(temp));
        call symput('ssecen',left(sse));
      end;
      if ((sse < &ssemin) & (sse > &ssecen)) then do;
```

```
        call symput('sigmin',left(temp));
        call symput('ssemin',left(sse));
      end;
  %put sigma= &sigma &temp2;
      stop;
    run;
    %put 'min' &sigmin &ssemin;
    %put 'cen' &sigcen &ssecen;
    %put 'max' &sigmax &ssemax;
    data _null_;
      signew=(&sigmax+&sigcen)/2;
      call symput('sigma',left(signew));
    run;
    %sigfind;
    data _null_;
      i=1;
      set ssefind point=i;
      temp=&sigma;
      call symput('temp2',(sse));
      if (sse < &ssecen) then do;
        call symput('sigcen',left(temp));
        call symput('ssecen',left(sse));
        stop;
      end;
      if ((sse < &ssemax) & (sse > &ssecen)) then do;
        call symput('sigmax',left(temp));
        call symput('ssemax',left(sse));
        stop;
      end;
  %put sigma= &sigma &temp2;
      stop;
    run;
    %put 'min' &sigmin &ssemin;
    %put 'cen' &sigcen &ssecen;
    %put 'max' &sigmax &ssemax;
  %end;
%mend;
%siglook;
```

APPENDIX C

C SOURCE CODE FOR PAC COMPUTATION

```
/*
  Program: PACGEN.C
  Written by: Patrick G. Drennan

  This program uses the Dill exposure model and the Mack PEB
  bake model to calculate the PAC concentration of conventional
  positive photoresist on Silicon. The parameters, A, B, C,
  resist thickness, resist refractive index, exposure dose,
  and PEB diffusion length constant are input via the file
  "PACTMP.IN". PAC concentrations and depths are output into
  the file "PACDATA.OUT".
*/

#include <stdio.h>
#include <math.h>
#include "complex.h"

#define numpts 250
#define numtint 50
#define pi 3.14159265
#define lambda 0.4358
#define nSi Complex(4.73,-0.138)
#define R 1.987
#define light 3.0e8
#define epsilon 8.85e-12

/* The universal gas constant above is in C/(mole*degreeK) */

void matmult();

main()
{
  FILE *fp, *fp2;
  float dilla,dillb,dillc,thick,refind,preea,prear,fpac,
    pebea,pebdo,dose,pretime,pretemp,pebtime,pebtemp,temp;
  float deltath,alpha,m[numpts],n,exparg,deltam1,deltam2,Kt
    ,relm;
  float tc,efield,inten,sigma,mnew[numpts],rate[numpts],time;
  fcomplex testa[4],testb[4],cumul[4],addon[4],ebotplus,nnow
    ,nnext,ij;
  fcomplex etopplus;
  double temp1,temp2;
  int j,k;
  if ((fp = fopen("PACTMP.IN","r"))==NULL){
    printf("cannot open read file\n");
    exit(1);
    }
  if ((fp2 = fopen("pacdata.out","w"))==NULL){
    printf("cannot open write file\n");
    exit(1);
    }

  /* input the appropriate parameters from pactmp.in */
    fscanf(fp,"%f",&tc);
```

```
    fscanf(fp,"%f",&dilla); fscanf(fp,"%f",&dillb);
    fscanf(fp,"%f",&dillc); fscanf(fp,"%f",&thick);
    fscanf(fp,"%f",&refind); fscanf(fp,"%f",&dose);
    fscanf(fp,"%f",&sigma);
  fclose(fp);
  /* find the real component of the refractive index */
  n=sqrt(refind*refind-(dilla+dillb)*(dilla+dillb)*(lambda/4/pi)
    *(lambda/4/pi));

  /* find the thickness of each sublayer */
  deltath=thick/numpts;

  for(j=0;j<numpts;j++) m[j]=1;

  /* since we have to approximate the partial derivative with
     respect to time in the Dill model, we find the exposure
     conditions for each increment in time */
  for(j=1;j<=numtint;j++){
    alpha=(dilla*m[0]+dillb)*lambda/4/pi;
    cumul[0]=cumul[3]=Complex((1+n)/2,-1.0*alpha/2.0);
    cumul[1]=cumul[2]=Complex((1-n)/2,alpha/2.0);

/* find the exposure condition for each sublayer. Remember that
   the physical constants of the sublayer are constant within
   a sublayer but are allowed to vary between layers */

    for(k=0;k<numpts;k++){
      exparg=deltath*(dilla*m[k]+dillb)/2.0;
      addon[3]=Complex(exp(-1.0*exparg)*cos(-2.0*n*pi*deltath
        /lambda),exp(-1.0*exparg)*sin(-2.0*n*pi*deltath/lambda));
      addon[1]=addon[2]=Complex(0,0);
      addon[0]=Complex(exp(exparg)*cos(2.0*n*pi*deltath/lambda),
        exp(exparg)*sin(2.0*n*pi*deltath/lambda));
      matmult(cumul,addon,0);
      if(k<numpts-1){
        nnow=Complex(n,(-1.0*lambda*(dilla*m[k]+dillb)/4.0/pi));
        nnext=Complex(n,(-1.0*lambda*(dilla*m[k+1]+dillb)/
          4.0/pi));
        addon[0]=addon[3]=Cmul(Complex(.5,0),Cadd(Complex(1.0,
          0),Cdiv(nnext,nnow)));
        addon[1]=addon[2]=Cmul(Complex(.5,0),Csub(Complex(1.0,
          0),Cdiv(nnext,nnow)));
        }
        else{
        addon[0]=addon[3]=Cmul(Complex(.5,0),Cadd(Complex(1.0,0),
          Cdiv(nSi,nnow)));
        addon[1]=addon[2]=Cmul(Complex(.5,0),Csub(Complex(1.0,0),
          Cdiv(nSi,nnow)));
        }
      matmult(cumul,addon,0);
    }

/* Now we found the electric field component entering the
   substrate. Since we know that there isn't an electric
```

```
   field component coming out of the substrate we work
   backwards from the bottom of the resist layer to find
   the exposure conditions throughout the resist.*/

    etopplus=Complex(sqrt(2.0*dose/numtint/light/epsilon),0.0);
    ebotplus=Cdiv(etopplus,cumul[0]);

    /* CALC PAC CONCENTRATION */

/* work backwards from the bottom of the resist to find the
   new PAC concentration profile for this increment in time. */

    for(k=numpts-1;k>=0;k--){
      nnow=Complex(n,(-1.0*lambda*(dilla*m[k]+dillb)/4.0/pi));
      if(k<numpts-1){
        nnext=Complex(n,(-1.0*lambda*(dilla*m[k+1]+dillb)/
          4.0/pi));
        addon[0]=addon[3]=Cmul(Complex(.5,0),Cadd(Complex(1.0
          ,0),Cdiv(nnext,nnow)));
        addon[1]=addon[2]=Cmul(Complex(.5,0),Csub(Complex(1.0
          ,0),Cdiv(nnext,nnow)));
        matmult(addon,cumul,1);
      }
      else{
        cumul[0]=cumul[3]=Cmul(Complex(.5,0.0),Cadd(Complex(1.0
          ,0.0),Cdiv(nSi,nnow)));
        cumul[1]=cumul[2]=Cmul(Complex(.5,0.0),Csub(Complex(1.0
          ,0.0),Cdiv(nSi,nnow)));
      }
      exparg=deltath*(dilla*m[k]+dillb)/2.0;
      addon[3]=Complex(exp(-1.0*exparg)*cos(-2.0*n*pi*deltath
        /lambda),exp(-1.0*exparg)*sin(-2.0*n*pi*deltath/lambda));
      addon[1]=addon[2]=Complex(0,0);
      addon[0]=Complex(exp(exparg)*cos(2.0*n*pi*deltath/lambda),
        exp(exparg)*sin(2.0*n*pi*deltath/lambda));
      matmult(addon,cumul,1);
      efield=Cabs(Cmul(Cadd(cumul[0],cumul[2]),ebotplus));
      inten=efield*efield*light*epsilon/2.0;
      m[k]=m[k]-1.0*inten*m[k]*dillc;


    }
  }

/* use the PEB diffusion length constant to find the PEB
   modified PAC profile after bake. */

  for(k=0;k<numpts;k++){
    for(mnew[k]=0,j=-50;j<=50;j++){
      if(((k+j)>=0) && ((k+j)<numpts)){
        mnew[k]+=m[k+j]*exp(-1.0*j*deltath*j*deltath/2.0
          /sigma/sigma)*deltath;
      }
      else{
```

```
        if ((k+j)<0)
          mnew[k]+=m[k-1*(k+j)]*exp(-1.0*j*deltath*j*deltath/2.0
            /sigma/sigma)*deltath;
        if ((k+j)>numpts)
          mnew[k]+=m[2*numpts-k-j]*exp(-1.0*j*deltath*j*deltath
            /2.0/sigma/sigma)*deltath;

      }
    }
    mnew[k]=mnew[k]/sqrt(2.0*pi)/sigma;
  }

  for(k=0;k<numpts;k++){
  fprintf(fp2,"%f %f %f\n",tc,k*deltath,mnew[k]);
/*  printf("%f %f %f\n",tc,k*deltath,mnew[k]); */
  }

  fclose(fp2);

}

/* routine for multiplying complex 2X2 matrices */
void matmult(mtra,mtrb,flag)
  fcomplex mtra[4],mtrb[4];

  int flag;
  {
    fcomplex temp[4]; int cnt1,cnt2;
    temp[0]=Cadd(Cmul(mtra[0],mtrb[0]),Cmul(mtra[1],mtrb[2]));
    temp[1]=Cadd(Cmul(mtra[0],mtrb[1]),Cmul(mtra[1],mtrb[3]));
    temp[2]=Cadd(Cmul(mtra[2],mtrb[0]),Cmul(mtra[3],mtrb[2]));
    temp[3]=Cadd(Cmul(mtra[2],mtrb[1]),Cmul(mtra[3],mtrb[3]));
    if(flag==0){
      for(cnt1=0;cnt1<=3;cnt1++){
        mtra[cnt1].r=temp[cnt1].r;
        mtra[cnt1].i=temp[cnt1].i;
      }
    }
    else{
      for(cnt1=0;cnt1<=3;cnt1++){
        mtrb[cnt1].r=temp[cnt1].r;
        mtrb[cnt1].i=temp[cnt1].i;
      }
    }
  }
```

APPENDIX D

SAS SOURCE CODE FOR IN-SITU DEVELOPMENT RATE CALCULATION

```
options bufno=4 ps=2000 nonotes;
/* Program: RATEGEN.SAS
   Written by: Patrick G. Drennan
   Date: 4/27/93

   This program calculates the development rate of any type of
   photoresist, in situ on the devlopment track. Signal data
   is taken from a Site Services Development Spray Monitor
   (DSM). Input data must be in a ASCII format for input.
   Signal data is input along with the time values of the peaks,
   valleys and endpoint (aka tags). The signals are normalized
   to values between -1.0 and +1.0 and the equation,
   S=cos(4*pi*n*(rate*time+thick)/Lambda) is used to solve for
   the development rate. This program uses the Marquardt-
   Levenberg non-linear regression technique to find the
   development rate from the signal data.

   */

proc printto;
%macro seltag;
  /* tag values are given in terms of time so we need to find
     the magnitude at these time. Tags are in chronological
     order so they alternate peak/valley/peak/valley...
  */
  data temp(keep=time sig);
    if _n_=1 then j=1;
    set tag(rename=(t&wvln=tm) keep=t&wvln) nobs=last1 point=j;
    if tm^=. then do;
      call symput('endpt',left(tm));
      set sig(rename=(n&wvln=sig) keep=n&wvln time) nobs=tot;
      call symput('total',left(tot));
      if time >= tm then do;
        retain last1 j;
        output;
        j=j+1;
      end;
      if j>last1 then stop;
    end;
    if tm=. then stop;
  run;
  /* Normalize the signals wrt the nearest peak and valley.
     Create a new data set for each wavelength so that for a
     given sample time we can access all eight wavelengths
     in parallel.
  */
  data c&wvln(keep=delta signl time);
    if _n_=1 then do;
      pt=1;
      set temp(rename=(time=tm)) point=pt;
      tmold=tm; sigold=sig;
      pt=pt+1;
      set temp(rename=(time=tm)) point=pt;
      timeold=tmold;
```

```
    end;
    set sig(keep=time n&wvln);
    if (time^=&endpt) & (time = tm) then do;
      tmold=tm; sigold=sig;
      pt=pt+1;
      set temp(rename=(time=tm)) point=pt;
    end;
  /*  if sig ^= sigold then*/
      signl=(n&wvln-(sig+sigold)/2)/(abs(sig-sigold)/2);
    if signl<-1 then signl=-1.0;
    if signl>1 then signl=1.0;
    delta=abs(time-timeold);
    timeold=time;
    retain pt timeold tmold sigold tm sig;
    output;
  run;
  proc sort;
    by descending time;
  run;
%mend;
%macro each;
  /* Now we're calculating the development rate. First, for
     a given sample time we want to get together the normalized
     signals for all eight wavelengths. The macro variable
     "select" choses which sample time.
  */
  data incre;
    pi=3.14159265;
    n=1.68;
    d0=&dvalue;
    pnt=&select;
    set c700 point=pnt; lambda=700; output;
    set c767 point=pnt; lambda=767; output;
    set c800 point=pnt; lambda=800; output;
    set c830 point=pnt; lambda=830; output;
    set c840 point=pnt; lambda=840; output;
    set c900 point=pnt; lambda=900; output;
    set c930 point=pnt; lambda=930; output;
    set c960 point=pnt; lambda=960; output;
    stop;
  run;
  /* Use the Marquardt-Levenberg technique for regressing on
     the signal data. Confidence intervals, errors, and etc.
     are dumped to "temp.lis" and are rewritten over for each
     sample time in order to save memory.
  */
  proc printto print='temp.lis' new;
  proc nlin method=marquardt outest=work.nest maxiter=200
  convergeparm=1e-10 convergeparm=1e-10 save data=incre;
    parms rate=1.0,10.0,20.0;
    bounds 500.0>rate>0;
    model signl=cos(4.0*pi*n/lambda*(rate*delta+d0));
    der.rate=-1*sin(4.0*pi*n/lambda*(rate*delta+d0))
             *(4.0*pi*n/lambda*delta*(pi/180));
```

```
  run;
  proc printto;
  /* For the given development rate that was just calculated,
     we need to find how much thickness in resist that accounts
     for. The value do keeps a running total of the thickness
     of the exposed areas. Needs to search through the non-
     linear regression output in order to find the converged
     development rate.
  */
  data temp(keep=rate d0 time);
    if i=. then i=1;
    retain i;
    set nest(keep=_type_ rate) nobs=last1;
    if rate>=500.0 then rate=0.0;
    if _TYPE_ = "FINAL" then do;
      set incre(keep=d0 time);
      output;
      stop;
    end;
    if i=last1 then do;
      set incre(keep=d0 time);
      output;
      stop;
    end;
    i=i+1;
  run;
  /* Add the newly calculated development rate and thickness
     added onto the list for output.
  */
  proc append base=esti;
%mend;
%macro dummy;
  %do select=1 %to &total;
    %each;
    data pat /*_null_*/;
      set temp;
      thick=rate*0.025+d0;
      call symput('dvalue',left(thick));
    run;
  %end;
%mend;

%macro master;
  /* clear the last estimates */
  proc datasets library=work;
     delete esti;
  run;
  /* read in tag data */
  data tag;
    infile tags;
    input t700 t767 t800 t830 t900 t930 t960 t840;
  run;
  /* read in the crude signal data */
  data sig(drop=dummy dummy1 dummy2 dummy3);
```

```
    infile signal;
    input dummy time n700 dummy1 dummy2 dummy3;
    input dummy time n767 dummy1 dummy2 dummy3;
    input dummy time n800 dummy1 dummy2 dummy3;
    input dummy time n830 dummy1 dummy2 dummy3;
    input dummy time n900 dummy1 dummy2 dummy3;
    input dummy time n930 dummy1 dummy2 dummy3;
    input dummy time n960 dummy1 dummy2 dummy3;
    input dummy time n840 dummy1 dummy2 dummy3;
    if time > 3.5 then output;
    if time > &tmax then stop;
  run;
  /* normalize each curve with respect to the tag values */
  %let wvln=700;
  %seltag;
  %let wvln=767;
  %seltag;
  %let wvln=800;
  %seltag;
  %let wvln=830;
  %seltag;
  %let wvln=840;
  %seltag;
  %let wvln=900;
  %seltag;
  %let wvln=930;
  %seltag;
  %let wvln=960;
  %seltag;
  %let dvalue=0.0;
  %dummy;
%mend;

/**** Find the development rates for a wafer exposed with
      90mJ/cm2 *.asc contains the ascii converted crude
      signal data. The DSM stores the data in a binary format.
      tags*.dat contains the time values for the peaks, valleys
      and endpoint. tmax is some time value right after endpoint.
 ****/
filename signal 'c:\thesis\array\act35.asc';
filename tags 'c:\thesis\array\tags35.dat';
%let tmax=30.20;
%master;
/**** output the development rate data */
proc printto print='rate35.dat' new;
proc print data=esti;
run;
proc printto;

/**** Find the development rates for a replicate wafer
      exposed with 90mJ/cm2
 ****/
filename signal 'c:\thesis\array\act37.asc';
filename tags 'c:\thesis\array\tags37.dat';
```

```
%let tmax=33.00;
%master;
proc printto print='rate37.dat' new;
proc print data=esti;
run;
proc printto;

/**** Find the development rates for a replicate wafer
      exposed with 90mJ/cm2
 ****/
filename signal 'c:\thesis\array\act43.asc';
filename tags 'c:\thesis\array\tags43.dat';
%let tmax=33.00;
%master;
proc printto print='rate43.dat' new;
proc print data=esti;
run;
proc printto;

/**** Find the development rates for a wafer exposed with
      66mJ/cm2
 ****/
filename signal 'c:\thesis\array\act8.asc';
filename tags 'c:\thesis\array\tags8.dat';
%let tmax=41.30;
%master;
proc printto print='rate8.dat' new;
proc print data=esti;
run;
proc printto;

/**** Find the development rates for a wafer exposed with
      114mJ/cm2
 ****/
filename signal 'c:\thesis\array\act9.asc';
filename tags 'c:\thesis\array\tags9.dat';
%let tmax=23.20;
%master;
proc printto print='rate9.dat' new;
proc print data=esti;
run;
proc printto;
```

APPENDIX E

CRUDE SIGNAL DATA

DOSE = 66 mJ/cm^2

OBS	TIME	N700	N767	N800	N830	N900	N930	N960	N840
1	0.000	0	0	0	0	0	0	0	0
2	0.125	0	-3	0	5	1	-1	-2	3
3	0.250	-1	-21	1	32	10	-10	-14	24
4	0.375	-1	-68	6	108	34	-40	-52	84
5	0.500	2	-151	19	251	79	-102	-128	199
6	0.625	12	-256	48	448	142	-195	-236	363
7	0.750	28	-363	93	661	212	-304	-358	544
8	0.875	45	-456	148	853	274	-413	-473	710
9	1.000	55	-533	200	1006	320	-514	-571	844
10	1.125	58	-598	242	1122	347	-604	-655	944
11	1.250	58	-651	276	1213	362	-682	-726	1021
12	1.375	62	-687	310	1290	375	-745	-784	1086
13	1.500	71	-708	347	1360	392	-792	-830	1146
14	1.625	84	-716	385	1426	412	-827	-865	1200
15	1.750	94	-718	418	1481	429	-854	-893	1245
16	1.875	100	-721	443	1524	440	-877	-917	1276
17	2.000	101	-730	458	1554	443	-898	-938	1293
18	2.125	98	-746	461	1571	436	-920	-958	1299
19	2.250	91	-770	452	1576	418	-944	-978	1300
20	2.375	79	-798	432	1570	392	-969	-1000	1297
21	2.500	66	-824	407	1560	362	-995	-1021	1293
22	2.625	54	-844	387	1554	339	-1015	-1040	1289
23	2.750	47	-855	377	1557	327	-1028	-1054	1290
24	2.875	42	-864	373	1565	323	-1037	-1065	1293
25	3.000	33	-881	367	1568	315	-1046	-1077	1294
26	3.125	19	-910	354	1562	298	-1058	-1089	1292
27	3.250	4	-944	337	1551	275	-1074	-1102	1286
28	3.375	-9	-973	320	1542	254	-1090	-1114	1278
29	3.500	-19	-993	305	1538	239	-1105	-1125	1268
30	3.625	-27	-1008	289	1534	226	-1116	-1135	1256
31	3.750	-36	-1023	273	1526	211	-1126	-1145	1243
32	3.875	-49	-1045	255	1511	192	-1134	-1157	1230
33	4.000	-65	-1073	237	1493	171	-1140	-1169	1220
34	4.125	-84	-1106	217	1477	150	-1147	-1182	1213
35	4.250	-103	-1139	195	1467	135	-1156	-1193	1208
36	4.375	-120	-1167	173	1463	125	-1164	-1202	1206
37	4.500	-132	-1185	157	1462	120	-1170	-1206	1205
38	4.625	-138	-1191	149	1464	121	-1173	-1207	1205
39	4.750	-139	-1190	148	1470	124	-1172	-1205	1207
40	4.875	-135	-1184	154	1486	133	-1166	-1201	1212
41	5.000	-125	-1171	161	1515	153	-1153	-1193	1227
42	5.125	-109	-1154	158	1560	192	-1127	-1183	1256
43	5.250	-93	-1141	128	1621	251	-1085	-1175	1297
44	5.375	-78	-1143	61	1696	322	-1029	-1175	1345
45	5.500	-66	-1159	-32	1779	400	-965	-1182	1396
46	5.625	-53	-1179	-136	1867	479	-900	-1195	1448
47	5.750	-38	-1191	-235	1958	561	-837	-1208	1501
48	5.875	-21	-1191	-324	2049	647	-774	-1220	1555
49	6.000	0	-1181	-401	2140	741	-708	-1229	1613
50	6.125	28	-1163	-464	2229	843	-640	-1234	1677
51	6.250	60	-1142	-511	2320	956	-569	-1236	1748

E4

OBS	TIME	N700	N767	N800	N830	N900	N930	N960	N840
52	6.375	95	-1119	-544	2413	1083	-498	-1236	1824
53	6.500	128	-1098	-574	2508	1222	-426	-1235	1904
54	6.625	156	-1090	-611	2597	1369	-356	-1238	1986
55	6.750	175	-1110	-665	2673	1515	-292	-1247	2063
56	6.875	179	-1166	-742	2735	1657	-238	-1268	2135
57	7.000	170	-1257	-838	2789	1796	-194	-1300	2204
58	7.125	154	-1375	-945	2848	1942	-154	-1341	2280
59	7.250	138	-1507	-1048	2919	2105	-116	-1388	2370
60	7.375	122	-1648	-1139	3008	2284	-81	-1440	2476
61	7.500	107	-1793	-1215	3113	2468	-55	-1500	2591
62	7.625	88	-1939	-1274	3230	2645	-40	-1568	2713
63	7.750	65	-2082	-1320	3354	2806	-36	-1641	2837
64	7.875	38	-2218	-1348	3481	2951	-43	-1717	2960
65	8.000	11	-2342	-1358	3612	3078	-59	-1793	3078
66	8.125	-10	-2449	-1351	3744	3190	-82	-1868	3191
67	8.250	-25	-2536	-1331	3879	3292	-110	-1940	3300
68	8.375	-31	-2601	-1300	4014	3388	-140	-2008	3409
69	8.500	-30	-2641	-1253	4155	3484	-171	-2070	3522
70	8.625	-18	-2651	-1180	4310	3587	-195	-2123	3646
71	8.750	9	-2626	-1079	4489	3705	-209	-2166	3787
72	8.875	55	-2570	-952	4693	3841	-209	-2201	3945
73	9.000	112	-2495	-809	4907	3985	-197	-2228	4108
74	9.125	167	-2421	-670	5108	4114	-187	-2253	4256
75	9.250	211	-2363	-549	5269	4205	-193	-2278	4370
76	9.375	238	-2328	-454	5376	4244	-220	-2308	4441
77	9.500	245	-2315	-383	5427	4234	-267	-2341	4471
78	9.625	236	-2321	-329	5435	4184	-332	-2378	4469
79	9.750	214	-2339	-286	5418	4102	-409	-2417	4446
80	9.875	185	-2361	-252	5389	3996	-495	-2456	4409
81	10.000	153	-2380	-223	5356	3872	-586	-2494	4364
82	10.125	120	-2396	-199	5318	3730	-683	-2531	4311
83	10.250	84	-2410	-180	5267	3565	-787	-2567	4242
84	10.375	44	-2420	-164	5199	3373	-900	-2602	4157
85	10.500	1	-2420	-151	5115	3156	-1019	-2634	4057
86	10.625	-41	-2406	-135	5016	2915	-1141	-2661	3945
87	10.750	-80	-2376	-114	4907	2658	-1263	-2679	3824
88	10.875	-114	-2332	-89	4786	2386	-1388	-2690	3694
89	11.000	-142	-2278	-61	4652	2106	-1511	-2691	3553
90	11.125	-163	-2214	-37	4508	1824	-1629	-2684	3403
91	11.250	-176	-2143	-19	4357	1544	-1734	-2665	3245
92	11.375	-182	-2069	-11	4200	1273	-1822	-2635	3083
93	11.500	-181	-1995	-17	4041	1014	-1893	-2595	2921
94	11.625	-178	-1927	-39	3879	770	-1949	-2548	2762
95	11.750	-173	-1870	-78	3715	546	-1990	-2497	2606
96	11.875	-170	-1828	-131	3552	344	-2018	-2445	2453
97	12.000	-167	-1798	-195	3390	164	-2033	-2394	2304
98	12.125	-163	-1777	-266	3237	9	-2037	-2344	2167
99	12.250	-158	-1760	-340	3097	-116	-2028	-2294	2046
100	12.375	-150	-1745	-412	2973	-211	-2006	-2244	1943
101	12.500	-139	-1733	-482	2865	-278	-1972	-2192	1856
102	12.625	-126	-1727	-547	2770	-320	-1932	-2142	1782

OBS	TIME	N700	N767	N800	N830	N900	N930	N960	N840
103	12.750	-113	-1729	-611	2685	-343	-1887	-2096	1721
104	12.875	-100	-1740	-678	2611	-349	-1840	-2054	1671
105	13.000	-88	-1758	-751	2545	-338	-1789	-2016	1631
106	13.125	-79	-1782	-828	2488	-305	-1729	-1977	1602
107	13.250	-71	-1809	-902	2445	-242	-1656	-1934	1588
108	13.375	-59	-1835	-970	2425	-142	-1567	-1887	1597
109	13.500	-36	-1858	-1029	2434	-7	-1463	-1839	1633
110	13.625	-5	-1877	-1081	2472	155	-1350	-1793	1695
111	13.750	32	-1895	-1127	2539	344	-1231	-1750	1780
112	13.875	70	-1914	-1166	2630	556	-1107	-1710	1885
113	14.000	102	-1940	-1202	2738	786	-984	-1675	2003
114	14.125	121	-1983	-1239	2853	1022	-869	-1650	2127
115	14.250	122	-2049	-1280	2965	1248	-769	-1636	2245
116	14.375	102	-2139	-1325	3071	1457	-685	-1636	2353
117	14.500	69	-2241	-1365	3174	1654	-614	-1647	2455
118	14.625	30	-2340	-1390	3282	1851	-550	-1665	2562
119	14.750	-3	-2423	-1390	3407	2058	-486	-1685	2684
120	14.875	-25	-2483	-1359	3554	2275	-421	-1704	2825
121	15.000	-35	-2517	-1299	3726	2498	-355	-1725	2983
122	15.125	-36	-2526	-1217	3915	2720	-293	-1748	3153
123	15.250	-32	-2514	-1122	4111	2933	-236	-1773	3324
124	15.375	-28	-2490	-1023	4301	3125	-192	-1801	3486
125	15.500	-27	-2464	-927	4471	3286	-164	-1833	3629
126	15.625	-33	-2439	-839	4618	3414	-154	-1871	3749
127	15.750	-42	-2414	-753	4748	3513	-155	-1912	3851
128	15.875	-49	-2380	-664	4871	3594	-161	-1953	3942
129	16.000	-49	-2334	-567	4993	3662	-171	-1993	4026
130	16.125	-45	-2280	-466	5104	3715	-188	-2032	4100
131	16.250	-41	-2227	-369	5190	3742	-220	-2072	4155
132	16.375	-43	-2182	-287	5239	3732	-269	-2117	4182
133	16.500	-52	-2148	-224	5254	3680	-333	-2164	4183
134	16.625	-63	-2119	-176	5245	3595	-410	-2213	4164
135	16.750	-73	-2088	-136	5223	3486	-496	-2264	4129
136	16.875	-79	-2051	-100	5192	3359	-590	-2315	4082
137	17.000	-81	-2007	-66	5151	3219	-688	-2365	4026
138	17.125	-78	-1952	-34	5101	3067	-786	-2410	3963
139	17.250	-69	-1889	-2	5042	2905	-881	-2448	3893
140	17.375	-56	-1823	26	4973	2733	-973	-2481	3812
141	17.500	-40	-1764	47	4889	2546	-1064	-2509	3716
142	17.625	-24	-1718	55	4786	2341	-1157	-2534	3603
143	17.750	-7	-1682	47	4668	2121	-1253	-2555	3478
144	17.875	11	-1648	27	4541	1897	-1346	-2569	3350
145	18.000	37	-1608	-2	4413	1680	-1431	-2576	3227
146	18.125	67	-1566	-41	4289	1474	-1505	-2576	3108
147	18.250	97	-1530	-90	4164	1278	-1568	-2569	2989
148	18.375	122	-1509	-150	4033	1090	-1624	-2558	2867
149	18.500	140	-1509	-223	3896	910	-1673	-2541	2742
150	18.625	151	-1529	-307	3752	740	-1716	-2521	2614
151	18.750	157	-1568	-403	3604	583	-1753	-2497	2487
152	18.875	157	-1618	-505	3459	442	-1781	-2473	2365
153	19.000	154	-1677	-612	3318	318	-1799	-2450	2251

OBS	TIME	N700	N767	N800	N830	N900	N930	N960	N840
154	19.125	146	-1744	-720	3181	212	-1807	-2426	2145
155	19.250	135	-1817	-827	3052	126	-1805	-2402	2051
156	19.375	130	-1887	-922	2946	74	-1791	-2372	1977
157	19.500	138	-1936	-994	2883	70	-1756	-2331	1939
158	19.625	164	-1954	-1038	2870	123	-1697	-2279	1944
159	19.750	201	-1952	-1062	2898	222	-1616	-2220	1982
160	19.875	233	-1953	-1082	2939	341	-1529	-2160	2033
161	20.000	248	-1979	-1112	2969	454	-1448	-2106	2076
162	20.125	238	-2036	-1160	2980	550	-1378	-2064	2102
163	20.250	209	-2116	-1220	2981	634	-1316	-2031	2119
164	20.375	168	-2205	-1282	2983	720	-1255	-2003	2137
165	20.500	121	-2296	-1340	2995	816	-1192	-1978	2161
166	20.625	72	-2385	-1389	3019	923	-1126	-1954	2195
167	20.750	23	-2469	-1427	3058	1043	-1061	-1933	2242
168	20.875	-22	-2541	-1448	3119	1178	-995	-1914	2306
169	21.000	-61	-2597	-1448	3204	1332	-925	-1895	2389
170	21.125	-93	-2633	-1422	3313	1504	-849	-1874	2492
171	21.250	-118	-2647	-1373	3441	1693	-766	-1852	2611
172	21.375	-137	-2643	-1310	3580	1889	-682	-1830	2738
173	21.500	-155	-2631	-1242	3720	2079	-603	-1814	2864
174	21.625	-173	-2618	-1177	3854	2256	-534	-1804	2981
175	21.750	-190	-2603	-1110	3980	2416	-474	-1802	3090
176	21.875	-205	-2579	-1038	4105	2562	-423	-1805	3195
177	22.000	-216	-2543	-962	4228	2694	-380	-1813	3297
178	22.125	-224	-2500	-884	4346	2807	-347	-1825	3393
179	22.250	-230	-2452	-809	4452	2901	-323	-1839	3478
180	22.375	-234	-2403	-736	4545	2981	-304	-1853	3553
181	22.500	-233	-2352	-661	4628	3052	-291	-1869	3620
182	22.625	-227	-2296	-583	4705	3114	-285	-1887	3681
183	22.750	-214	-2232	-502	4784	3168	-287	-1909	3739
184	22.875	-196	-2158	-418	4866	3213	-297	-1933	3796
185	23.000	-173	-2077	-337	4944	3245	-311	-1959	3847
186	23.125	-150	-1998	-265	5006	3255	-332	-1987	3885
187	23.250	-127	-1928	-207	5043	3239	-361	-2020	3904
188	23.375	-106	-1870	-162	5054	3193	-400	-2055	3899
189	23.500	-85	-1823	-133	5043	3121	-451	-2095	3874
190	23.625	-67	-1786	-119	5009	3022	-514	-2139	3829
191	23.750	-55	-1762	-121	4952	2897	-588	-2186	3765
192	23.875	-47	-1754	-134	4873	2751	-670	-2234	3683
193	24.000	-42	-1760	-156	4774	2594	-757	-2282	3590
194	24.125	-39	-1774	-184	4660	2428	-846	-2328	3491
195	24.250	-39	-1791	-222	4534	2257	-937	-2372	3387
196	24.375	-40	-1812	-271	4400	2078	-1029	-2414	3277
197	24.500	-41	-1840	-332	4260	1891	-1123	-2454	3161
198	24.625	-41	-1874	-404	4119	1697	-1218	-2492	3039
199	24.750	-42	-1915	-483	3975	1499	-1314	-2530	2913
200	24.875	-45	-1961	-567	3827	1299	-1406	-2565	2783
201	25.000	-51	-2012	-653	3677	1103	-1492	-2595	2652
202	25.125	-59	-2062	-739	3532	917	-1569	-2619	2526
203	25.250	-61	-2105	-819	3403	750	-1636	-2637	2415
204	25.375	-58	-2141	-891	3292	605	-1692	-2650	2320

OBS	TIME	N700	N767	N800	N830	N900	N930	N960	N840
205	25.500	-57	-2179	-962	3189	474	-1738	-2659	2234
206	25.625	-65	-2230	-1040	3082	347	-1781	-2666	2145
207	25.750	-82	-2294	-1127	2968	221	-1822	-2671	2051
208	25.875	-104	-2365	-1215	2856	107	-1860	-2672	1961
209	26.000	-123	-2433	-1299	2755	15	-1891	-2669	1884
210	26.125	-140	-2496	-1374	2670	-52	-1912	-2662	1821
211	26.250	-152	-2553	-1435	2601	-95	-1922	-2651	1771
212	26.375	-162	-2602	-1485	2551	-115	-1919	-2635	1735
213	26.500	-169	-2642	-1523	2523	-111	-1900	-2613	1714
214	26.625	-176	-2675	-1555	2516	-88	-1872	-2587	1708
215	26.750	-185	-2702	-1583	2524	-50	-1839	-2559	1715
216	26.875	-197	-2728	-1607	2544	0	-1803	-2530	1733
217	27.000	-209	-2749	-1625	2572	60	-1761	-2500	1759
218	27.125	-217	-2762	-1634	2615	140	-1710	-2468	1801
219	27.250	-213	-2754	-1625	2685	250	-1646	-2430	1868
220	27.375	-194	-2718	-1594	2795	398	-1567	-2384	1968
221	27.500	-161	-2655	-1535	2943	584	-1469	-2330	2097
222	27.625	-118	-2572	-1454	3117	796	-1357	-2270	2245
223	27.750	-75	-2484	-1361	3297	1020	-1237	-2207	2401
224	27.875	-37	-2403	-1266	3470	1242	-1120	-2148	2553
225	28.000	-9	-2336	-1178	3628	1453	-1012	-2095	2693
226	28.125	5	-2287	-1101	3764	1641	-919	-2050	2811
227	28.250	6	-2256	-1035	3875	1807	-841	-2013	2908
228	28.375	-1	-2233	-972	3968	1961	-773	-1979	2994
229	28.500	-4	-2201	-901	4064	2121	-706	-1946	3084
230	28.625	9	-2147	-814	4183	2297	-634	-1909	3190
231	28.750	39	-2073	-711	4326	2482	-556	-1869	3310
232	28.875	74	-1987	-603	4482	2663	-477	-1832	3432
233	29.000	108	-1901	-499	4630	2824	-404	-1799	3546
234	29.125	136	-1824	-403	4757	2958	-341	-1775	3645
235	29.250	160	-1762	-320	4854	3063	-291	-1758	3726
236	29.375	179	-1715	-245	4926	3149	-252	-1745	3792
237	29.500	192	-1676	-177	4978	3224	-221	-1734	3846
238	29.625	200	-1641	-113	5017	3287	-197	-1725	3886
239	29.750	203	-1612	-57	5044	3334	-183	-1722	3911
240	29.875	205	-1595	-16	5057	3356	-182	-1728	3919
241	30.000	202	-1593	6	5054	3353	-194	-1741	3914
242	30.125	196	-1602	15	5034	3328	-213	-1759	3898
243	30.250	185	-1614	14	5001	3286	-240	-1780	3871
244	30.375	172	-1625	7	4958	3226	-275	-1802	3834
245	30.500	161	-1634	-4	4907	3151	-318	-1827	3788
246	30.625	153	-1639	-18	4856	3070	-366	-1855	3739
247	30.750	150	-1642	-30	4807	2990	-414	-1884	3694
248	30.875	151	-1642	-39	4758	2912	-461	-1915	3655
249	31.000	154	-1643	-50	4707	2831	-508	-1947	3615
250	31.125	156	-1651	-69	4650	2738	-559	-1982	3570
251	31.250	154	-1666	-102	4586	2633	-615	-2018	3515
252	31.375	150	-1687	-145	4515	2518	-676	-2057	3449
253	31.500	143	-1710	-195	4438	2397	-741	-2097	3376
254	31.625	136	-1734	-249	4357	2271	-810	-2138	3299
255	31.750	129	-1761	-307	4272	2137	-883	-2181	3218

OBS	TIME	N700	N767	N800	N830	N900	N930	N960	N840
256	31.875	122	-1790	-369	4181	1992	-957	-2224	3132
257	32.000	112	-1827	-437	4081	1838	-1031	-2268	3038
258	32.125	100	-1873	-514	3969	1676	-1106	-2314	2937
259	32.250	82	-1929	-596	3849	1507	-1183	-2360	2829
260	32.375	60	-1988	-679	3725	1336	-1261	-2404	2721
261	32.500	36	-2045	-761	3603	1169	-1338	-2444	2617
262	32.625	16	-2098	-838	3488	1011	-1414	-2479	2522
263	32.750	1	-2145	-909	3383	869	-1484	-2510	2436
264	32.875	-10	-2186	-973	3288	745	-1549	-2538	2356
265	33.000	-19	-2222	-1029	3202	636	-1606	-2561	2283
266	33.125	-28	-2253	-1078	3124	540	-1655	-2579	2219
267	33.250	-34	-2276	-1119	3056	460	-1695	-2593	2166
268	33.375	-37	-2293	-1152	3002	397	-1725	-2602	2124
269	33.500	-38	-2305	-1181	2964	349	-1748	-2609	2092
270	33.625	-39	-2313	-1207	2943	313	-1763	-2613	2067
271	33.750	-40	-2317	-1230	2933	286	-1772	-2617	2050
272	33.875	-42	-2318	-1245	2930	273	-1774	-2619	2041
273	34.000	-42	-2316	-1251	2933	272	-1770	-2616	2040
274	34.125	-40	-2315	-1249	2938	281	-1764	-2610	2045
275	34.250	-40	-2316	-1247	2947	299	-1756	-2600	2057
276	34.375	-41	-2322	-1247	2960	325	-1746	-2589	2073
277	34.500	-44	-2332	-1247	2978	361	-1733	-2576	2094
278	34.625	-48	-2340	-1242	3003	407	-1713	-2561	2119
279	34.750	-50	-2340	-1227	3039	462	-1687	-2544	2153
280	34.875	-49	-2331	-1201	3086	529	-1653	-2523	2196
281	35.000	-47	-2316	-1165	3144	609	-1611	-2498	2247
282	35.125	-47	-2301	-1127	3208	699	-1564	-2471	2301
283	35.250	-49	-2290	-1093	3271	792	-1518	-2441	2355
284	35.375	-55	-2283	-1063	3327	883	-1474	-2410	2406
285	35.500	-64	-2281	-1038	3377	968	-1432	-2380	2456
286	35.625	-77	-2283	-1014	3424	1047	-1391	-2353	2502
287	35.750	-94	-2288	-992	3465	1124	-1350	-2329	2547
288	35.875	-117	-2299	-972	3499	1202	-1310	-2307	2587
289	36.000	-143	-2316	-952	3526	1281	-1269	-2285	2623
290	36.125	-168	-2336	-928	3549	1363	-1226	-2261	2656
291	36.250	-191	-2358	-898	3573	1446	-1182	-2236	2688
292	36.375	-209	-2374	-864	3600	1529	-1140	-2210	2722
293	36.500	-221	-2378	-827	3640	1617	-1095	-2183	2765
294	36.625	-221	-2362	-784	3703	1720	-1045	-2153	2824
295	36.750	-206	-2318	-730	3794	1842	-986	-2120	2905
296	36.875	-180	-2254	-664	3905	1979	-921	-2086	3003
297	37.000	-151	-2184	-594	4017	2115	-856	-2053	3101
298	37.125	-123	-2123	-523	4118	2241	-796	-2023	3189
299	37.250	-98	-2067	-452	4214	2358	-740	-1996	3267
300	37.375	-73	-2011	-376	4312	2474	-681	-1968	3345
301	37.500	-46	-1953	-297	4415	2596	-618	-1937	3425
302	37.625	-19	-1898	-220	4512	2718	-553	-1905	3502
303	37.750	3	-1853	-154	4597	2830	-495	-1876	3570
304	37.875	22	-1820	-103	4666	2925	-447	-1851	3628
305	38.000	38	-1795	-68	4724	3004	-408	-1831	3679
306	38.125	52	-1773	-42	4778	3072	-374	-1814	3729

OBS	TIME	N700	N767	N800	N830	N900	N930	N960	N840
307	38.250	65	-1752	-22	4826	3131	-342	-1799	3775
308	38.375	74	-1736	-7	4865	3183	-314	-1786	3812
309	38.500	75	-1732	1	4889	3222	-294	-1776	3832
310	38.625	65	-1746	4	4893	3248	-284	-1768	3836
311	38.750	49	-1768	5	4888	3266	-276	-1760	3835
312	38.875	38	-1780	17	4890	3292	-261	-1750	3845
313	39.000	43	-1768	48	4918	3340	-232	-1734	3878
314	39.125	64	-1729	100	4975	3417	-192	-1713	3938
315	39.250	95	-1673	160	5052	3510	-145	-1690	4014
316	39.375	128	-1612	216	5138	3605	-102	-1669	4094
317	39.500	160	-1550	267	5226	3693	-65	-1650	4171
318	39.625	194	-1487	316	5316	3777	-27	-1630	4243
319	39.750	230	-1425	372	5409	3865	13	-1610	4313
320	39.875	264	-1368	433	5498	3954	58	-1590	4379
321	40.000	291	-1323	490	5576	4033	98	-1574	4435
322	40.125	308	-1293	530	5634	4091	126	-1566	4474
323	40.250	318	-1274	553	5673	4130	141	-1563	4500
324	40.375	324	-1260	566	5702	4160	149	-1561	4519
325	40.500	328	-1252	574	5722	4183	155	-1558	4531
326	40.625	326	-1254	574	5726	4193	159	-1552	4532
327	40.750	322	-1267	567	5714	4189	160	-1547	4522
328	40.875	320	-1276	562	5702	4184	163	-1542	4512
329	41.000	326	-1269	569	5705	4191	171	-1537	4516
330	41.125	340	-1247	587	5726	4214	183	-1531	4534
331	41.250	351	-1225	607	5747	4238	192	-1527	4551
332	41.375	351	-1223	615	5749	4247	191	-1525	4551
333	41.500	342	-1241	609	5729	4237	181	-1526	4535
334	41.625	328	-1267	597	5698	4217	169	-1529	4512
335	41.750	316	-1289	586	5668	4198	160	-1532	4490
336	41.875	306	-1305	577	5643	4180	154	-1535	4469
337	42.000	296	-1320	571	5616	4165	149	-1536	4449
338	42.125	287	-1338	568	5585	4153	146	-1536	4429
339	42.250	280	-1357	564	5555	4146	143	-1535	4414
340	42.375	278	-1370	555	5530	4140	138	-1535	4399
341	42.500	275	-1378	543	5512	4131	130	-1538	4383
342	42.625	270	-1383	531	5496	4113	119	-1546	4365
343	42.750	264	-1391	522	5480	4089	106	-1555	4344
344	42.875	255	-1406	512	5462	4058	95	-1563	4322
345	43.000	246	-1428	497	5440	4025	85	-1570	4299
346	43.125	236	-1453	476	5420	3995	78	-1573	4277
347	43.250	226	-1477	454	5403	3970	73	-1574	4261
348	43.375	214	-1500	430	5385	3946	68	-1576	4247
349	43.500	201	-1526	404	5361	3920	57	-1581	4229
350	43.625	189	-1550	378	5334	3893	43	-1589	4212
351	43.750	185	-1559	362	5321	3881	35	-1594	4208
352	43.875	195	-1542	365	5340	3898	41	-1591	4231
353	44.000	221	-1496	391	5400	3949	66	-1579	4281
354	44.125	258	-1429	435	5488	4022	101	-1564	4347
355	44.250	294	-1361	483	5580	4097	134	-1550	4413
356	44.375	320	-1307	523	5654	4155	157	-1542	4464
357	44.500	331	-1279	546	5695	4187	169	-1539	4493

OBS	TIME	N700	N767	N800	N830	N900	N930	N960	N840
358	44.625	331	-1275	555	5707	4198	173	-1538	4504
359	44.750	327	-1279	561	5710	4202	176	-1537	4510
360	44.875	329	-1274	575	5724	4219	187	-1534	4527
361	45.000	339	-1253	598	5756	4252	206	-1527	4559
362	45.125	354	-1224	629	5795	4294	231	-1517	4599
363	45.250	369	-1197	660	5828	4333	255	-1506	4633
364	45.375	376	-1184	681	5842	4356	271	-1498	4647
365	45.500	372	-1193	684	5829	4358	272	-1496	4636
366	45.625	357	-1225	667	5790	4334	257	-1500	4599
367	45.750	333	-1272	629	5730	4285	229	-1509	4546
368	45.875	304	-1327	579	5655	4216	197	-1521	4483
369	46.000	272	-1383	524	5572	4138	165	-1533	4418
370	46.125	239	-1439	465	5488	4057	133	-1547	4354
371	46.250	206	-1495	406	5405	3975	99	-1564	4293
372	46.375	174	-1551	350	5326	3899	62	-1585	4237
373	46.500	144	-1606	302	5253	3832	24	-1607	4187
374	46.625	115	-1659	263	5184	3776	-10	-1625	4143
375	46.750	87	-1709	232	5119	3728	-41	-1639	4100
376	46.875	60	-1755	203	5055	3680	-68	-1649	4055
377	47.000	32	-1800	172	4992	3628	-93	-1658	4004
378	47.125	5	-1847	141	4931	3575	-118	-1666	3953
379	47.250	-19	-1894	113	4877	3525	-142	-1673	3906
380	47.375	-40	-1936	92	4832	3482	-160	-1679	3872
381	47.500	-54	-1964	79	4803	3452	-171	-1685	3851
382	47.625	-59	-1975	73	4791	3436	-174	-1689	3843
383	47.750	-58	-1971	73	4797	3435	-174	-1691	3843
384	47.875	-53	-1961	82	4811	3447	-174	-1691	3845
385	48.000	-48	-1950	99	4824	3467	-173	-1688	3847
386	48.125	-41	-1935	122	4836	3491	-170	-1683	3855
387	48.250	-26	-1908	146	4857	3524	-162	-1675	3874
388	48.375	0	-1861	175	4901	3571	-145	-1665	3914
389	48.500	39	-1792	211	4974	3634	-119	-1654	3974
390	48.625	82	-1715	253	5063	3705	-87	-1643	4043
391	48.750	121	-1646	295	5147	3769	-55	-1634	4104
392	48.875	148	-1599	329	5209	3816	-30	-1627	4147
393	49.000	163	-1577	349	5246	3841	-14	-1621	4168
394	49.125	165	-1580	355	5259	3845	-8	-1619	4171
395	49.250	157	-1601	348	5250	3830	-13	-1622	4161
396	49.375	141	-1632	330	5226	3801	-27	-1629	4142
397	49.500	123	-1665	309	5191	3767	-45	-1638	4119
398	49.625	108	-1689	288	5153	3734	-61	-1645	4097
399	49.750	99	-1703	273	5121	3710	-72	-1648	4083
400	49.875	97	-1707	265	5098	3699	-76	-1646	4077

DOSE = 90 mJ/cm^2

OBS	TIME	N700	N767	N800	N830	N900	N930	N960	N840
1	0.000	0	0	0	0	0	0	0	0
2	0.125	0	-1	1	6	1	-3	-3	3
3	0.250	1	-13	7	39	10	-21	-22	22
4	0.375	4	-51	24	137	31	-71	-77	76
5	0.500	6	-127	55	326	70	-167	-181	182
6	0.625	7	-237	96	603	120	-302	-328	334
7	0.750	6	-360	141	924	169	-453	-494	507
8	0.875	5	-475	182	1243	210	-596	-652	670
9	1.000	5	-569	215	1526	241	-722	-792	809
10	1.125	5	-645	242	1765	265	-828	-909	922
11	1.250	7	-706	263	1967	286	-915	-1006	1016
12	1.375	10	-756	281	2137	303	-985	-1086	1094
13	1.500	13	-798	296	2282	315	-1043	-1152	1157
14	1.625	17	-834	308	2401	323	-1093	-1208	1206
15	1.750	20	-863	317	2494	326	-1136	-1253	1245
16	1.875	24	-890	324	2564	327	-1171	-1289	1275
17	2.000	27	-917	328	2616	327	-1197	-1316	1297
18	2.125	30	-942	331	2655	325	-1216	-1338	1315
19	2.250	32	-965	333	2683	323	-1233	-1356	1330
20	2.375	33	-980	332	2706	322	-1251	-1373	1343
21	2.500	32	-989	332	2726	321	-1270	-1389	1356
22	2.625	29	-993	332	2745	322	-1286	-1404	1364
23	2.750	24	-995	333	2764	323	-1298	-1419	1370
24	2.875	18	-997	333	2780	321	-1304	-1434	1375
25	3.000	13	-998	333	2793	318	-1309	-1446	1380
26	3.125	11	-995	334	2805	318	-1311	-1455	1385
27	3.250	11	-989	336	2817	321	-1313	-1460	1391
28	3.375	14	-981	339	2830	330	-1312	-1462	1399
29	3.500	19	-973	343	2844	341	-1312	-1461	1410
30	3.625	24	-968	345	2860	350	-1311	-1460	1421
31	3.750	28	-968	346	2875	355	-1312	-1460	1429
32	3.875	31	-974	347	2888	357	-1313	-1462	1433
33	4.000	32	-983	347	2897	360	-1313	-1464	1436
34	4.125	33	-992	349	2901	364	-1313	-1465	1440
35	4.250	34	-998	351	2901	367	-1312	-1467	1445
36	4.375	34	-1001	354	2899	370	-1311	-1468	1447
37	4.500	34	-1001	356	2897	371	-1311	-1468	1446
38	4.625	34	-1001	357	2893	368	-1311	-1469	1443
39	4.750	34	-1001	357	2888	361	-1311	-1470	1439
40	4.875	34	-998	356	2884	353	-1311	-1471	1440
41	5.000	35	-990	358	2884	355	-1308	-1470	1446
42	5.125	32	-971	362	2882	374	-1298	-1466	1458
43	5.250	25	-941	365	2867	411	-1279	-1457	1470
44	5.375	13	-907	365	2833	460	-1250	-1445	1481
45	5.500	0	-876	356	2784	514	-1213	-1431	1490
46	5.625	-10	-857	338	2731	568	-1173	-1419	1501
47	5.750	-19	-851	306	2681	626	-1131	-1412	1513
48	5.875	-25	-858	265	2640	693	-1086	-1410	1528
49	6.000	-28	-875	216	2610	779	-1037	-1411	1550
50	6.125	-28	-901	162	2601	890	-982	-1414	1583
51	6.250	-25	-938	101	2619	1034	-922	-1421	1631

OBS	TIME	N700	N767	N800	N830	N900	N930	N960	N840
52	6.375	-18	-989	33	2673	1216	-856	-1436	1700
53	6.500	-8	-1058	-39	2768	1441	-784	-1462	1795
54	6.625	6	-1148	-111	2910	1709	-709	-1500	1919
55	6.750	23	-1260	-177	3100	2014	-633	-1553	2071
56	6.875	41	-1389	-228	3330	2341	-563	-1622	2248
57	7.000	58	-1528	-255	3590	2677	-502	-1705	2445
58	7.125	75	-1664	-253	3873	3007	-455	-1799	2653
59	7.250	91	-1791	-221	4169	3317	-425	-1900	2862
60	7.375	106	-1903	-163	4467	3595	-413	-2006	3062
61	7.500	118	-1997	-82	4761	3838	-418	-2112	3248
62	7.625	127	-2073	19	5045	4044	-440	-2216	3419
63	7.750	133	-2129	135	5311	4213	-477	-2317	3575
64	7.875	135	-2171	257	5551	4343	-526	-2416	3713
65	8.000	134	-2202	379	5760	4437	-586	-2512	3831
66	8.125	130	-2226	497	5934	4497	-652	-2603	3929
67	8.250	122	-2243	610	6080	4525	-727	-2688	4009
68	8.375	110	-2251	720	6202	4521	-810	-2769	4071
69	8.500	97	-2250	828	6308	4487	-901	-2846	4118
70	8.625	85	-2235	936	6399	4423	-1000	-2920	4150
71	8.750	72	-2204	1049	6472	4325	-1106	-2989	4163
72	8.875	58	-2156	1169	6519	4184	-1219	-3052	4155
73	9.000	42	-2089	1299	6533	3997	-1342	-3106	4126
74	9.125	24	-2005	1432	6506	3760	-1477	-3148	4073
75	9.250	6	-1905	1559	6432	3468	-1625	-3174	3993
76	9.375	-12	-1793	1668	6305	3121	-1786	-3182	3877
77	9.500	-32	-1674	1754	6121	2723	-1952	-3173	3724
78	9.625	-51	-1553	1813	5885	2291	-2111	-3145	3541
79	9.750	-65	-1435	1841	5606	1848	-2254	-3098	3336
80	9.875	-72	-1326	1832	5298	1415	-2373	-3034	3117
81	10.000	-73	-1228	1785	4977	1009	-2465	-2957	2895
82	10.125	-67	-1145	1707	4659	641	-2532	-2870	2676
83	10.250	-57	-1079	1607	4355	322	-2571	-2776	2466
84	10.375	-43	-1030	1492	4069	56	-2583	-2678	2272
85	10.500	-29	-1000	1365	3802	-153	-2569	-2581	2097
86	10.625	-15	-988	1228	3557	-310	-2533	-2486	1944
87	10.750	0	-992	1083	3336	-415	-2479	-2395	1816
88	10.875	13	-1009	937	3146	-469	-2411	-2307	1714
89	11.000	26	-1039	790	2987	-470	-2332	-2221	1639
90	11.125	38	-1086	641	2862	-418	-2241	-2139	1589
91	11.250	50	-1148	491	2773	-312	-2138	-2061	1562
92	11.375	63	-1224	342	2730	-150	-2020	-1989	1563
93	11.500	78	-1311	201	2741	69	-1886	-1923	1596
94	11.625	90	-1409	76	2809	343	-1741	-1865	1663
95	11.750	96	-1520	-30	2929	665	-1591	-1820	1763
96	11.875	96	-1639	-113	3096	1025	-1441	-1792	1895
97	12.000	90	-1756	-164	3304	1411	-1296	-1780	2054
98	12.125	79	-1862	-177	3548	1810	-1157	-1784	2238
99	12.250	63	-1951	-151	3823	2207	-1028	-1801	2441
100	12.375	46	-2020	-86	4119	2589	-913	-1828	2654
101	12.500	29	-2070	9	4426	2944	-817	-1864	2866
102	12.625	11	-2101	130	4732	3263	-742	-1910	3070

OBS	TIME	N700	N767	N800	N830	N900	N930	N960	N840
103	12.750	-9	-2113	267	5022	3532	-691	-1966	3257
104	12.875	-33	-2110	411	5286	3744	-664	-2034	3419
105	13.000	-60	-2093	557	5516	3899	-660	-2112	3556
106	13.125	-87	-2064	703	5713	4006	-675	-2196	3671
107	13.250	-110	-2022	849	5886	4074	-704	-2284	3767
108	13.375	-128	-1964	997	6039	4106	-747	-2374	3844
109	13.500	-142	-1892	1140	6164	4097	-807	-2465	3898
110	13.625	-152	-1807	1272	6249	4038	-887	-2557	3927
111	13.750	-160	-1714	1386	6282	3923	-988	-2649	3930
112	13.875	-163	-1617	1480	6263	3751	-1108	-2741	3905
113	14.000	-161	-1520	1555	6195	3524	-1240	-2828	3852
114	14.125	-154	-1428	1609	6081	3249	-1382	-2909	3766
115	14.250	-142	-1347	1639	5917	2931	-1531	-2978	3648
116	14.375	-125	-1279	1640	5709	2581	-1684	-3036	3499
117	14.500	-103	-1224	1612	5467	2210	-1838	-3079	3328
118	14.625	-77	-1180	1555	5204	1832	-1986	-3106	3142
119	14.750	-48	-1148	1473	4929	1459	-2126	-3118	2947
120	14.875	-19	-1132	1367	4649	1104	-2251	-3114	2751
121	15.000	6	-1133	1239	4371	774	-2357	-3096	2559
122	15.125	31	-1152	1093	4098	481	-2441	-3065	2376
123	15.250	55	-1187	938	3839	233	-2498	-3023	2206
124	15.375	80	-1235	781	3602	31	-2531	-2971	2054
125	15.500	103	-1296	625	3397	-120	-2541	-2911	1924
126	15.625	123	-1367	475	3223	-222	-2532	-2844	1818
127	15.750	140	-1446	331	3079	-274	-2503	-2771	1736
128	15.875	154	-1531	193	2968	-277	-2454	-2695	1679
129	16.000	163	-1620	62	2890	-229	-2385	-2616	1648
130	16.125	165	-1712	-56	2853	-130	-2297	-2536	1644
131	16.250	161	-1805	-158	2862	20	-2195	-2457	1670
132	16.375	151	-1890	-233	2922	223	-2081	-2378	1727
133	16.500	136	-1964	-277	3034	473	-1957	-2300	1811
134	16.625	117	-2024	-287	3194	762	-1822	-2225	1923
135	16.750	95	-2068	-264	3394	1081	-1676	-2154	2058
136	16.875	71	-2095	-209	3623	1418	-1526	-2091	2213
137	17.000	46	-2108	-128	3869	1762	-1381	-2037	2382
138	17.125	21	-2105	-25	4124	2104	-1244	-1993	2559
139	17.250	-3	-2088	94	4381	2436	-1118	-1961	2740
140	17.375	-30	-2057	227	4636	2745	-1006	-1940	2917
141	17.500	-56	-2013	368	4882	3024	-911	-1930	3081
142	17.625	-82	-1959	513	5113	3269	-836	-1931	3232
143	17.750	-104	-1895	660	5326	3481	-776	-1943	3367
144	17.875	-120	-1825	805	5517	3659	-731	-1965	3486
145	18.000	-132	-1752	942	5676	3792	-702	-2000	3586
146	18.125	-141	-1679	1062	5798	3871	-695	-2048	3660
147	18.250	-147	-1606	1163	5880	3896	-709	-2110	3707
148	18.375	-150	-1533	1249	5927	3874	-742	-2183	3732
149	18.500	-150	-1462	1324	5946	3809	-791	-2263	3736
150	18.625	-148	-1396	1388	5938	3705	-856	-2348	3720
151	18.750	-142	-1340	1439	5897	3560	-938	-2435	3685
152	18.875	-134	-1299	1470	5815	3376	-1035	-2522	3630
153	19.000	-123	-1271	1475	5690	3153	-1143	-2608	3553

OBS	TIME	N700	N767	N800	N830	N900	N930	N960	N840
154	19.125	-109	-1254	1447	5527	2896	-1260	-2695	3454
155	19.250	-92	-1244	1388	5336	2608	-1385	-2782	3332
156	19.375	-74	-1245	1305	5126	2300	-1516	-2866	3190
157	19.500	-55	-1257	1208	4906	1982	-1653	-2944	3036
158	19.625	-39	-1286	1100	4679	1662	-1791	-3013	2878
159	19.750	-23	-1330	981	4446	1348	-1924	-3069	2721
160	19.875	-9	-1387	851	4210	1048	-2047	-3113	2567
161	20.000	2	-1450	712	3979	768	-2160	-3146	2416
162	20.125	11	-1516	571	3762	513	-2263	-3167	2271
163	20.250	15	-1586	431	3565	289	-2354	-3176	2133
164	20.375	18	-1658	295	3388	99	-2429	-3176	2007
165	20.500	18	-1733	164	3228	-54	-2486	-3168	1894
166	20.625	18	-1810	42	3087	-170	-2523	-3153	1799
167	20.750	15	-1886	-66	2975	-247	-2542	-3129	1725
168	20.875	10	-1961	-158	2894	-283	-2542	-3096	1673
169	21.000	3	-2028	-231	2848	-273	-2524	-3053	1646
170	21.125	-2	-2084	-280	2844	-211	-2485	-2999	1648
171	21.250	-8	-2124	-303	2885	-100	-2425	-2936	1679
172	21.375	-13	-2147	-304	2973	54	-2347	-2865	1733
173	21.500	-17	-2154	-285	3099	245	-2255	-2789	1810
174	21.625	-22	-2145	-244	3255	470	-2150	-2709	1905
175	21.750	-25	-2121	-179	3436	726	-2036	-2625	2019
176	21.875	-28	-2086	-92	3637	1006	-1916	-2540	2148
177	22.000	-29	-2041	11	3849	1301	-1794	-2458	2286
178	22.125	-29	-1989	126	4060	1598	-1673	-2383	2427
179	22.250	-28	-1932	249	4262	1886	-1552	-2313	2569
180	22.375	-25	-1870	380	4460	2163	-1429	-2248	2711
181	22.500	-20	-1801	518	4659	2427	-1306	-2189	2853
182	22.625	-13	-1727	656	4856	2673	-1188	-2136	2991
183	22.750	-5	-1652	787	5040	2894	-1083	-2094	3118
184	22.875	1	-1579	907	5202	3082	-996	-2061	3230
185	23.000	5	-1509	1017	5343	3240	-925	-2038	3329
186	23.125	10	-1443	1119	5466	3372	-869	-2024	3414
187	23.250	16	-1381	1210	5574	3476	-826	-2021	3484
188	23.375	24	-1326	1287	5661	3550	-796	-2030	3536
189	23.500	33	-1279	1349	5724	3589	-782	-2050	3570
190	23.625	41	-1240	1397	5758	3591	-782	-2077	3587
191	23.750	47	-1212	1432	5761	3557	-795	-2109	3590
192	23.875	51	-1194	1451	5730	3487	-819	-2148	3578
193	24.000	52	-1188	1454	5669	3388	-858	-2194	3549
194	24.125	51	-1192	1441	5588	3264	-912	-2247	3505
195	24.250	50	-1207	1410	5489	3116	-980	-2304	3444
196	24.375	48	-1235	1355	5367	2938	-1062	-2368	3364
197	24.500	44	-1278	1272	5214	2723	-1157	-2440	3265
198	24.625	36	-1336	1166	5032	2477	-1265	-2521	3149
199	24.750	24	-1402	1045	4831	2210	-1385	-2608	3022
200	24.875	9	-1471	919	4625	1937	-1509	-2694	2891
201	25.000	-6	-1541	792	4425	1669	-1634	-2776	2759
202	25.125	-23	-1612	664	4235	1414	-1754	-2850	2629
203	25.250	-41	-1687	539	4055	1171	-1870	-2917	2500
204	25.375	-60	-1763	418	3885	941	-1980	-2977	2376

OBS	TIME	N700	N767	N800	N830	N900	N930	N960	N840
205	25.500	-80	-1837	302	3725	722	-2085	-3031	2258
206	25.625	-99	-1902	192	3575	521	-2183	-3079	2148
207	25.750	-116	-1958	88	3440	343	-2268	-3121	2050
208	25.875	-129	-2007	-4	3326	193	-2340	-3154	1966
209	26.000	-140	-2052	-85	3234	74	-2397	-3179	1896
210	26.125	-148	-2090	-149	3167	-13	-2443	-3196	1844
211	26.250	-156	-2118	-196	3124	-70	-2479	-3203	1806
212	26.375	-163	-2134	-226	3106	-93	-2503	-3200	1784
213	26.500	-166	-2137	-236	3115	-79	-2510	-3188	1782
214	26.625	-165	-2127	-225	3152	-24	-2496	-3164	1802
215	26.750	-160	-2103	-190	3219	67	-2462	-3130	1844
216	26.875	-154	-2068	-136	3313	190	-2414	-3087	1903
217	27.000	-147	-2026	-66	3426	336	-2357	-3039	1974
218	27.125	-137	-1980	11	3552	499	-2293	-2987	2054
219	27.250	-123	-1930	100	3692	684	-2221	-2930	2144
220	27.375	-106	-1872	205	3855	893	-2136	-2868	2248
221	27.500	-85	-1807	327	4044	1129	-2040	-2798	2368
222	27.625	-61	-1736	464	4255	1384	-1935	-2723	2503
223	27.750	-35	-1660	607	4475	1648	-1823	-2643	2644
224	27.875	-11	-1582	746	4691	1909	-1709	-2564	2783
225	28.000	11	-1502	875	4893	2159	-1598	-2490	2916
226	28.125	31	-1424	994	5078	2396	-1490	-2420	3039
227	28.250	51	-1351	1105	5247	2623	-1388	-2354	3155
228	28.375	71	-1284	1209	5400	2837	-1290	-2288	3266
229	28.500	92	-1223	1305	5540	3039	-1197	-2224	3371
230	28.625	114	-1170	1395	5671	3229	-1109	-2161	3469
231	28.750	133	-1124	1484	5795	3405	-1028	-2103	3557
232	28.875	148	-1086	1572	5913	3566	-956	-2052	3637
233	29.000	160	-1053	1657	6021	3710	-893	-2006	3709
234	29.125	172	-1023	1734	6116	3842	-836	-1967	3777
235	29.250	185	-995	1802	6202	3965	-780	-1930	3843
236	29.375	199	-967	1863	6281	4082	-724	-1897	3906
237	29.500	213	-937	1916	6352	4190	-669	-1867	3963
238	29.625	225	-906	1964	6415	4288	-618	-1840	4010
239	29.750	236	-876	2009	6477	4375	-577	-1816	4049
240	29.875	246	-849	2052	6543	4450	-547	-1796	4081
241	30.000	253	-828	2095	6610	4510	-524	-1779	4105
242	30.125	256	-818	2134	6666	4554	-507	-1767	4117
243	30.250	255	-819	2163	6697	4584	-496	-1757	4117
244	30.375	255	-824	2181	6708	4607	-489	-1747	4114
245	30.500	257	-825	2194	6710	4632	-480	-1735	4116
246	30.625	262	-818	2204	6715	4660	-469	-1721	4124
247	30.750	269	-805	2212	6725	4688	-454	-1707	4136
248	30.875	275	-791	2220	6739	4714	-436	-1696	4151
249	31.000	282	-780	2228	6755	4742	-419	-1685	4168
250	31.125	288	-772	2237	6775	4772	-404	-1677	4190
251	31.250	293	-764	2247	6797	4804	-390	-1669	4213
252	31.375	297	-755	2259	6823	4837	-375	-1663	4232
253	31.500	300	-747	2273	6852	4867	-359	-1658	4249
254	31.625	302	-741	2285	6879	4891	-346	-1653	4263
255	31.750	304	-738	2290	6893	4904	-339	-1651	4270

OBS	TIME	N700	N767	N800	N830	N900	N930	N960	N840
256	31.875	305	-739	2287	6889	4903	-340	-1652	4267
257	32.000	304	-741	2276	6868	4893	-344	-1656	4256
258	32.125	302	-742	2262	6841	4881	-350	-1659	4241
259	32.250	300	-741	2250	6819	4873	-357	-1659	4228
260	32.375	300	-739	2244	6808	4870	-365	-1657	4221
261	32.500	301	-738	2245	6806	4871	-368	-1652	4221
262	32.625	303	-737	2252	6811	4876	-364	-1645	4225
263	32.750	304	-735	2264	6820	4887	-352	-1638	4232
264	32.875	305	-732	2279	6835	4905	-338	-1632	4239
265	33.000	306	-732	2294	6856	4927	-328	-1628	4244
266	33.125	307	-735	2309	6881	4950	-323	-1625	4248
267	33.250	308	-739	2321	6907	4965	-320	-1624	4251
268	33.375	309	-739	2331	6931	4970	-316	-1626	4254
269	33.500	310	-736	2338	6949	4966	-312	-1631	4256
270	33.625	311	-733	2342	6955	4955	-308	-1638	4256
271	33.750	311	-733	2341	6947	4943	-304	-1646	4254
272	33.875	311	-736	2337	6924	4934	-302	-1652	4251
273	34.000	310	-743	2328	6893	4929	-300	-1655	4247
274	34.125	310	-750	2317	6864	4927	-299	-1655	4245
275	34.250	310	-752	2306	6842	4926	-298	-1655	4243
276	34.375	310	-749	2297	6832	4928	-297	-1656	4243
277	34.500	311	-739	2297	6839	4938	-293	-1656	4246
278	34.625	313	-723	2305	6854	4952	-283	-1654	4254
279	34.750	315	-709	2315	6868	4963	-271	-1649	4261
280	34.875	316	-702	2320	6871	4965	-263	-1646	4265
281	35.000	318	-703	2319	6872	4964	-258	-1645	4272
282	35.125	321	-707	2317	6881	4970	-253	-1645	4284
283	35.250	324	-705	2318	6904	4984	-247	-1644	4300
284	35.375	326	-700	2320	6930	4997	-241	-1642	4316
285	35.500	327	-695	2321	6951	5002	-239	-1642	4324
286	35.625	325	-693	2320	6964	5001	-242	-1645	4326
287	35.750	324	-694	2319	6970	4996	-247	-1648	4323
288	35.875	323	-695	2317	6970	4989	-255	-1651	4321
289	36.000	321	-695	2313	6959	4978	-262	-1652	4319
290	36.125	319	-696	2304	6937	4962	-266	-1652	4314
291	36.250	317	-698	2293	6915	4946	-264	-1653	4310
292	36.375	318	-701	2287	6906	4942	-261	-1657	4309
293	36.500	321	-701	2291	6916	4952	-257	-1660	4315
294	36.625	324	-698	2304	6940	4972	-255	-1660	4326
295	36.750	325	-692	2318	6963	4993	-254	-1657	4340
296	36.875	325	-687	2325	6973	5008	-255	-1654	4353
297	37.000	326	-681	2325	6976	5020	-254	-1653	4365
298	37.125	328	-675	2325	6984	5037	-248	-1653	4380
299	37.250	330	-667	2332	7007	5059	-239	-1652	4395
300	37.375	330	-655	2344	7042	5084	-231	-1649	4408
301	37.500	330	-643	2359	7080	5107	-225	-1644	4419
302	37.625	331	-631	2373	7115	5129	-220	-1639	4430
303	37.750	334	-622	2383	7144	5148	-213	-1634	4441
304	37.875	335	-619	2385	7164	5163	-203	-1633	4448
305	38.000	333	-621	2381	7171	5169	-194	-1636	4449
306	38.125	331	-628	2371	7167	5166	-190	-1641	4446

OBS	TIME	N700	N767	N800	N830	N900	N930	N960	N840
307	38.250	331	-636	2360	7155	5159	-190	-1646	4443
308	38.375	333	-643	2353	7140	5152	-193	-1649	4447
309	38.500	336	-652	2350	7122	5148	-192	-1650	4455

DOSE = 114 mJ/cm^2

OBS	TIME	N700	N767	N800	N830	N900	N930	N960	E20 N840
1	0.000	0	0	0	0	0	0	0	0
2	0.125	0	-3	0	4	0	-2	-2	3
3	0.250	1	-20	4	28	6	-16	-18	23
4	0.375	1	-68	12	94	20	-58	-63	78
5	0.500	0	-158	28	217	43	-140	-150	182
6	0.625	-6	-283	50	383	68	-259	-272	324
7	0.750	-14	-420	76	560	85	-397	-408	476
8	0.875	-23	-546	105	717	90	-534	-537	611
9	1.000	-32	-655	133	839	82	-658	-649	714
10	1.125	-45	-750	155	928	63	-768	-743	787
11	1.250	-62	-835	170	990	37	-863	-823	836
12	1.375	-81	-910	179	1032	9	-944	-892	870
13	1.500	-97	-971	186	1064	-16	-1012	-949	897
14	1.625	-104	-1009	196	1096	-31	-1063	-994	926
15	1.750	-96	-1018	218	1143	-29	-1096	-1024	966
16	1.875	-77	-1002	249	1203	-7	-1111	-1041	1015
17	2.000	-56	-978	280	1263	22	-1119	-1052	1062
18	2.125	-45	-967	301	1306	41	-1128	-1065	1094
19	2.250	-52	-979	305	1324	41	-1146	-1085	1106
20	2.375	-72	-1012	293	1321	23	-1173	-1109	1099
21	2.500	-101	-1060	269	1303	-5	-1202	-1135	1083
22	2.625	-134	-1119	234	1277	-44	-1231	-1161	1062
23	2.750	-167	-1185	193	1245	-89	-1257	-1186	1038
24	2.875	-199	-1250	150	1213	-137	-1282	-1208	1014
25	3.000	-228	-1309	110	1185	-184	-1307	-1229	990
26	3.125	-253	-1359	74	1159	-226	-1331	-1248	967
27	3.250	-274	-1401	43	1136	-262	-1355	-1263	947
28	3.375	-290	-1435	19	1116	-290	-1374	-1275	930
29	3.500	-305	-1463	4	1100	-310	-1388	-1282	917
30	3.625	-321	-1486	-4	1090	-326	-1398	-1290	907
31	3.750	-336	-1507	-14	1083	-342	-1406	-1299	898
32	3.875	-349	-1533	-32	1075	-362	-1416	-1310	887
33	4.000	-361	-1563	-58	1061	-385	-1428	-1324	873
34	4.125	-370	-1592	-86	1042	-407	-1439	-1337	857
35	4.250	-379	-1616	-110	1023	-427	-1450	-1346	842
36	4.375	-389	-1637	-131	1007	-445	-1462	-1353	829
37	4.500	-402	-1657	-147	993	-464	-1474	-1357	818
38	4.625	-414	-1674	-158	984	-480	-1484	-1359	810
39	4.750	-421	-1678	-161	982	-487	-1487	-1360	808
40	4.875	-418	-1669	-153	988	-480	-1483	-1359	813
41	5.000	-410	-1656	-149	999	-466	-1473	-1358	820
42	5.125	-409	-1661	-173	1011	-454	-1460	-1362	827
43	5.250	-420	-1694	-245	1027	-448	-1443	-1375	830
44	5.375	-441	-1752	-368	1048	-441	-1418	-1399	832
45	5.500	-467	-1823	-520	1078	-424	-1383	-1432	836
46	5.625	-487	-1891	-676	1120	-388	-1338	-1467	850
47	5.750	-497	-1949	-818	1175	-326	-1282	-1501	882
48	5.875	-494	-1999	-946	1247	-230	-1216	-1532	936
49	6.000	-482	-2047	-1063	1335	-98	-1142	-1560	1012
50	6.125	-467	-2101	-1174	1441	72	-1063	-1591	1112
51	6.250	-451	-2169	-1280	1573	283	-982	-1627	1242

OBS	TIME	N700	N767	N800	N830	N900	N930	N960	N840
52	6.375	-433	-2252	-1373	1740	538	-900	-1674	1407
53	6.500	-412	-2346	-1441	1946	836	-819	-1730	1608
54	6.625	-391	-2446	-1479	2184	1161	-745	-1796	1836
55	6.750	-374	-2549	-1488	2436	1482	-688	-1869	2075
56	6.875	-363	-2651	-1475	2688	1769	-653	-1950	2307
57	7.000	-357	-2748	-1441	2929	2004	-642	-2035	2522
58	7.125	-354	-2835	-1389	3151	2190	-650	-2120	2712
59	7.250	-353	-2910	-1322	3352	2335	-674	-2203	2876
60	7.375	-351	-2967	-1248	3535	2447	-711	-2283	3017
61	7.500	-345	-2998	-1163	3710	2532	-758	-2356	3144
62	7.625	-329	-2996	-1058	3892	2604	-810	-2421	3270
63	7.750	-302	-2956	-922	4090	2670	-865	-2478	3403
64	7.875	-266	-2882	-756	4297	2727	-923	-2528	3536
65	8.000	-224	-2775	-568	4502	2760	-987	-2570	3662
66	8.125	-179	-2632	-364	4694	2750	-1063	-2604	3769
67	8.250	-131	-2458	-153	4856	2676	-1156	-2628	3841
68	8.375	-86	-2269	43	4959	2520	-1270	-2640	3856
69	8.500	-54	-2092	200	4972	2273	-1403	-2636	3794
70	8.625	-40	-1947	297	4882	1946	-1543	-2615	3652
71	8.750	-42	-1838	331	4706	1571	-1676	-2579	3449
72	8.875	-51	-1757	314	4476	1190	-1786	-2529	3213
73	9.000	-56	-1694	261	4227	837	-1864	-2468	2971
74	9.125	-57	-1644	180	3980	533	-1909	-2400	2740
75	9.250	-54	-1610	77	3744	285	-1924	-2328	2528
76	9.375	-50	-1595	-42	3518	92	-1915	-2258	2337
77	9.500	-52	-1609	-179	3301	-52	-1888	-2191	2166
78	9.625	-63	-1661	-334	3088	-155	-1847	-2129	2010
79	9.750	-86	-1749	-509	2885	-213	-1793	-2075	1875
80	9.875	-115	-1867	-697	2708	-216	-1724	-2027	1771
81	10.000	-146	-2001	-882	2581	-149	-1633	-1984	1712
82	10.125	-174	-2141	-1047	2520	-4	-1520	-1945	1711
83	10.250	-199	-2281	-1180	2530	213	-1389	-1912	1770
84	10.375	-223	-2416	-1276	2607	484	-1250	-1890	1883
85	10.500	-249	-2541	-1335	2739	782	-1117	-1885	2037
86	10.625	-276	-2648	-1354	2912	1084	-999	-1897	2219
87	10.750	-303	-2734	-1338	3107	1374	-904	-1924	2411
88	10.875	-332	-2800	-1292	3307	1640	-833	-1963	2600
89	11.000	-362	-2844	-1224	3499	1870	-787	-2011	2774
90	11.125	-394	-2867	-1140	3680	2058	-764	-2068	2930
91	11.250	-424	-2867	-1040	3849	2203	-764	-2131	3066
92	11.375	-450	-2845	-927	4003	2302	-786	-2198	3181
93	11.500	-472	-2805	-809	4132	2347	-831	-2267	3269
94	11.625	-489	-2749	-694	4226	2332	-901	-2340	3324
95	11.750	-498	-2681	-590	4279	2255	-995	-2415	3338
96	11.875	-495	-2602	-503	4288	2116	-1112	-2490	3310
97	12.000	-483	-2517	-440	4252	1916	-1248	-2563	3238
98	12.125	-466	-2436	-406	4169	1659	-1397	-2628	3124
99	12.250	-445	-2369	-406	4039	1357	-1550	-2679	2972
100	12.375	-423	-2323	-437	3866	1031	-1699	-2715	2790
101	12.500	-403	-2302	-496	3661	701	-1836	-2733	2588
102	12.625	-386	-2301	-578	3438	384	-1955	-2735	2380

OBS	TIME	N700	N767	N800	N830	N900	N930	N960	E22 N840
103	12.750	-368	-2312	-678	3219	101	-2046	-2721	2180
104	12.875	-341	-2319	-783	3025	-124	-2101	-2688	2010
105	13.000	-302	-2314	-881	2874	-276	-2113	-2639	1882
106	13.125	-251	-2298	-967	2773	-349	-2082	-2573	1803
107	13.250	-196	-2284	-1042	2716	-349	-2015	-2497	1767
108	13.375	-150	-2286	-1117	2690	-292	-1924	-2416	1764
109	13.500	-121	-2319	-1195	2678	-191	-1819	-2338	1782
110	13.625	-115	-2387	-1274	2674	-60	-1709	-2265	1813
111	13.750	-132	-2481	-1342	2682	95	-1598	-2200	1856
112	13.875	-168	-2588	-1392	2711	272	-1485	-2142	1917
113	14.000	-218	-2693	-1422	2767	466	-1374	-2092	1996
114	14.125	-275	-2786	-1432	2852	673	-1270	-2056	2095
115	14.250	-333	-2856	-1418	2965	890	-1173	-2032	2211
116	14.375	-386	-2898	-1374	3102	1113	-1086	-2020	2341
117	14.500	-431	-2910	-1299	3260	1338	-1007	-2015	2482
118	14.625	-462	-2886	-1197	3439	1562	-933	-2016	2636
119	14.750	-470	-2821	-1068	3642	1785	-864	-2021	2804
120	14.875	-453	-2714	-916	3863	1999	-801	-2031	2983
121	15.000	-416	-2577	-753	4084	2188	-751	-2048	3156
122	15.125	-368	-2430	-592	4283	2329	-724	-2074	3305
123	15.250	-320	-2291	-446	4438	2407	-726	-2111	3413
124	15.375	-276	-2173	-328	4533	2410	-763	-2159	3468
125	15.500	-240	-2082	-249	4558	2336	-836	-2218	3463
126	15.625	-215	-2025	-217	4512	2183	-941	-2289	3399
127	15.750	-201	-2001	-233	4403	1962	-1071	-2366	3283
128	15.875	-194	-2006	-292	4246	1688	-1216	-2445	3127
129	16.000	-191	-2034	-381	4055	1381	-1368	-2520	2945
130	16.125	-194	-2083	-491	3839	1061	-1518	-2587	2745
131	16.250	-203	-2152	-613	3607	743	-1661	-2643	2535
132	16.375	-221	-2240	-745	3366	439	-1794	-2687	2321
133	16.500	-250	-2350	-888	3120	155	-1914	-2720	2109
134	16.625	-289	-2479	-1044	2873	-104	-2017	-2741	1905
135	16.750	-333	-2615	-1204	2644	-324	-2097	-2748	1723
136	16.875	-369	-2737	-1349	2459	-484	-2142	-2740	1583
137	17.000	-387	-2823	-1458	2345	-563	-2146	-2717	1506
138	17.125	-382	-2861	-1519	2319	-550	-2106	-2676	1499
139	17.250	-359	-2852	-1536	2377	-450	-2028	-2619	1561
140	17.375	-323	-2805	-1515	2509	-272	-1918	-2548	1679
141	17.500	-279	-2732	-1461	2692	-36	-1781	-2467	1840
142	17.625	-235	-2648	-1377	2907	242	-1628	-2381	2029
143	17.750	-196	-2558	-1268	3137	545	-1466	-2296	2233
144	17.875	-159	-2462	-1140	3377	862	-1304	-2213	2447
145	18.000	-122	-2361	-998	3616	1181	-1148	-2135	2661
146	18.125	-88	-2262	-852	3843	1486	-1003	-2066	2864
147	18.250	-62	-2174	-711	4048	1759	-877	-2009	3046
148	18.375	-47	-2102	-583	4222	1990	-773	-1969	3199
149	18.500	-45	-2050	-473	4359	2173	-695	-1945	3315
150	18.625	-54	-2021	-387	4454	2301	-647	-1936	3391
151	18.750	-72	-2014	-330	4500	2368	-630	-1942	3425
152	18.875	-95	-2024	-302	4505	2376	-644	-1963	3423
153	19.000	-119	-2038	-296	4483	2339	-678	-1995	3397

OBS	TIME	N700	N767	N800	N830	N900	N930	N960	N840
154	19.125	-136	-2046	-299	4447	2271	-727	-2036	3357
155	19.250	-145	-2048	-308	4394	2178	-785	-2083	3303
156	19.375	-155	-2058	-331	4312	2049	-860	-2136	3225
157	19.500	-173	-2091	-382	4191	1874	-955	-2199	3115
158	19.625	-200	-2142	-460	4037	1659	-1068	-2268	2977
159	19.750	-223	-2194	-545	3877	1429	-1188	-2337	2834
160	19.875	-229	-2226	-619	3737	1213	-1302	-2401	2706
161	20.000	-213	-2231	-675	3629	1023	-1402	-2456	2605
162	20.125	-183	-2218	-721	3546	856	-1491	-2502	2524
163	20.250	-153	-2206	-770	3469	698	-1571	-2543	2448
164	20.375	-138	-2215	-831	3378	537	-1649	-2582	2365
165	20.500	-141	-2249	-905	3272	374	-1726	-2618	2268
166	20.625	-157	-2303	-985	3160	222	-1796	-2651	2168
167	20.750	-176	-2356	-1057	3065	101	-1852	-2674	2085
168	20.875	-188	-2394	-1109	3006	30	-1884	-2683	2034
169	21.000	-194	-2413	-1137	2984	10	-1891	-2676	2021
170	21.125	-198	-2424	-1150	2988	31	-1878	-2656	2032
171	21.250	-208	-2436	-1156	3004	77	-1852	-2629	2056
172	21.375	-225	-2451	-1155	3029	145	-1816	-2596	2090
173	21.500	-244	-2464	-1142	3069	235	-1769	-2562	2137
174	21.625	-260	-2469	-1111	3126	350	-1710	-2522	2198
175	21.750	-271	-2467	-1067	3197	491	-1640	-2477	2272
176	21.875	-277	-2456	-1010	3282	652	-1560	-2428	2358
177	22.000	-276	-2431	-939	3388	836	-1468	-2373	2460
178	22.125	-262	-2383	-847	3522	1044	-1361	-2313	2584
179	22.250	-235	-2314	-735	3680	1274	-1243	-2249	2728
180	22.375	-199	-2230	-612	3852	1518	-1121	-2181	2884
181	22.500	-158	-2137	-483	4028	1769	-999	-2113	3046
182	22.625	-112	-2036	-352	4208	2022	-879	-2047	3211
183	22.750	-59	-1926	-218	4394	2273	-762	-1985	3376
184	22.875	-4	-1815	-90	4577	2510	-654	-1927	3532
185	23.000	40	-1724	17	4732	2712	-563	-1877	3660
186	23.125	62	-1675	90	4836	2857	-499	-1837	3745
187	23.250	54	-1677	120	4878	2937	-462	-1812	3781
188	23.375	25	-1716	118	4869	2961	-447	-1802	3778
189	23.500	-15	-1775	99	4830	2950	-447	-1802	3752
190	23.625	-59	-1841	75	4777	2924	-453	-1809	3718
191	23.750	-101	-1910	48	4718	2891	-462	-1820	3680
192	23.875	-139	-1976	20	4662	2860	-472	-1830	3644
193	24.000	-170	-2027	-2	4624	2838	-479	-1837	3618
194	24.125	-189	-2055	-12	4614	2835	-479	-1838	3611
195	24.250	-198	-2061	-9	4627	2850	-471	-1834	3619
196	24.375	-200	-2056	5	4652	2877	-458	-1826	3638
197	24.500	-196	-2041	29	4686	2917	-439	-1814	3666
198	24.625	-181	-2007	68	4741	2980	-409	-1801	3713
199	24.750	-151	-1945	125	4830	3073	-366	-1784	3784
200	24.875	-110	-1865	192	4946	3183	-315	-1763	3871
201	25.000	-71	-1789	252	5061	3285	-268	-1743	3953
202	25.125	-44	-1737	294	5151	3362	-236	-1727	4012
203	25.250	-31	-1711	315	5204	3409	-219	-1718	4043
204	25.375	-27	-1708	321	5223	3431	-215	-1715	4049

OBS	TIME	N700	N767	N800	N830	N900	N930	N960	N840
205	25.500	-28	-1718	320	5219	3435	-217	-1715	4038
206	25.625	-34	-1736	315	5200	3428	-224	-1716	4020
207	25.750	-47	-1759	303	5168	3407	-235	-1721	3999
208	25.875	-67	-1788	283	5124	3368	-248	-1731	3973
209	26.000	-91	-1825	256	5069	3312	-265	-1746	3940
210	26.125	-114	-1865	229	5013	3252	-284	-1760	3901
211	26.250	-133	-1897	209	4972	3206	-298	-1769	3868
212	26.375	-138	-1908	206	4960	3191	-303	-1771	3855
213	26.500	-125	-1887	226	4989	3218	-294	-1765	3874
214	26.625	-92	-1837	270	5057	3282	-269	-1750	3925
215	26.750	-45	-1767	329	5150	3368	-234	-1730	3997
216	26.875	3	-1691	388	5247	3455	-195	-1710	4075
217	27.000	49	-1620	437	5335	3528	-161	-1693	4148
218	27.125	89	-1554	474	5408	3589	-132	-1682	4216
219	27.250	125	-1493	505	5472	3647	-107	-1671	4282
220	27.375	158	-1434	537	5535	3706	-83	-1658	4347
221	27.500	190	-1381	574	5599	3769	-56	-1643	4408
222	27.625	219	-1334	616	5659	3834	-25	-1627	4461
223	27.750	244	-1297	658	5713	3895	6	-1612	4504
224	27.875	264	-1268	693	5758	3947	34	-1601	4535
225	28.000	278	-1246	713	5796	3986	56	-1593	4556
226	28.125	288	-1230	722	5830	4014	73	-1586	4570
227	28.250	294	-1220	722	5860	4031	86	-1580	4580
228	28.375	296	-1215	717	5883	4039	93	-1579	4585
229	28.500	294	-1215	710	5897	4038	93	-1583	4586
230	28.625	289	-1217	703	5902	4032	88	-1590	4582
231	28.750	283	-1220	700	5901	4028	83	-1596	4577
232	28.875	279	-1222	703	5897	4033	82	-1598	4572
233	29.000	276	-1223	709	5892	4046	85	-1597	4572
234	29.125	276	-1225	713	5884	4063	89	-1593	4575
235	29.250	277	-1229	712	5870	4075	91	-1589	4578
236	29.375	277	-1235	706	5848	4072	90	-1587	4576
237	29.500	276	-1246	695	5820	4051	84	-1590	4565
238	29.625	272	-1261	678	5791	4016	73	-1595	4544
239	29.750	263	-1280	660	5764	3977	61	-1601	4517
240	29.875	250	-1299	645	5740	3948	52	-1604	4491
241	30.000	237	-1316	640	5718	3933	47	-1604	4468
242	30.125	227	-1331	641	5701	3924	44	-1604	4452
243	30.250	221	-1342	641	5686	3917	40	-1605	4442
244	30.375	217	-1355	637	5671	3907	34	-1606	4434
245	30.500	211	-1372	631	5652	3891	25	-1609	4423
246	30.625	203	-1392	624	5630	3869	14	-1614	4409
247	30.750	190	-1414	615	5607	3842	-1	-1624	4390
248	30.875	171	-1442	596	5580	3808	-21	-1639	4365
249	31.000	146	-1482	562	5540	3761	-46	-1656	4326
250	31.125	110	-1541	508	5476	3695	-78	-1676	4269
251	31.250	64	-1619	438	5384	3606	-119	-1697	4192
252	31.375	10	-1710	359	5267	3501	-166	-1719	4101
253	31.500	-47	-1805	280	5140	3394	-216	-1740	4005
254	31.625	-101	-1894	210	5020	3295	-261	-1755	3918
255	31.750	-145	-1967	154	4918	3214	-297	-1765	3846

OBS	TIME	N700	N767	N800	N830	N900	N930	N960	N840
256	31.875	-180	-2023	112	4840	3152	-323	-1775	3793
257	32.000	-207	-2063	80	4785	3104	-342	-1784	3756
258	32.125	-230	-2092	54	4743	3063	-360	-1793	3728
259	32.250	-250	-2118	29	4708	3026	-378	-1801	3705
260	32.375	-265	-2142	1	4676	2994	-394	-1809	3681
261	32.500	-276	-2165	-25	4652	2971	-407	-1820	3659
262	32.625	-282	-2185	-50	4635	2957	-417	-1831	3640
263	32.750	-285	-2201	-74	4624	2948	-427	-1839	3627
264	32.875	-288	-2213	-95	4615	2941	-434	-1844	3622
265	33.000	-289	-2219	-111	4609	2938	-438	-1845	3624
266	33.125	-292	-2225	-122	4601	2937	-438	-1844	3627
267	33.250	-298	-2235	-130	4587	2932	-438	-1843	3626
268	33.375	-307	-2251	-139	4570	2922	-440	-1841	3618
269	33.500	-313	-2261	-141	4566	2917	-442	-1838	3613
270	33.625	-306	-2251	-130	4589	2932	-436	-1831	3624
271	33.750	-286	-2218	-100	4640	2974	-420	-1821	3656
272	33.875	-257	-2170	-59	4702	3031	-397	-1812	3700
273	34.000	-231	-2127	-19	4752	3083	-376	-1806	3740
274	34.125	-214	-2101	6	4780	3115	-363	-1803	3765
275	34.250	-207	-2095	18	4787	3128	-359	-1801	3773
276	34.375	-206	-2099	21	4782	3133	-358	-1800	3772
277	34.500	-206	-2102	23	4775	3137	-357	-1800	3770
278	34.625	-204	-2100	29	4775	3142	-354	-1799	3773
279	34.750	-201	-2090	37	4783	3147	-348	-1798	3781
280	34.875	-195	-2074	49	4802	3159	-339	-1797	3795
281	35.000	-184	-2052	65	4832	3184	-325	-1793	3816
282	35.125	-168	-2024	86	4868	3218	-309	-1786	3842
283	35.250	-149	-1997	106	4901	3249	-294	-1777	3865
284	35.375	-133	-1981	117	4918	3261	-289	-1770	3875
285	35.500	-127	-1983	116	4908	3249	-298	-1769	3867
286	35.625	-128	-1998	106	4875	3217	-317	-1773	3842
287	35.750	-133	-2013	92	4835	3178	-341	-1781	3812
288	35.875	-135	-2018	82	4803	3145	-360	-1787	3786
289	36.000	-133	-2015	78	4783	3125	-371	-1790	3769
290	36.125	-133	-2015	78	4768	3116	-375	-1789	3755
291	36.250	-140	-2026	78	4753	3111	-377	-1787	3739
292	36.375	-150	-2040	82	4741	3107	-379	-1787	3724
293	36.500	-151	-2039	93	4750	3117	-374	-1785	3727
294	36.625	-131	-2005	120	4794	3157	-354	-1778	3763
295	36.750	-90	-1938	165	4876	3231	-321	-1765	3830
296	36.875	-40	-1857	218	4973	3321	-282	-1748	3911
297	37.000	4	-1782	269	5064	3407	-244	-1729	3988
298	37.125	37	-1724	313	5140	3475	-210	-1713	4053
299	37.250	61	-1682	350	5202	3528	-179	-1698	4103
300	37.375	80	-1654	379	5251	3572	-153	-1686	4141
301	37.500	96	-1639	396	5287	3607	-132	-1678	4163
302	37.625	103	-1640	401	5305	3625	-121	-1675	4170
303	37.750	96	-1657	395	5305	3623	-119	-1675	4164
304	37.875	80	-1684	384	5289	3605	-125	-1678	4148
305	38.000	60	-1718	365	5260	3577	-137	-1682	4122
306	38.125	38	-1759	334	5221	3538	-158	-1689	4086

OBS	TIME	N700	N767	N800	N830	N900	N930	N960	N840
307	38.250	10	-1807	288	5169	3484	-188	-1703	4041
308	38.375	-23	-1861	231	5106	3415	-226	-1724	3988
309	38.500	-60	-1914	174	5038	3340	-266	-1745	3935
310	38.625	-91	-1959	131	4977	3272	-300	-1762	3888
311	38.750	-108	-1984	110	4938	3230	-320	-1773	3862
312	38.875	-113	-1986	114	4931	3222	-324	-1775	3861
313	39.000	-109	-1970	138	4947	3240	-316	-1772	3881
314	39.125	-104	-1952	167	4967	3266	-303	-1766	3904
315	39.250	-101	-1940	188	4980	3285	-292	-1763	3920
316	39.375	-100	-1936	199	4989	3297	-283	-1762	3929
317	39.500	-96	-1934	203	5003	3309	-274	-1763	3937
318	39.625	-89	-1929	206	5026	3328	-262	-1761	3949
319	39.750	-74	-1914	213	5061	3359	-248	-1756	3970
320	39.875	-51	-1884	232	5109	3405	-228	-1746	4003
321	40.000	-21	-1839	265	5167	3464	-203	-1729	4049
322	40.125	10	-1787	307	5230	3527	-176	-1711	4105
323	40.250	37	-1737	348	5290	3586	-152	-1696	4162
324	40.375	56	-1699	379	5339	3628	-135	-1688	4207
325	40.500	65	-1684	390	5363	3644	-132	-1687	4228
326	40.625	58	-1699	375	5352	3631	-143	-1696	4219
327	40.750	33	-1744	340	5301	3593	-167	-1713	4179
328	40.875	-6	-1810	293	5222	3541	-198	-1732	4120
329	41.000	-51	-1881	245	5133	3480	-230	-1749	4055
330	41.125	-92	-1946	197	5050	3415	-260	-1761	3994
331	41.250	-125	-2003	149	4980	3349	-289	-1773	3942
332	41.375	-152	-2049	103	4924	3287	-315	-1785	3897
333	41.500	-171	-2083	64	4884	3237	-335	-1795	3863
334	41.625	-178	-2099	41	4867	3208	-344	-1799	3847
335	41.750	-171	-2091	39	4880	3210	-338	-1797	3854
336	41.875	-151	-2060	60	4924	3245	-317	-1791	3889
337	42.000	-117	-2006	102	4998	3313	-282	-1778	3949
338	42.125	-72	-1930	161	5098	3410	-236	-1760	4031
339	42.250	-15	-1835	236	5221	3529	-183	-1735	4130
340	42.375	48	-1729	321	5356	3657	-126	-1709	4236
341	42.500	111	-1625	403	5489	3776	-72	-1687	4337
342	42.625	169	-1532	474	5607	3876	-25	-1668	4425
343	42.750	217	-1456	529	5703	3959	11	-1653	4497
344	42.875	256	-1396	571	5783	4032	39	-1640	4556
345	43.000	288	-1348	608	5853	4101	62	-1628	4606
346	43.125	315	-1306	644	5920	4166	85	-1617	4651
347	43.250	339	-1268	678	5981	4224	108	-1608	4694
348	43.375	357	-1236	704	6030	4268	127	-1604	4727
349	43.500	370	-1213	719	6063	4293	140	-1602	4747
350	43.625	378	-1199	724	6081	4304	150	-1602	4756
351	43.750	382	-1191	725	6092	4313	159	-1601	4761
352	43.875	383	-1185	727	6105	4326	169	-1597	4769
353	44.000	384	-1179	732	6122	4345	179	-1593	4783
354	44.125	388	-1173	743	6138	4367	187	-1586	4798
355	44.250	398	-1165	763	6148	4386	194	-1577	4813
356	44.375	413	-1156	789	6151	4400	201	-1566	4824
357	44.500	429	-1144	813	6153	4406	209	-1557	4833

OBS	TIME	N700	N767	N800	N830	N900	N930	N960	N840
358	44.625	441	-1134	829	6158	4405	214	-1551	4836
359	44.750	449	-1128	835	6164	4399	215	-1548	4832
360	44.875	455	-1123	837	6172	4392	216	-1545	4827
361	45.000	461	-1115	842	6184	4393	219	-1542	4827
362	45.125	464	-1102	852	6201	4407	227	-1539	4839
363	45.250	467	-1087	864	6216	4429	237	-1536	4860
364	45.375	468	-1075	875	6223	4450	245	-1532	4882
365	45.500	469	-1070	885	6224	4467	250	-1528	4898
366	45.625	472	-1068	892	6222	4482	252	-1526	4907
367	45.750	480	-1066	898	6221	4499	254	-1523	4913
368	45.875	492	-1059	903	6227	4522	258	-1520	4920
369	46.000	506	-1044	911	6242	4548	265	-1518	4933
370	46.125	520	-1023	923	6262	4573	271	-1518	4950
371	46.250	531	-1002	939	6282	4596	277	-1518	4967
372	46.375	539	-988	954	6299	4616	279	-1519	4977
373	46.500	542	-984	963	6310	4631	278	-1519	4980
374	46.625	541	-988	961	6318	4634	274	-1519	4978
375	46.750	537	-996	946	6323	4626	270	-1521	4974
376	46.875	533	-1004	924	6326	4615	266	-1523	4972
377	47.000	530	-1007	905	6327	4610	265	-1523	4971
378	47.125	530	-1007	894	6327	4617	269	-1522	4972
379	47.250	533	-1006	894	6330	4634	277	-1520	4975
380	47.375	538	-1003	903	6340	4654	287	-1519	4982
381	47.500	542	-999	916	6357	4670	297	-1519	4993
382	47.625	545	-995	929	6375	4678	304	-1519	5005
383	47.750	545	-991	936	6391	4677	306	-1520	5013
384	47.875	544	-990	934	6403	4665	303	-1523	5017
385	48.000	543	-989	922	6414	4648	298	-1528	5022
386	48.125	543	-985	911	6426	4636	297	-1532	5031
387	48.250	544	-976	908	6439	4634	301	-1534	5044
388	48.375	545	-964	913	6454	4643	308	-1533	5060
389	48.500	545	-955	924	6474	4655	315	-1531	5074
390	48.625	545	-948	936	6501	4667	318	-1532	5087
391	48.750	547	-941	946	6531	4680	321	-1534	5104
392	48.875	552	-931	955	6561	4698	326	-1534	5124
393	49.000	557	-921	961	6580	4715	332	-1531	5141
394	49.125	562	-917	963	6584	4724	335	-1527	5148
395	49.250	562	-924	965	6574	4724	335	-1525	5144
396	49.375	559	-941	967	6556	4720	334	-1524	5132
397	49.500	552	-963	966	6534	4717	331	-1525	5118
398	49.625	543	-985	959	6509	4711	326	-1525	5100
399	49.750	534	-1009	944	6480	4696	317	-1525	5078
400	49.875	522	-1034	923	6449	4676	306	-1527	5052